Morphological studies on lymphoid tissues locally formed in the ductal organs of animals

動物の管状臓器に局所的に形成されるリンパ組織の形態学的研究

Tsolmon CHULUUNBAATAR

Contents

Abbreviations

APCs: antigen-presenting cells

BALT: bronchus-associated lymphoid tissue

CALT: conjunctiva-associated lymphoid tissue

CB: citrate buffer

DC: dendritic cell

DLT: diffuse lymphoid tissue

EPGO: external parts of genital organ

Erβ: estrogen receptor β

GALT: gut-associated lymphoid tissue

GIT: gastrointestinal tract

GOALT: genital organ-associated lymphoid tissue

HE: hematoxylin-eosin

HEV: high endothelial venule

HSLF: horseshoe-like flexure

IF: immunofluorescence

IgA: immunoglobulin A

IgG: immunoglobulin G

IHC: immunohistochemistry

LN: lymphatic nodule

MALT: mucosa-associated lymphoid tissue

NALT: nose (or nasopharynx)-associated lymphoid tissue

NBF: neutral buffered formalin

NDS: normal donkey serum

NGS: normal goat serum

OsO_4: osmium tetroxide

PAS-H: periodic acid Schiff-hematoxylin

PSR: picrosirius red

SE: standard error

SEM: scanning electron microscopy

SILT: solitary intestinal lymphoid tissue

SLLF: spiral loop-like flexure

SLMF: single longitudinal mucosal fold

TB: tris buffer

VEDC: vaginal epithelial dendritic cell

List of published articles

1. Chuluunbaatar T, Ichii O, Nakamura T, Irie T, Namba T, Islam MR, Otani Y, Masum MA, Okamatsu-Ogura Y, Elewa YHA, Kon Y. Unique Running Pattern and Mucosal Morphology Found in the Colon of Cotton Rats. *Front. Physiol*., **11**:587214, 2020.
2. Chuluunbaatar T, Ichii O, Masum MA, Namba T, Islam MR, Otani Y, Elewa YHA, Kon Y. Genital organ-associated lymphoid tissues arranged in a ring in the mucosa of cow vaginal vestibules. *Res. Vet. Sci*., **145**, 147-158, 2022.
3. Chuluunbaatar T, Ichii O, Masum MA, Namba T, Kon Y. Morphological characteristics of genital organ-associated lymphoid tissue in the vaginal vestibule of goats and pigs.

Preface

The ductal organs of mammals face the outer environment at their entrance or exit. Mucosal epithelium and secreted mucus covering these organs are important for a physical barrier against the invasion by pathogens or commensal microorganisms, which could be harmful for the ductal tissue parenchyma [103]. Mucosal surfaces need a certain protection, but their thin epithelial layer can be easily damaged. Therefore, the mammalian body has a mechanism to supply additional immunological protections [59], such as mucosa-associated lymphoid tissues (MALTs) which compose of a complex of lymphoid cell aggregation and occupy about 50% of systemic immune system. MALTs include T cells, B cells, those in intraepithelial area, and antigen presenting cells (APCs) such as macrophages and dendritic cells (DCs), and these cells are localized to catch and respond to antigens at each entrance or exit of ductal organ [8]. The distribution, occurrence, morphology, ontogeny, and evolution of MALTs differ among species. In mammals, MALTs are classified according to their anatomical localizations; Waldeyer's ring (tonsils) in the oropharynx, conjunctiva-associated lymphoid tissue (CALT), nose (or nasopharynx)-associated lymphoid tissue (NALT), bronchus-associated lymphoid tissue (BALT), and gut-associated lymphoid tissue (GALT) [5,15,116].

Several lymphoid tissues (LTs) are defined as MALTs according to following morphological and functional characteristics; 1) LTs closely contact to the mucosal surface, 2) single (isolated) lymphatic nodules (LNs) or several LNs are covered by mucosal epithelium containing lymphocytes, 3) mucosal epithelium covering LTs lays out the morphologically distinct cells designed to uptake antigens, such as microfold cells (M cells), M cell-like cells, or DCs, 4) circulating lymphocytes enter LTs through high endothelial venules (HEVs) in the interfollicular areas. Specific receptors on HEVs control the tissue-specific immigration of lymphocytes [16]. These characteristics distinguish MALT structures from local cell infiltrations in the mucosa; they do not show compartmental organization. MALT formations would be induced at several disease status as found in isolated LNs in the large intestine of pigs in the granulomas [41], BALTs in the pneumonic lesions [1] or GALTs in the gastric lesions [35].

Furthermore, MALTs in the ductal organs can be functionally subdivided into inductive or effector sites. GALT, BALT, NALT, and CALT in mice, dogs, [34] and baboons [3], and duct-associated lymphoid tissue in cynomolgus macaques [88,115] are considered as inductive sites. Briefly, inductive sites include secondary LTs in which immunoglobulin A (IgA) switches and clonal expansion of B cells occur for the activation of antigen-specific T cells. After activation and IgA class switching, T and B cells migrate from inductive sites to effector sites. Effector sites exist in all mucosal tissues as dispersed LTs and diffusely distributed throughout the lamina propria or submucosa [131]. In effector sites, IgA is secreted over the mucosal epithelium [101]. Although the localization of each MALT is anatomically distinct, they can functionally connected as a common mucosal immune system; therefore antigen presentation and B cell activation at one mucosal site

can result in IgA productions at the mucosa of different organs [25,61].

The ductal genital organs and anal canal show anatomically close localization, and the formers in females are directly contact with the outer environment and susceptible to various infectious or non-infectious diseases including gynecologic cancer, pyometra, and vaginitis. In particular, the vaginal vestibule is the terminal part of the femal genital organs, extending from the external urethral orifice to the vulva, composed of the caudal part of the genital organs and urinary system, localized ventrally to the anus [119]. This region intensively contacts with high exposure of antigenic substances, such as urine or feces. Importantly, at healthy conditions, cows, dolphins, and non-human primates develop MALTs in their vaginal vestibule, uterus, and vagina, respectively [12,71,118]. In contrast, human and mouse vaginal mucosa do not develop clear MALTs; however, immune cells aggregate the genital organs during infectious status [122]. Furthermore, the morpho-function of female genital organs such as uterine and vagina are cyclically controlled by the sex hormones; estradiol and progesterone[70]. In addition, estrogens have closely association with the function of gastrointestinal mucosa and regulate immunological intestinal environments in various inflammatory bowel diseases that exhibit sex differences in incidence [36,93]. The MALT system around the cranial part of ductal organs (NALTs, CALTs, tonsils) is well characterized in several studies; however, their morpho-functional characteristics at the caudal part in each animal remains still unclear points [9,21,115].

In the thesis, the author focused on the morphology of MALTs found in the ductal organs of farm animals and experimental rodents, especially in females. The thesis contains three Chapters; the first and second Chapters characterized the morphology of MALTs, its immune cell composition, and mucosal epithelium structure in the vaginal vestibules of cow, goat, and pig which titled “genital lymphoid ring”. And then, author moved to the MALT in the reproductive organs of cotton rats and mice in third Chapter. Unfortunately, the author could not find the genital lymphoid ring in rodents because they lack the vaginal vestibule, but be able to observe a very unique morphology in the large intestine of cotton rats. Although this study does not reveal direct relationship between the genital lymphoid ring of the vaginal vestibule and large intestinal MALT, it provides important insight in the health and pathology of large intestine.

This thesis provides an important morphological basic knowledge of MALTs found in lower tubular organs of female body in several animals and would contribute to understanding the exact border between normal or pathological conditions and to developing the diagnosis and treatment for female-related disorders in animals and humans.

Chapter 1

Genital organ-associated lymphoid tissues

arranged in a ring in the mucosa of cow vaginal vestibules

Introduction

MALT is a local immune system beneath the mucosal epithelium [59,69]. MALTs are located in systemic organs that directly contact the outer environment, including alimentary tracts, salivary gland ducts, conjunctiva, nasopharynx, and respiratory tracts [32,59,62,66,67,85,88,106]. GALT is a well-known MALT and also known as Peyer's patches [32]. In the oropharynx, there are ring-shaped localized MALTs, including the lingual, palatine, and pharyngeal areas and the tubal tonsils [43]. Waldeyer's pharyngeal ring is the sentinel for the oral, nasal, and auditory tracts toward to the pharynx and basically functions in antibody production to protect against regular environmental antigens [73,80].

MALTs mainly consist of LTs with two types of morphology. Briefly, the lamina propria of several MALT-forming organs exhibit diffused arrangement of immune cells, and this type is called diffuse lymphoid tissue (DLT). However, in several MALTs, the accumulation of immune cells is separated by connective tissue from surrounding tissues, and these are called LNs [128]. Furthermore, the MALT is composed of B cells, $CD4^+$, or $CD8^+$ T cells, APCs, macrophages, and occasionally, mast cells and eosinophils. Each cell is well-situated to initiate an immune reaction when encountering antigens passing through the mucosal epithelium [21].

Mammalian female genital organs are also in close contact with the outer environment and maintain innate and adaptive immune systems constructed by the epithelial barrier, the production of antimicrobial agents, cytokines secreted by the epithelial cells, and the innate immune cells [44,79]. Importantly, the genital organs of humans or other animal species contain MALT with species- or disease-specific variations in morphology. A series of studies on LT have recently been pursued in some female genital organs, including the vaginal vestibule, vagina, cervix, uterus, and oviducts in non-human primates, pigs, and cows to evaluate the effects of drug administration or mucosal vaccination [12,57,71]. Specifically, the guiana dolphin (*Sotalia guianensis*) exhibited aggregations of LNs in the lamina propria of their uterine [118]. Importantly, healthy female mice did not have MALT in their genital organs, but they exhibited a MALT-like structure in their vaginal mucosa after receiving intravaginal immunization with a specific peptide [124]. Furthermore, locally organized MALT in the vaginal vestibule observed in patients with provoked vulvodynia compared with healthy women, indicated the MALT emerged because of the local alternation of vaginal vestibule morpho-function [73,122].

The reproductive management of animals is crucial in veterinary medicine. In cattle, gross anatomically and functionally, MALT in the alimentary and respiratory tract has been well-investigated in several studies [1,80,104]. Briefly, several types of MALTs were established according to their anatomical localization, including GALTs, CALTs, and BALTs [1,22]. Importantly, epithelium-associated LN aggregations were suggested throughout the genital organs in cattle, including the vaginal vestibule [12]. Additionally, in cow vaginal

vestibule is comparatively short pair of major vestibular glands located in the lateral walls underneath the constrictor vulvae[119]. The LN aggregations located in the lamina propria of the clitoris and vaginal vestibule could play an important role in immune induction sites because of their appearance during infection with cow reproductive tract pathogens [13,123]; however, structural information on genital organ-associated MALTs, in particular their localizations, morphological types, and cellular composition, has received limited attention.

In this Chapter, the author characterized a MALT-like structure arranged in a ring around the cow vaginal vestibule, and the stratified epithelium covering the LT was partially or completely disrupted, which permitted direct passage of immune cells and erythrocytes into the intraluminal space. The author named these LTs the “genital lymphoid ring” and discussed the similarities with Waldeyer’s pharyngeal ring, which acts as an immunological gate.

Materials and methods

Animal and sample preparation

Animal experimentation procedures were approved by the Institutional Animal Care and Use Committee of the Faculty of Veterinary Medicine, Hokkaido University (approval no. 19-0097, 19-0125). Investigators adhered to the Guidelines for the Care and Use of Laboratory Animals of Hokkaido University, Faculty of Veterinary Medicine. All animal experimental protocols were approved by the Association for Assessment and Accreditation of Laboratory Animal Care International. Holstein breed, normal non-pregnant cows (*Bos taurus*, total n = 8, over 2-year-old) were sedated with xylazine (3.0 mg/kg body weight) through an intramuscular route followed by general anesthesia with pentobarbital sodium (500 mg/kg body weight) via the intravascular route. The cows were sacrificed by intravenous administration of a saturated potassium chloride solution of at least 0.1 mL/kg body weight. Then, the jugular vein was exsanguinated. After euthanasia, female genital organs were obtained, and the vagina, vaginal vestibule, and external parts of genital organs (EPGOs), including the clitoris and vulva were separated. They were immediately fixed in 10% neutral buffered formalin (NBF) for more than 7 days. These specimens were dissected using scissors at the dorsal commissure along the median line of the vulva to the vagina.

Whole-mount observation

Separated genital organs were pinned flat, with the mucosa uppermost, and immersed in Mayer's hematoxylin for approximately 10 minutes (min) (examining at 3–4 min intervals) to visualize LTs. LTs were then visible as small navy-blue spots. To decrease the intensity of the staining background, specimens were rinsed in 70% alcohol containing 1% hydrochloric acid.

Counting of hematoxylin-positive ($^{+}$) spots was performed for the vaginal vestibule and EPGOs. Flattened vaginal vestibule and EPGOs were divided into six regions (Fig. 1-1). Briefly, the author divided the vaginal vestibule and EPGOs into two equal regions (cranial and caudal) along the horizontal line (the length of the external urethral orifice to the ventral commissure was divided into two equal lengths). Then, the cranial and caudal regions were subdivided by two vertical lines into three equal subregions. The external urethral orifice was located at the center of the cranial median region (Fig. 1-1, region II), and the clitoris was located at the center of the caudal median region (Fig. 1-1, region V). Each area was measured using ImageJ (National Institutes of Health; MD, Bethesda, USA) after taking photos with a DMC-FX3799 device (Panasonic; Osaka, Japan). The number of hematoxylin^{+} spots was counted, and their density in each region was calculated.

Histoplanimetry

The vaginal vestibule of each cow was cut into more than 15 pieces according to their size. Then, whole-mount specimens with hematoxylin were embedded into paraffin and cut to a thickness of 5 μm. Sections were stained with hematoxylin and eosin (HE) or picrosirius red (PSR) for histological analysis. Stained sections were scanned with a NanoZoomer 2.0 RS virtual slide scanner (Hamamatsu Photonics; Shizuoka, Japan). Histological images for microscopic examinations were observed using a model BZ-X710 microscope (Keyence; Osaka, Japan). The number of LNs and DLTs was counted after HE staining. This measurement was performed for more than 120 sections of eight cows. The author also characterized the LNs according to their localization (isolated, migrating, bordering) and the DLTs according to their shape (oval, c-shaped, triangle, amorphous), and their appearance % was calculated.

Immunohistochemistry (IHC)

IHC was performed to evaluate the presence of B cells (CD20), T cells (CD3), macrophages (IBA1), APCs (major histocompatibility complex, MHCII), HEVs (peripheral lymph node addressin, PNAd), and tight junctions (Occludin). The staining conditions of each antibody are listed in Table 1-1. In brief, sections were deparaffinized and incubated in 10 mM citrate buffer (CB, pH 6.0) or Tris-HCl buffer (pH 9.0) for 15 min at 110 °C. Thereafter, slides were submerged in methanol containing 0.3% H_2O_2 for 20 min at 20–22 °C and blocked with normal goat serum (SABPO kit, Nichirei Bioscience; Tokyo, Japan) for 1 hour at room temperature. Sections were incubated with primary antibody overnight at 4 °C. After rinsing in phosphate-buffered saline (PBS), sections were incubated with biotinylated secondary antibody (goat anti-rabbit or goat anti-rat) for 30 min and streptavidin-horseradish peroxidase (Nichirei Bioscience) for 30 min at room temperature. To develop the color, sections were incubated in a 3,3'-diaminobenzidine tetrahydrochloride–hydrogen peroxide solution for 4 min. Finally, the sections were counterstained with hematoxylin and dehydrated with ascending grades of alcohols. After rinsing with three steps of xylene, the sections were mounted and examined as explained in histoplanimetry.

Next, the author performed the histoplanimetrical analysis of LTs using the IHC sections for CD20, CD3, IBA1, and MHCII. More than 10 LNs and DLTs were examined. Firstly, total area of LNs or DLTs and the positive reaction area for each marker were measured, and percentage of the latter to the former was calculated.

Electron microscopy

For scanning electron microscopy (SEM), small pieces of vaginal vestibule were treated with tannic acid and post-fixed with 1% osmium tetroxide (OsO_4) for 1 hour (h). Then, the specimens were dehydrated in

ascending grades of alcohol, immersed in 3-methylbutyl acetate, and dried with the HCP-2 critical point dryer (Hitachi; Tokyo, Japan). The specimens were then observed under an S-4100 scanning electron microscope (Hitachi).

Statistical analyses

The results are expressed as the mean ± standard error (SE). Multiple comparisons were performed using the Kruskal–Wallis test followed by the Scheffé method when a significant difference was observed ($P < 0.05$).

Results

LT found in the vaginal vestibule and EPGO mucosa of cows

The author investigated the mucosa of the vagina and vaginal vestibule extending from the external urethral orifice to the vulva, and the vulva along with the pudendal labia and clitoris were also examined as EPGOs (Fig. 1-1A). Whole-mount specimens were visualized for hematoxylin$^+$ spots in the examined mucosae; in particular, the author focused on vaginal vestibule and EPGOs, because these areas are close to the outer environment and have contact with urine and feces. All examined cows had numerous hematoxylin$^+$ spots in the mucosal surface of the vaginal vestibule and EPGOs, and these spots were distributed at an approximately 1 cm distance from the boundary of the un-haired pudendal labia (Fig. 1-1B, C). Furthermore, 37.5% of examined cows showed these spots in EPGOs (three of eight cows), especially in the area close to the clitoris (Fig. 1-1D). Then, these spots were histologically identified as LTs (Fig. 1-1E), and classified as genital organ associated LTs (GOALTs). They were further investigated in subsequent experiments.

The author also examined the localizations of GOALTs by dividing the vaginal vestibule and EPGOs into six regions (Fig. 1-1F). During the histometry of the density of GOALT spots for the six examined regions, regions II and V, located along the ventral median line of the vaginal vestibule, including the external urethral orifice, clitoris, and ventral commissure of the labia, tended to exhibit a higher density without significance (Fig. 1-1G). These results indicated that GOALTs were distributed in the mucosa of the vaginal vestibule and EPGOs in a ring shape; therefore, the author denoted the GOALT distributions as a "genital lymphoid ring," based on "Waldeyer's lymphoid pharyngeal ring". In subsequent analysis, the author focused on vaginal vestibule mucosa.

Histology of GOALTs found in the cow vaginal vestibule mucosa

The histological observation was performed in the vaginal vestibule. The mucosa was covered by non-keratinized and stratified squamous epithelium (Fig. 1-2). The GOALTs were mainly localized in the lamina propria in the vaginal vestibule. Importantly, regarding the LT structures, two different types of GOALTs were found in the vaginal vestibule; LN (Fig. 1-2A-D) and DLT (Fig. 1-2E-H). For LN, three types were primarily observed in the vaginal vestibule mucosa based on their morphology. First, several LNs were localized in the deep portion of the lamina propria and fully surrounded by connective tissues. In this type, the vaginal vestibule epithelium completely maintained the structure (Fig. 1-2A). Second, scattered lymphocytes were observed between the LN and vaginal vestibule epithelium, and these lymphocytes were also thoroughly or partially observed within the vaginal vestibule epithelium structure (Fig. 1-2B). Third, LN directly faced the vaginal vestibule lumen, and the vaginal vestibule epithelium was occupied by lymphocytes (Fig. 1-2C). Further, most of the LNs were solitarily, but paired LNs were also noticed (Fig. 1-2D).

Additionally, several shapes of DLTs were observed, such as triangle-, C-shaped-, amorphous-, and oval-types (Fig. 1-2E-H).

In the histometry of the vaginal vestibule mucosa, LN- and DLT-types accounted for 35% and 65%, respectively (Fig. 1-2I). Furthermore, as a result of morphometry according to the LN localization, migrating-, isolated-, and bordering-types accounted for 51%, 37%, and 12%, respectively (Fig. 1-2J). Finally, for the DLT shapes, amorphous-, oval-, C-shaped-, and triangle-types accounted for 57%, 30%, 9%, and 4%, respectively (Fig. 1-2K).

Cell composition of GOALTs in the cow vaginal vestibule mucosa

Regarding LNs of the GOALT in the vaginal vestibule mucosa, numerous $CD20^+$ B cells were found, and the germinal center and an area between the LN and vaginal vestibule epithelium were located (Fig. 1-3A). Further, $CD3^+$ T cells were diffusely distributed in LNs, including the germinal center, and tended to mainly localize along the border area between the LN and vaginal vestibule epithelium (Fig. 1-3B). $IBA1^+$ macrophages and $MHCII^+$ APCs were similar in localization and were located in the germinal center and the border area between the LN and vaginal vestibule epithelium; the former was also localized in the vaginal vestibule epithelium (Fig. 1-3C, D). Next, $PNAd^+$ HEVs were localized around the LNs and in the border area between the LN and vaginal vestibule epithelium (Fig. 1-3E). In agreement with histological observations, the percentage of B cells was statistically significantly higher in LNs than the percentage of T cells, macrophages, and APCs ($P < 0.01$, Fig. 1-3F).

In the DLT, B cells, T cells, macrophages, APCs, and HEVs were dispersed diffusely (Fig. 1-4A-E). Similar to LNs, DLTs had a statistically significantly higher percentage of B cells than that of other examined immune cells ($P < 0.01$, Fig. 1-4F).

Histology of epithelial cells covering the GOALT in the cow vaginal vestibule mucosa

Histologically, the vaginal vestibule mucosa was covered by stratified epithelial cells, wherein the basal layer was smaller with narrow cytoplasm, and their nuclei were located close to one another (Fig. 1-5A). Follicular epithelial cells found in MALTs were not identified. Importantly, in several LTs, the thickness of the epithelium gradually became smaller towards the epithelium covering LTs (Fig. 1-5A). Furthermore, the epithelium covering LTs showed complete destruction of each junction of epithelial cell with numerous lymphocytes and erythrocytes, and several epithelial cells peeled off and created a large junctional gap, which permitted direct passage of immune cells into the intraluminal space of the vaginal vestibule (Fig. 1-5B). $Occludin^+$ reactions were observed in the intercellular region of the epithelial cells, but these were unclear in the epithelium covering LTs (Fig. 1-5C, D).

Next, PSR staining revealed the developed connective tissue fibers in the lamina propria of the vaginal vestibule mucosa. Under polarized light observation, well-developed collagen fibers were visualized as bright orange to red, whereas thinner reticular fibers appeared yellow to green (Fig. 1-5E). In GOALTs, the DLT-types contained abundant collagen and reticular fibers, but they were scarce in the LN-type (Fig. 1-5E). The vaginal vestibule mucosa exhibited well-developed collagen and reticular fibers beneath the epithelium (Fig. 1-5F), but they were obscure in the LN (Fig. 1-5H-J).

Ultrastructure of surface of LT in the vaginal vestibule

Next, the author observed the GOALT surface in the vaginal vestibule mucosa (Fig. 1-6). Whole-mount staining with hematoxylin revealed the GOALTs as spots (Fig. 1-6A). Using SEM, the epithelium covering GOALTs was found to partially lack in several areas (Fig. 1-6B). Briefly, at these regions, several polygonal-shaped epithelial cells were peeled off, and lymphocytes appeared to be directly exposed to the intraluminal space through the hole (Fig. 1-6C, D). Figure 1-6E shows the large sized, dome-shaped LN covered by the vaginal vestibule epithelium, which was approximately 350–480 μm in a diameter. Several differently sized destroyed areas of the epithelium fused with each other and formed a complicated cleft. From the inside of the GOALT, erythrocytes were also exposed directly to the intraluminal space (Fig. 1-6F, G). Additionally, small protrusions occurred that appeared to be lymphocytes pushed up to the surface of the epithelium (Fig. 1-6F, G). Some connective tissue fibers were also observed inside of the GOALT and opened to the lumen (Fig. 1-6G).

Discussion

This Chapter clarified the morphological characteristics of GOALTs found in the vaginal vestibule and EPGOs of the cow. Cow is one of the most important farm animal for meat, milk, hides, and its reproductive performance directly affects to the economy. In cows, the vaginal vestibule extends from the external urethral orifice to the ventral commissure of the labia and is composed of the caudal part of the reproductive and/or urinary system, localized ventral to the anus, with a length of approximately 7–11 cm [17,64]. The LTs in the bovine vaginal vestibule were previously suggested in cows [13,23,40], but detailed morphological information was lacking. The high abundance of LTs along the vaginal vestibule may relate to increased antigenic stimulation in this region. In this Chapter, the ventral median region (II and V containing EPGOs) of the vaginal vestibule and EPGOs tended to have a greater number of GOALTs than other areas. The author considered that the developed GOALTs in this area reflected the possibility of high exposure to antigenic substances, such as urine or feces, because of the anatomical localization of the vaginal vestibule. These relationships between antigenic challenge and the localizations of LTs are compatible with statements regarding the amount and type of MALTs being partially dependent on the antigenic challenge [54,106]. Additionally, the age of the cow appeared to be a factor influencing the amount of LT, and the vaginal vestibule of adult cows contained a significantly higher number of LTs than 6–8-week-old calves [12].

GOALTs were morphologically divided into LNs and DLTs, and the latter was dominant in the vaginal vestibule. LNs were usually dispersed solitarily in a random manner throughout the mucosa of the vaginal vestibule or EPGOs. Most LNs had a germinal center, which initiated a series of events that included lymphocyte activation and proliferation, plasma cell differentiation, and antibody production. Mitotic patterns were frequently seen in the germinal center, indicating that new lymphocytes were proliferating *in situ* [128]. Although this histological data showed different morphology of LNs, the dominant was the migrating-type, and sectioning of LNs also could have affected their shape observed during microscopical examination. SEM analysis revealed both an epithelium-covered area (isolated-type) and non-covered area (migrating-, bordering-type) in the same LN. Furthermore, three-dimensional analysis of LNs could clarify their fine structure.

DLTs typically do not have a distinct border with surrounding tissues, rather have an amorphous shape and are tactically localized to intercept antigens and initiate an immune response. In general, after contact with antigen, lymphocytes located in the LT move to regional lymph nodes, where they can sustain proliferation and differentiation. Then, the progenies of these cells return to the lamina propria as B and T cells with effector functions. Therefore, combined localization of LNs and DLTs in the vaginal vestibule or EPGO mucosa could act as a protector of the genital organ against pathogenic substances. Furthermore, this histological data showed the different morphology of LNs; the dominant amorphous-type, with variation in

the morphology of DLT that might reflect the difference in the activation phase of GOALTs.

Subsequently, the percentage of the positive area for the immune cells calculated in GOALT and both DLTs and LNs was dominated by B cells in comparison with T cells, macrophages, and APCs. This was an expected finding, which is in agreement with other research data, including those for the mice spleen, Peyer's patches, isolated LNs, and cow and rabbit GALT [38,63,104,117].

The cell components of the cow GOALT showed close similarities to those of other MALTs (GALT and Waldeyer's pharyngeal ring); however, the cell distribution was generally solitarily and randomly localized within the vaginal vestibule and EPGOs [100]. One of the most important cell components in MALTs is the APC. In this Chapter, APCs were found around the DLT and LN in different regions of the mucosal epithelium, such as the germinal center, mantle zone, submucosa, and middle layers of stratified squamous epithelium of the vaginal vestibule. These strategically positioned localizations might play important roles in the initiation of immune reactions and maintenance of peripheral tolerance. Therefore, various types of APCs in the LTs have different ways to take up antigens from the lumen, including endocytosis, phagocytosis, or transcytosis [134]. Although, in this Chapter, the epithelium that covered GOALTs was thinner than areas not covering GOALTs, and in some areas, the epithelium structure was completely lost, and LT and the intraluminal area were directly bordered without any edge. This formation of LT allows direct passage of antigens to the LT and immune cells from the intraluminal area. As described in the literature [15], MALT is divided into two specific types, an organized MALT delimited by organized collagen fiber tissue and a disorganized or diffuse MALT, comprising populations of lymphocytes from the lamina propria and the base of the epithelial lining, which are consistent with LNs and DLTs. LNs located in the conjunctiva have a lenticular shape, and occasionally around this area, the basement membrane is mostly discontinuous, and the epithelium is thinner [24]. The author classified DLTs by shape, and each shape might reflect the different LT activity in the vaginal vestibule mucosa.

The author studied the normal histomorphology of the GOALT, and unfortunately, the phase of the estrus cycle was impossible to identify in the examined cows. Importantly, the immune system in the female genital organ is precisely influenced and regulated by sex steroid hormones, estradiol and progesterone, which are produced in cyclic variations by the ovary during the estrus cycles. Throughout the estrus cycle, immune cells are present in considerable numbers and inconsistently distributed in the stromal layer and the epithelium of the female genital organ [19,48]. Moreover, the epithelial barrier of the genital organ, which includes various tight junction conditions, provides immune protection by maintaining a strong physical barrier, transferring antibodies to the mucosa, producing antibacterial composites, and recruiting immune cells, all of which are influenced by hormones [112)96]. Additionally, the various shapes of GOALTs found in the vaginal vestibule and EPGOs may be affected by different phases of the estrus cycle. A limitation of this

Chapter was the small sample size available to identify whether or not the estrus cycle influences the amount of GOALT in the vaginal vestibule in cows. Further study is needed to clarify the GOALT amount at every stage of the estrous cycle.

In conclusion, this Chapter morphologically and histologically evaluated GOALTs in the vaginal vestibule and EPGOs of cows, which constituted a “genital lymphoid ring.” Regarding GOALT morphology (Fig. 7), the mucosal epithelium covering DLTs and LNs was partially or completely demolished, making a direct passage for immune cells to reach the luminal side. The clarification of the morphology of GOALTs in cow genital organs would contribute to understanding of its immune-associated function, the pathogenesis of diseases, and the development of therapeutic strategy by applying mucosal vaccinations targeting GOALTs in farm animals.

Summary

Female genital organs are equipped with local and mucosal immune systems; however, structural information remains unclear among farm animals. In this Chapter, the MALTs in cow genital organs were investigated, and their vaginal vestibule and EPGOs, including the clitoris and vulva, were morphologically analyzed. Whole-mount specimens revealed several hematoxylin^{+} spots arranged in a ring in the mucosa. Histologically, these spots were aggregated immune cells and defined as GOALTs. GOALTs were composed of LNs or DLTs at different depths of lamina propria. LNs frequently contained germinal centers. Scattered lymphocytes occupied the border area between follicles and epithelium, whereas DLTs had indefinite shapes. GOALTs contained immune cells and HEVs. B cells were dominant both in LNs and DLTs. Abundant collagenous fibers were stretched across vaginal vestibule lamina propria, whereas reticular fibers were primarily observed in the DLT rather than LN. The epithelium covering of GOALTs was partially or fully disrupted by the invasion of immune cells toward the vaginal vestibule lumen. These findings suggest GOALTs function as a “genital lymphoid ring” as in Waldeyer's pharyngeal ring and act as immunological gate systems in lower ductal organs of cows.

Figures

Table 1-1. Antibodies

Primary antibody	Source	Detection (Application)	Dilution	Blocking	Antigen retrieval	Secondary antibody
Rabbit anti-CD20	Spring Bioscience (Pleasanton, USA)	B-cell	1:300	10% NGS (SABPO(R) Kit, Nichirei)	20mM TB (pH 9.0) 115C	Goat anti-rabbit IgG antibody (SABPO(R) Kit, Nichirei)
Rabbit anti-CD3	Nichirei (Tokyo, Japan)	T-cell	1:200	10% NGS (SABPO(R) Kit, Nichirei)	10mM CB (pH 6.0) 115°C, 15 min	Goat anti-rabbit IgG antibody (SABPO kit, Nichirei)
Rabbit anti-Iba1	Wako (Osaka, Japan)	Macrophage	1: 1200	10% NGS (SABPO(R) Kit, Nichirei)	10mM CB (pH 6.0) 115°C, 15 min	Goat anti-rabbit IgG antibody (SABPO kit, Nichirei)
Rat anti-PNAd	Biolegend (California, USA)	High endothelial venule	1: 200	10% NGS (SABPO(R) Kit, Nichirei)	10mM CB (pH 6.0) 115°C, 15 min	Goat anti-rat IgG (Biolegend) (California, USA)
Rabbit anti-Occludin	Abcam (Cambridge, UK)	Tight junction	1: 100	10% NGS (SABPO(R) Kit, Nichirei)	10mM CB (pH 6.0) 115°C, 15 min	Goat anti-rabbit IgG antibody (SABPO kit, Nichirei)
Mouse anti-MHC-II	Washington State University (Washington, USA)	Antigen-presenting cell	1: 100	10% NGS (SABPO(R) Kit, Nichirei)	20mM TB (pH 9.0) 115°C, 15 min	Goat anti-mouse IgG (Southern Biotech, Birmingham, AL, USA)

CB: citrate buffer. TB: tris buffer. NGS: normal goat serum

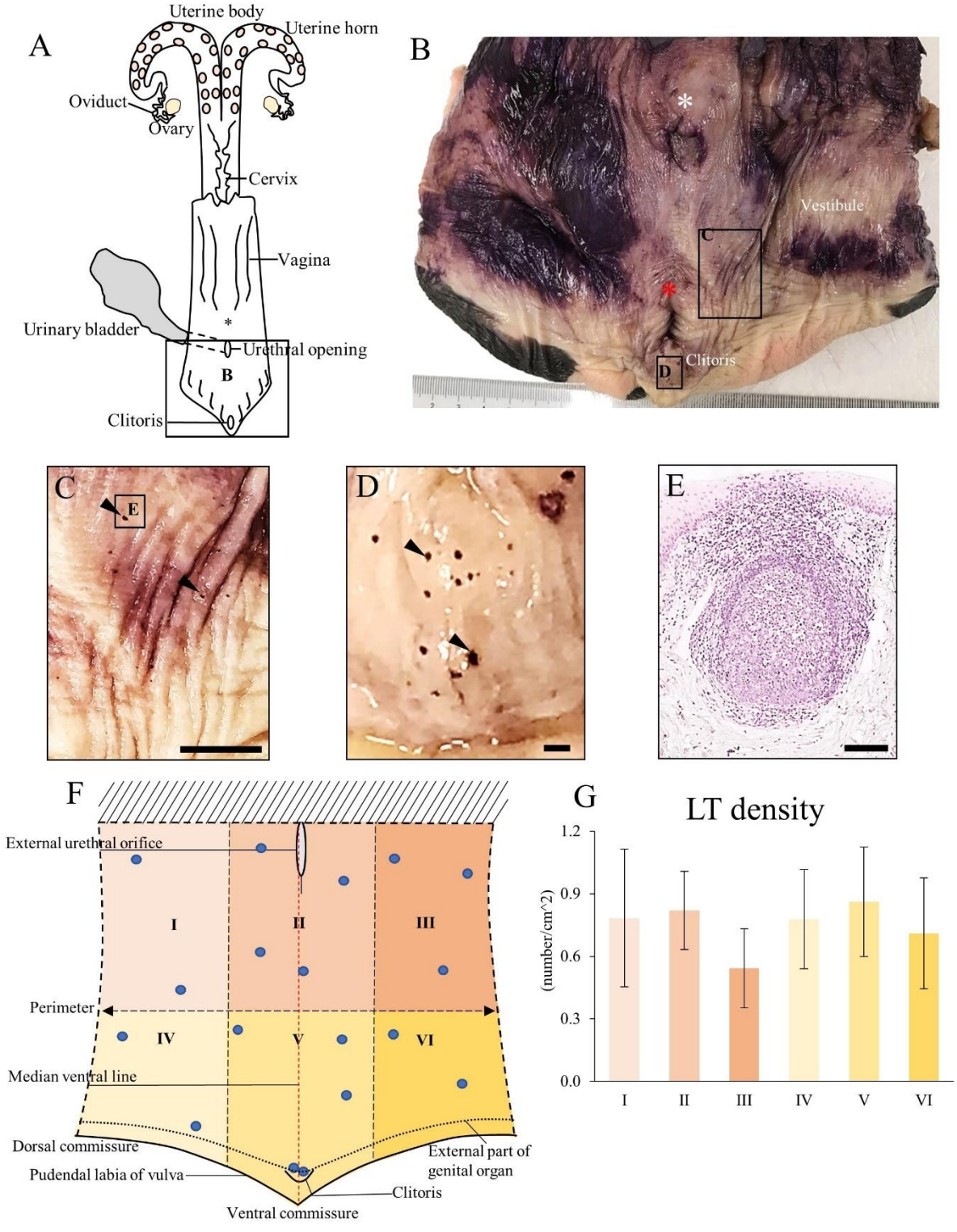

Figure 1-1. Distribution of GOALTs in the mucosa of the vaginal vestibule and EPGOs of cows

(A) Illustration of reproductive organs in a cow. Vagina and vaginal vestibule are cut open. The square indicates vaginal vestibule, and EPGO area, examined in this study. (B) Gross anatomical features of the vaginal vestibule and EPGOs with whole-mount staining using hematoxylin. White and red asterisks indicate the external urethral orifice and clitoris, respectively. One scale of the ruler is 1 mm. (C) Magnified image of

the vaginal vestibule mucosa squared area in panel B. Scale bars = 1 cm. (D) Magnified image of the EPGO mucosa squared area in panel B. Black arrowheads indicate hematoxylin-positive spots. Scale bars = 1 mm. (E) Histology of hematoxylin-positive spot squared area in panel C. Histological observation revealed the spot is a cell aggregation, the GOALT, part of genital lymphoid ring. HE staining. Scale bar = 100 μm. (F) Schematic illustration of cutaway of the vaginal vestibule and EPGO area, including the vulva and clitoris. For morphometry, the mucosal area is divided into six regions. Blue circles indicate GOALTs. (G) The density of GOALTs in the vaginal vestibule mucosa (number/cm^2). Values = mean ± SE. n = 8.

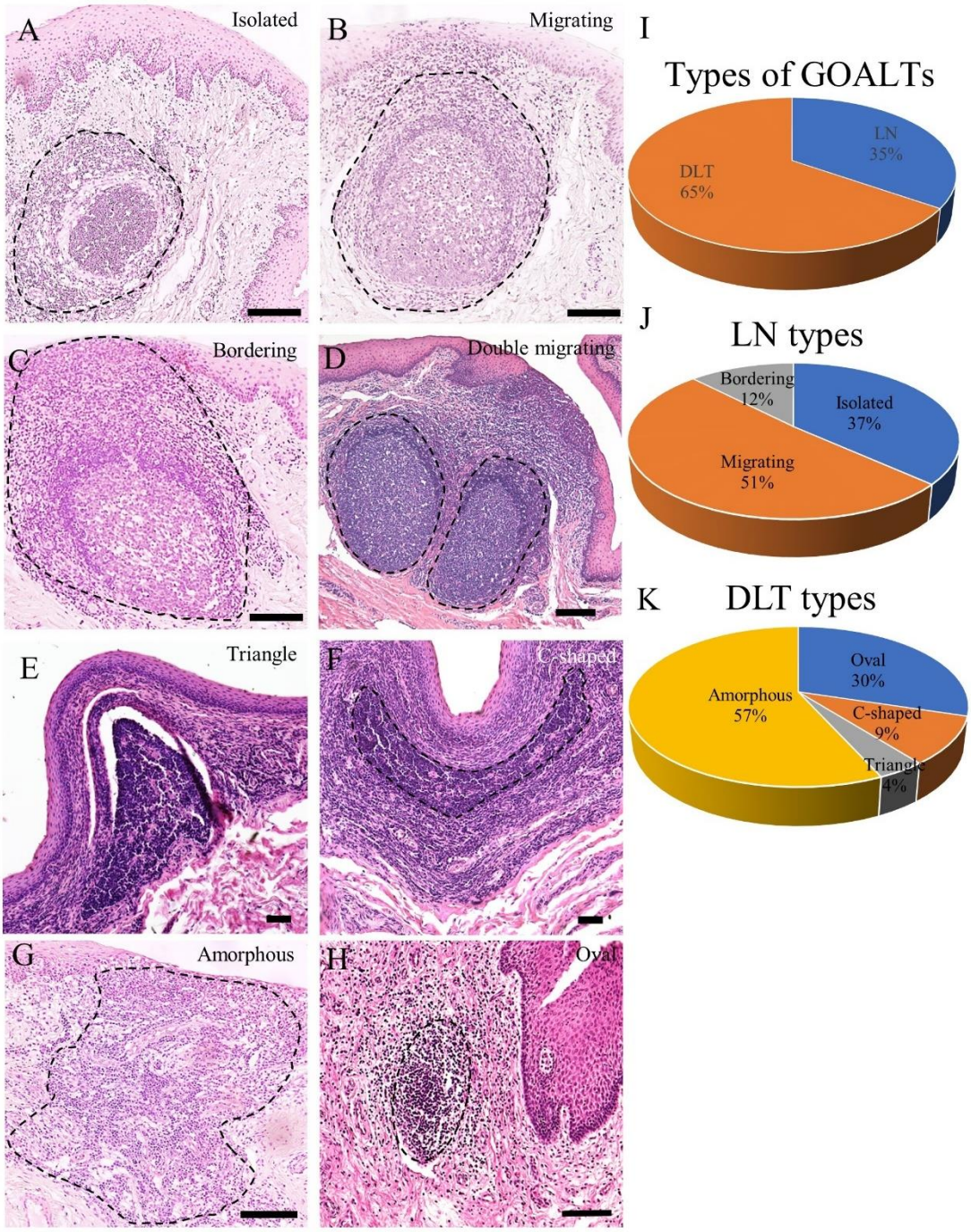

Figure 1-2. Histological characteristics of GOALTs in the cow vaginal vestibule

(A) Isolated-type LN. LN localizes in the deep portion of the lamina propria and is fully surrounded by connective tissues. (B) Migrating-type LN. Scattered lymphocytes are observed between LN and vaginal vestibule epithelium. (C) Bordering-type LN. LN directly faces the vaginal vestibule lumen, and the vaginal vestibule epithelium is occupied by lymphocytes. (D) Double migrating-type LN. Dotted lines indicate the border of LNs. HE staining. Scale bars = 100 μm. (E) Triangle-type DLT. (F) C-shaped-type DLT. (G)

Amorphous-type DLT. Dotted lines indicate the border of the DLT. (H) Oval-type DLT. Scale bars = 100 μm. (I) Appearance of the percentage of LNs and DLTs in the examined GOALTs of the vaginal vestibule. n = 8. (J) Appearance of the percentage of each type of LN in the examined LNs of the vaginal vestibule. n = 8. (K) Appearance of the percentage of each type of DLT in the examined DLTs of the vaginal vestibule. n = 8.

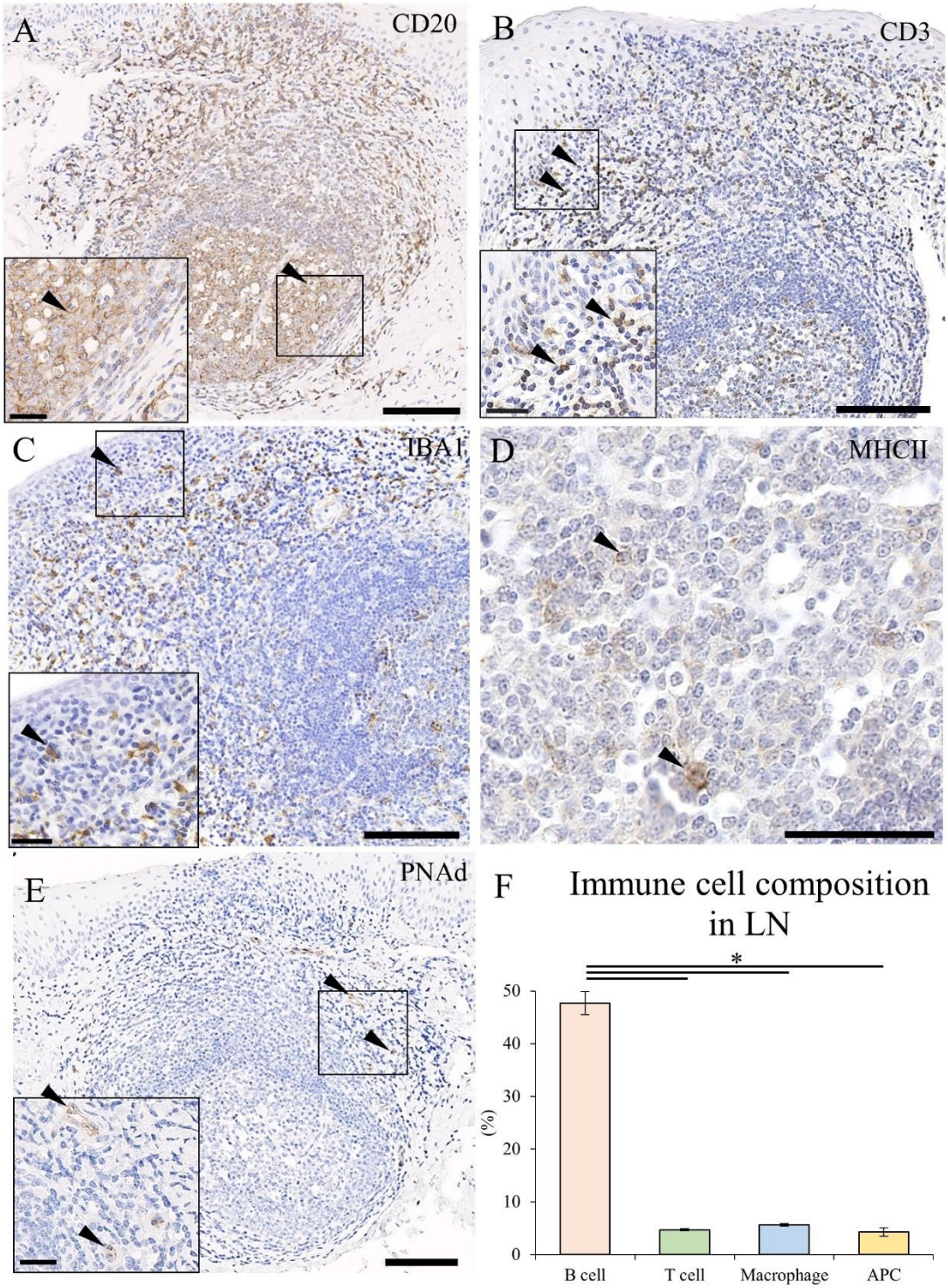

Figure 1-3. Immune cells composing the LN-type GOALT in the cow vaginal vestibule

IHC was performed in the vaginal vestibule mucosa, and immune cells and HEVs were found in the GOALTs. (A) CD20 for B-cells. (B) CD3 for T-cells. (C) IBA1 for macrophages. (D) MHCII for APCs. (E) PNAd for HEVs. Squares denote the magnified area. Black arrowheads indicate positive cells for the IHC. Scale bars = 100 and 25 μm (low and high magnifications, respectively). (F) Percentage of each examined cell

occupying the LN. Values = mean ± SE. $n \geq 4$. Significant differences between the immune cells indicated by ∗, $P < 0.01$; Kruskal–Wallis test followed by the Scheffé method.

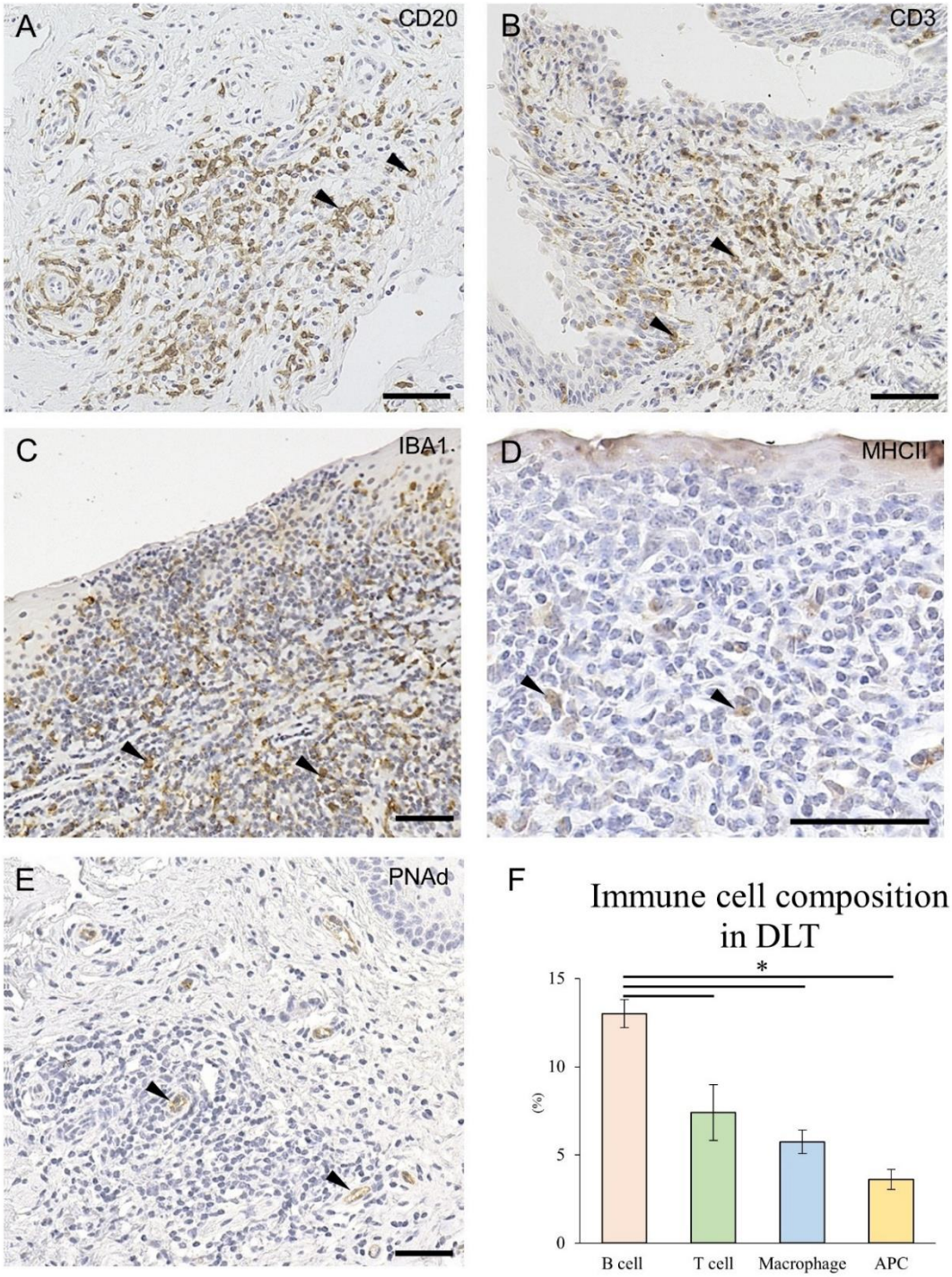

Figure 1-4. Immune cells composing the DLT-type GOALT in the cow vaginal vestibule

IHC was performed in the vaginal vestibule mucosa, and immune cells and HEVs were found in the GOALTs. (**A**) CD20 for B-cells. (**B**) CD3 for T-cells. (**C**) IBA1 for macrophages. (**D**) MHCII for APCs. (**E**) PNAd for HEVs. Black arrowheads indicate positive cells for the IHC. Scale bars = 100 μm. (**F**) Percentage of each examined cell occupying the DLT. Values = mean ± SE. $n \geq 4$. Significant differences between the immune cells indicated by ∗, $P < 0.01$; Kruskal–Wallis test followed by the Scheffé method.

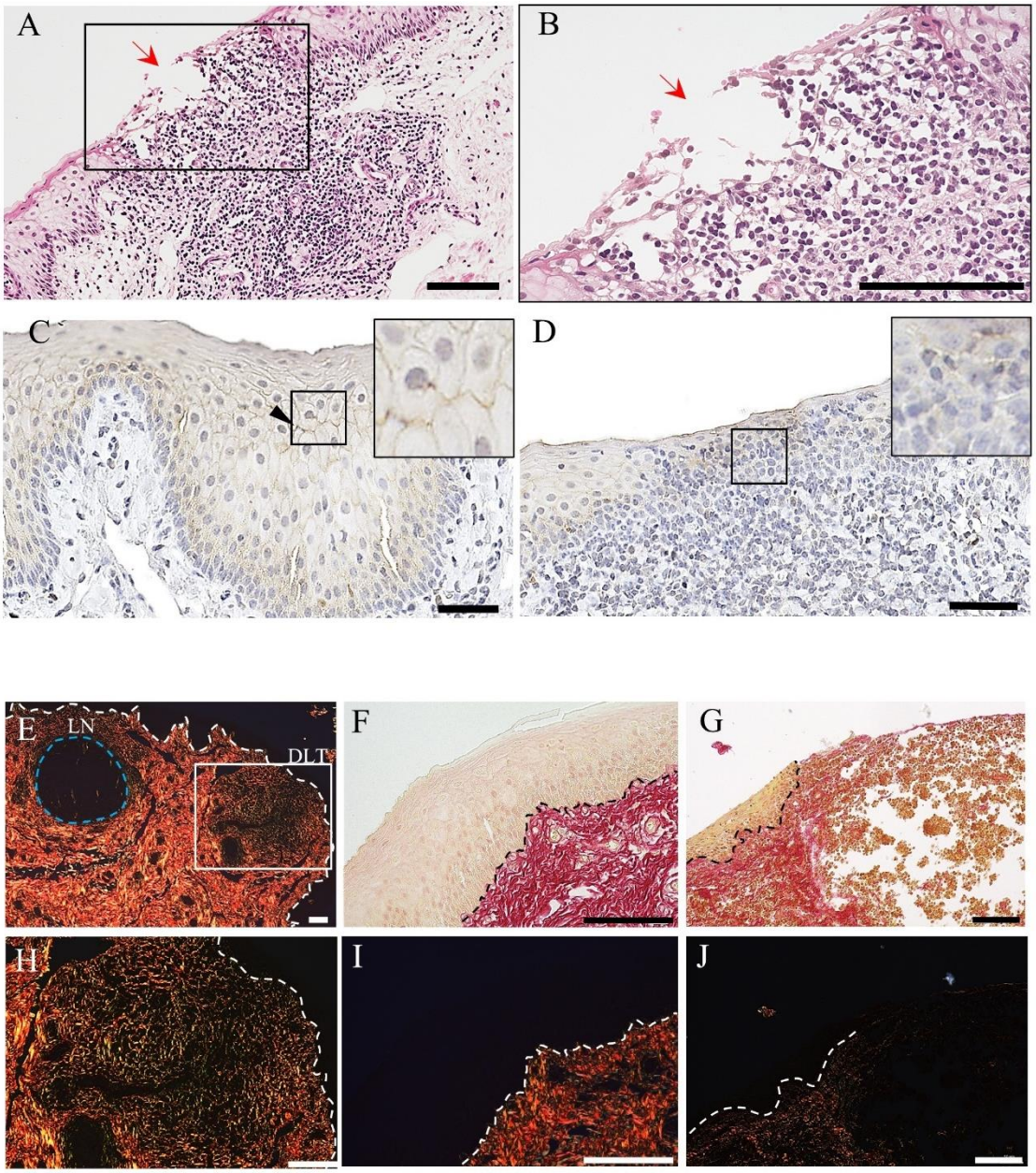

Figure 1-5. Epithelium covering and connective tissue fibers composing the GOALTs in the cow vaginal vestibule

(A, B) Amorphous-type DLT. Destroyed epithelium located between DLT and intralumenal area. The square indicates the magnified area. Red arrows denote peeled-off area of epithelial cells. HE staining. Scale bars = 100 μm. (C, D) Mucosal epithelium features stained using IHC for occludin. Panel C shows the epithelium that does not cover the lymphoid tissue. Panel D shows the epithelium covering the lymphoid tissue. Black arrowheads indicate positive reaction for the occludin. Scale bars = 50 μm. (E) Connective tissue fibers of

LN and DLT stained using PSR under polarized conditions. White dotted line indicates the border between the lamia propria and the epithelium. Blue dotted line denotes the border of the LN. Lower panel is a magnification of the squared area in the upper panel. (F, G) Mucosal epithelium and connective tissue fibers stained using PSR. Panel F shows the mucosa with epithelium that does not cover the DLT. Panel G shows the mucosa with epithelium covering the DLT. Upper and lower panels show optimal and polarized conditions, respectively. Black and white dotted lines indicate the border between the lamia propria and the epithelium. Scale bars = 100 μm.

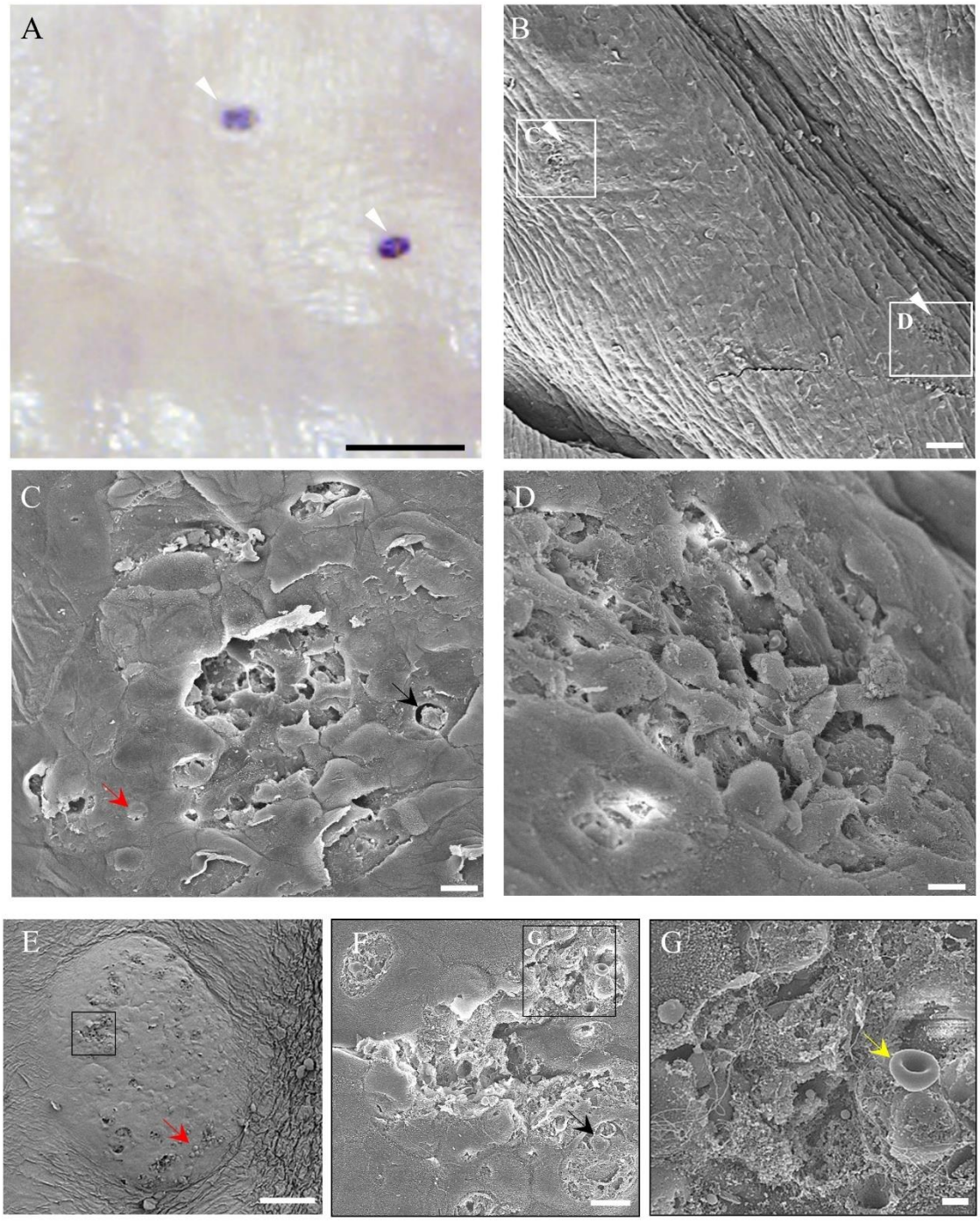

Figure 1-6. Ultrastructure of mucosal epithelium covering the GOALT of the cow vaginal vestibule

(A) vaginal vestibule mucosa stained in whole-mount with hematoxylin. GOALTs can be observed as hematoxylin-positive spots. Scale bars = 1 mm. (B) vaginal vestibule mucosa examined using SEM. The same area as in panel A was examined. Scale bars = 100 μm. White arrow heads indicate GOALTs. (C, D) High-magnified areas squared in panel B. Black arrow heads indicate migrating lymphocytes from the GOALT to the lumen of the vaginal vestibule. Red arrow represents small protrusions that could be

lymphocytes. Scale bars = 10 μm. (E) vaginal vestibule mucosa on large GOALTs examined using SEM. Red arrow represents small protrusions that could be lymphocytes. Scale bars = 100 μm. (F) High-magnified area of panel E. High-magnified areas squared in panel E. Black arrowhead indicates lymphocytes. Scale bars =10 μm. (G) High-magnified area of panel F. High-magnified areas squared in panel F. Yellow arrowhead indicates erythrocytes. Scale bars = 2 μm.

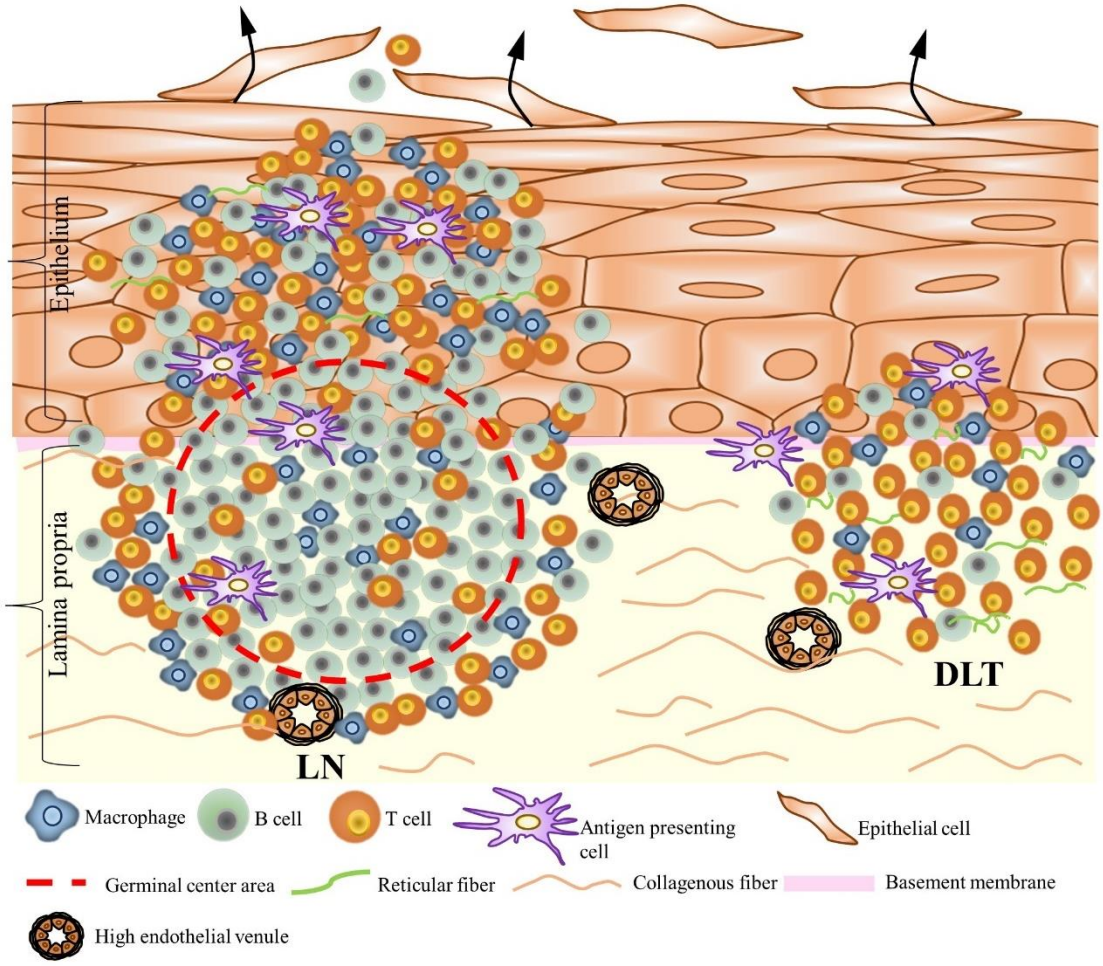

Figure 1-7. Schematic illustration of GOALTs in the mucosa of the vaginal vestibule and EPGOs in cows.

GOALTs consist of various shaped LNs and DLTs that localize in different regions in the lamina propria of the vaginal vestibule. Both lymphoid tissues contain B-cells, T-cells, macrophages, and APCs. B-cells are dominant. Germinal centers are frequently observed in the center of the LN. High endothelial venules also appeared between lymphoid tissues and surrounding connective tissues in the lamina propria. Moreover, collagenous fibers are stretched across the lamina propria, whereas reticular fibers are mainly observed in DLTs rather than in LNs. Characteristically, the epithelium covering GOALTs is partially or completely disrupted by the invasion of immune cells composing LNs and DLTs. These GOALTs are arranged as ring in the vaginal vestibule and EPGO mucosa and named the “genital lymphoid ring.”

Chapter 2

Morphological characteristics of GOALTs in the vaginal vestibule of goats and pigs

Introduction

In Chapter 1, the author clarified the morphological structure of GOALTs in cows which formed a genital lymphoid ring in the vaginal vestibule. Furthermore, the author hypothesized that goats and pigs also develop similar LT structures in their vaginal vestibule.

MALTs in pigs have been studied by several researchers because of their similarities to humans. The porcine large intestine harbors GALT, including multi-follicular submucosal lymphoid clusters, as well as smaller mucosal isolated LNs that contain high numbers of T, B cells [55]. BALTs are mostly found in bronchiolar bifurcations as a single dome-shaped LN, which bulges out from the mucosal surface into the airway [46]. The size of NALT found on the roof of the nasopharynx in pigs varied from 2 to 4 cm. Similar to pigs, GALT, BALT, and NALT have also been identified in goats. GALTs are densely found in the distal colon and rectum as solitary LNs with round tubercles and a central depression. In goats, BALT differs from other locally organized tissues, is not developed during the prenatal period, and is fully affected by antigenic stimuli [33].

The vaginal vestibule is the terminal part of the genital organ, and the urethra opens the border between the vagina and the vaginal vestibule. In adult pigs, the vaginal vestibule is relatively long since the urethra enters the genital organ rather far cranially, and the external urethral orifice is associated with a small suburethral diverticulum [28]. In adult goats, the vaginal vestibule slopes ventrally to the opening between the labia of the vulva and is less distensible than the vagina [28]. The vaginal vestibule of the goat is 2.5-3.0 cm in length and the major vestibular glands are not permanent structures, whereas the vaginal vestibule of the pig is comparatively longer (approximately 7.5 cm) and does not contain any major vestibular glands [7,119]. The mucosal epithelium of vaginal vestibule is composed of non-keratinized stratified squamous epithelium and forms longitudinal folds called rugae in both goats and pigs [47]. Therefore, innate and adaptive factors are involved in the immune system of reproductive organs, and both are regulated by sex hormones, fluctuate through estrous cycles [44,96,112].

A clear understanding of the species-specific features of GOALT is important for comparative research in order to understand the border between normal and pathological conditions in EPGO and the development of therapeutic methods such as mucosal vaccination. In this Chapter the author aimed to describe the morphology of GOALT in the vaginal vestibule of goats and pigs during adulthood.

Materials and methods

Sample preparations from healthy goats and pigs

All animal handling protocols and procedures were carried out as described in Chapter 1. Animal experimentation procedures were approved by the Institutional Animal Care and Use Committee of the Faculty of Veterinary Medicine, Hokkaido University (approval no. 19-0097, 20-0012). Over one year old healthy and non-pregnant Saanen breed goats (*Capra hircus*, total n = 8) were sedated with xylazine (3.0 mg/kg body weight) through an intramuscular or intravascular route. Same aged one mixed breed pigs (*Sus scrofa domestica*, total n = 8) were sedated and anesthetized by a combination of medetomidine hydrochloride (0.04 mg/kg body weight), midazolam (0.2 mg/kg body weight), and ketamine hydrochloride (20 mg/kg body weight). All the animals were deeply anesthetized with injections of pentobarbital sodium (500 mg/kg body weight) and sacrificed by intravenous administration of a saturated potassium chloride solution of at least 0.1 mL/kg body weight via the intravascular route. Method of tissue fixation and tissue sampling were carried out as previously described in Chapter 1.

Vaginal smear observation in goats

To determine the estrus stages, vaginal smears were collected from each goat at 1-day intervals using disposable sterile cotton vaginal swabs wetted with 0.01M PBS. The vulva and perineum were gently wiped with wet cotton pads prior to each examination. The swab was gently inserted into the anterior vagina to a depth of 5 cm. After rolling the swab a few times in the vagina, it was immediately inserted into tubes containing 15 mL 0.9% sodium chloride and centrifuged for 20 min at 1,885 x g (Kubota 8800, Kubota; Tokyo, Japan). The separated upper fraction of the liquid was discarded, and 500 μL of PBS was added for dilution. Ten microliters of the diluted solution were inserted into a hemocytometer counting chamber. The cells encountered in the vaginal smear were categorized as parabasal, intermediate, and superficial cells and their proportions were determined. Vaginal epithelial cells were identified using an inverted phase-contrast microscope (CK30; Olympus Optical, Tokyo, Japan), based on their morphological characteristics. The percentage of vaginal cells was calculated as the number of each cell type divided by the total number of cells counted in four microscopic fields. The same amount of diluted cell suspension was smeared on a glass slide, dried, and stained with Diff-Quik (Sysmex; Hyogo, Japan).

Determination of vaginal pH and temperature in goats

For goats, the vaginal pH level was measured using pH paper (Advantec; Tokyo, Japan) with a 5.8–8.2 indicator. The pH paper was gently inserted into the vagina, 5 cm deep, and soaked in vaginal mucus. The color change of the pH paper was compared with the attached standard color. Vaginal temperature was

measured using a thermometer MC-672L (Omron Healthcare; Kyoto, Japan) with an accuracy of ± 0.05 °C. A thermometer was inserted 5 cm deep into the vagina, and the results were recorded.

Whole-mount observation

Separated genital organs were immersed in Mayer's hematoxylin to visualize LTs. Staining condition and method described in Chapter 1.

Histological analysis

The vaginal vestibule of each animal was divided into more than five sections based on their size. The specimens were routinely dehydrated with ethanol and then embedded in paraffin. Paraffin sections (4–5 μm) stained with HE. The stained sections were analyzed as previously described in Chapter 1. The numbers and proportions of LNs and DLTs were determined after HE stain of the whole section. Above measurement was done on minimum eight sections of each animal.

IHC and immunofluorescence IF

NBF-fixed paraffin blocks were cut, and IHC and IF were performed to calculate the percentage of B cells (CD20), T cells (CD3), macrophages (IBA1), DCs (Langerin), plasma cells (IgA and immunoglobulin G, IgG), and HEV (PNAd). Staining was performed as previously described in Chapter 1. For histoplanimetry, the total area of LNs or DLTs and the positive reaction area for each immune cell marker or the number of $PNAd^+$ HEVs were determined based on measurements conducted on more than eight LNs or DLTs of each examined goat or pig. Subsequently, the positive reaction area or the number of $PNAd^+$ HEVs to the total area was calculated for LNs or DLTs.

SEM

For SEM, approximately 5 x 5 mm of vaginal vestibule tissue containing dark-blue spots in result of hematoxylin whole-mount staining were fixed using a fixing solution containing 2.5% glutaraldehyde and 4% paraformaldehyde in 0.1 M phosphate buffer. After six washes with 0.1 M phosphate buffer, the specimens were post-fixed with 1% OsO4 phosphate buffer (0.1 M) for 1 h at 4 °C. The tissue was then treated with tannic acid for 1.5 h at 4 °C. Subsequently, the specimens were dehydrated and analyzed as previously described in Chapter1.

Statistical analyses

All data are presented as mean ± SE. The Mann-Whitney *U* test was used to compare data between goats

384 and pigs ($P < 0.05$).

Results

GOALTs found in the vaginal vestibule of goats and pigs

According to Chapter 1, the author investigated GOALTs in goat and pig vaginal vestibule as small ruminant animal and non-ruminant animal. Goat (Fig. 2-1A-C) and pig (Fig. 2-1D-F) vaginal vestibule mucosa located between the external urethral orifice and vulva was examined. Whole-mount staining with hematoxylin was performed to visualize the LTs in the examined mucosa based on the aggregation of immune cell nuclei. Hematoxylin$^+$, small, dark-blue spots appeared on the mucosa, indicating LT, which was histologically identified after HE staining (Fig. 2-1C, F). All examined goats and pigs showed abundant hematoxylin$^+$ spots throughout the mucosal surface of the vaginal vestibule area, which were ring-shaped. Morphologically, the author did not observe an obvious difference between goat and pig LT, but the size of the dark blue spots on the mucosal surface seemed to be larger in pigs than in goats.

Histological description of GOALTs in the vaginal vestibule of goats and pigs

Histological observations were performed on the mucosa of the vaginal vestibule (Fig. 2-2). Both goat and pig vaginal vestibule were covered with non-keratinized and stratified squamous epithelium. The basal membrane separated the epithelium and lamina propria, however; in some cases their structure was partly or completely broken by the LTs (Fig. 2-2A-D). LTs were predominantly distributed in the lamina propria, but LTs bordered with lumen were also observed. Similar to cow results in Chapter 1, two different types of LTs were observed in both goats (Fig. 2-2A, C) and pigs (Fig. 2-2B, D) vaginal vestibule; LN- or DLT-type. Briefly, randomly localized LNs were mostly oval shaped and included a bright and centrally localized germinal center surrounded by densely aggregated cells (Fig. 2-2A, B). DLTs showed an undefined shape, and these composing cells were diffusely distributed (Fig. 2-2C, D). In the histometry of the vaginal vestibule mucosa, goat LNs accounted for 39.9% and pig one 25.1%, when as there were goat DLT 60.1%, and pig 74.9%; showing significant differences between LNs and DLTs in two animals (Fig. 2-2E). In the vaginal vestibule section, the author also examined the stratified squamous epithelium thickness, which was significantly thicker in goats than in pigs (Fig. 2-2F).

Immune cells characteristics composing GOALTs in the vaginal vestibule of goats and pigs

Various immune cells were found in goat and pig LNs of GOALT in the vaginal vestibule mucosa, including CD3$^+$ T cells, CD20$^+$ B cells, and IBA1$^+$ macrophages. The CD3$^+$ T cells were distributed throughout the LNs and their germinal center, as well as in the area surrounding the LNs (Fig. 2-3A, B). The percentage of CD3$^+$ T cells in the LN area was not significantly different between the two species (Fig. 2-3C). The CD20$^+$ B cells were densely distributed in the LN, and the percentage in the LN area was

significantly higher in pigs than in goats ($P < 0.05$, Fig. 2-3D-F). IBA1$^+$ macrophages were similarly localized in goats and pigs, being observed in the germinal center and the area surrounding LNs (Fig. 2-3G, H). There was no significant difference between goats and pigs regarding the percentage of IBA1$^+$ macrophages (Fig. 2-3I). Finally, the author found that PNAd$^+$ HEVs formed only around the LNs, and the numbers were not statistically different between the two species (Fig. 2-3J-L).

Goat and pig DLT of GOALT in the vaginal vestibule mucosa had a similar immune cell composition to that of the LN. CD3$^+$ T cells were diffusely found throughout the DLT (Fig. 2-4A, B). In pigs, CD3$^+$ T cells were found near the intraepithelial space (Fig. 2-4B). The percentage of CD3$^+$ T cells in the DLT area was not significantly different between the two species (Fig. 2-4C). CD20$^+$ B cells were distributed thoroughly in DLT (Fig. 2-4d, e), and the percentage in the DLT area was significantly higher in pigs than in goats ($P < 0.05$, Fig. 2-4f). Diffuse IBA1$^+$ macrophages were observed in the DLT (Fig. 2-4G, H), and no significant difference was found between goats and pigs (Fig. 2-4I). Finally, PNAd$^+$ HEVs formed diffusely inside the DLT, and this number was not statistically different between the two species (Fig. 2-4J-L).

Additionally, the author checked whether the percentage of immune cells was affected by the different stages of the estrus cycle in goats (Fig. 2-5). Although the stages of the estrus cycle in the two goats were determined using a visual assessment test (Fig. 2-5A, B), estradiol level in blood serum (Fig. 2-5C), vaginal cytology (Fig. 2-5D-I), vaginal temperature (Fig. 2-5J), vaginal pH (Fig. 2-5K), and vaginal vestibule epithelium thickness (Fig. 2-5L), the percentage of immune cells was not remarkably different between the estrus and diestrus stages (Fig. 2-5M, N).

Immunoglobulin producing cells and antigen presenting cells in the vaginal vestibule of goats and pigs

IgA$^+$ plasma cells were found within goat and pig LNs in small amounts and around the area surrounding the LN without significant differences in their quantified values (Fig. 2-6A-C). The presence of IgA$^+$ plasma cells was also observed diffusely in the DLT of both goats and pigs, without significant differences in their quantified values (Fig. 2-6D-F). IgG$^+$ plasma cells were distributed in the LN and DLT, similar to IgA$^+$ plasma cells, and no significant difference was observed between goats and pigs (Fig. 2-6G-L). Furthermore, IgA$^+$ plasma cells were aggregated to connective tissue papillae near the intraepithelial space in goats, whereas both goats (Fig. 2-6M, N) and pigs (Fig. 2-6O) contained IgA$^+$ plasma cells within the epithelium, resembling plasma cell migration from the lamina propria of the vaginal vestibule to the intraepithelial space.

Additionally, the author examined the localization of Langerin$^+$ cells [136] and DCs in the LN, DLT, and vaginal vestibule epithelium of goats and pigs (Fig. 2-7). No DCs were found in the LNs (Fig. 2-7A, B); however, in the DLT, Langerin$^+$ DCs with round-shaped morphology were observed (Fig. 2-7C, D). Abundant Langerin$^+$ DCs were found in the vaginal vestibule epithelium, whereas in goats, DCs were found in the

intermediate layers of the epithelium (Fig. 2-7E), and in pigs, DCs were found near the basement membrane area (Fig. 2-7F).

Surface structures of GOALTs in the vaginal vestibule of goats and pigs

Fig. 2-8 shows the ultrastructural characteristics of GOALTs on the surface of the vaginal vestibule epithelium in goats and pigs. Hematoxylin^{+} spots were distributed on the vaginal vestibule mucosal surface (Fig. 2-8A, B). The author used SEM to observe the epithelium structure covered the GOALTs and found partly disrupted areas where dark blue spots were formed (Fig. 2-8C, D). Briefly, epithelial cells were flattened and detached (data not shown) around the GOALTs area. The morphology of the GOALTs surface differed from that of a normal vaginal vestibule surface. In the center of the modified GOALTs surface, a hole was observed beneath the epithelium, which contained abundant connective tissue fibers that created a net-like structure, and lymphocytes were attached to the fibers (Fig. 2-8E, F). Finally, all these ultrastructural features are consistent with previously reported SEM data for cow vaginal vestibule tissue in Chapter 1.

Graphical representation of GOALTs in the vaginal vestibule and reproductive organs of goat and pig shown in Figure 2-9.

Discussion

In this Chapter, the author compared the GOALTs of adult, female, non-pregnant goats and pigs in terms of their vaginal vestibule. In Chapter 1, the author characterized GOALTs surrounding the vaginal vestibule mucosa area in a ring shape in cows. This anatomical formation is titled as genital lymphoid ring. In this Chapter, the genital lymphoid ring was also found in both goat and pig vaginal vestibules, and their general morphological structure was consistent with cow data previously described in Chapter 1. Briefly, as summarized in Figure 2-9, the GOALT of vaginal vestibule was anatomically and histologically similar between goats and pigs, being composed of LN and DLTs, including T cells, B cells, macrophages, IgA-producing cells, and HEVs.

Species-related differences in MALT-related structures have been previously reported; palatine tonsils are absent in pigs, but those in ovine species are sequentially formed from the first day of birth [97,132]. Furthermore, mice have uniform-sized follicles, whereas pigs, dogs, and ruminants have distinct and long continuous follicles in their gastrointestinal tracts (GITs) [53]. LTs in the genital organs have also been previously introduced in pigs and goats [75,76,107]. In the vaginal vestibule of goats and pigs, the majority type of GOALT is DLT (73%), but goats showed a comparable appearance rate between LN and DLT. Cows showed a higher percentage of DLT (65%) compared to LN (35%), indicating that the morphology of pig GOALT differed from that of ruminants. Furthermore, both LNs and DLTs of pigs contained a significantly higher percentage of $CD20^+$ B cells than those of goats. In a related report, LNs in the ileal Peyer's patches of sheep were reported to contain approximately 77.8 ± 8.6% B cells and 3.9 ± 4.4% T cells, whereas in pigs the respective percentages were 3.1 ± 7.8% and 6.3 ± 1.3% [108,110], indicating species-related differences. Additionally, in histological sections, pig lymph nodes show inverted localization of the cortex and medulla due to their different localization from other species [110]. These morphological characteristics of lymphocyte arrangements might also affect the structural characteristics of pig MALT. In MALTs, LNs are clearly bordered by surrounding tissues, and their germinal centers initiate activation and proliferation of lymphocytes, differentiation of plasma cells, and production of antibodies [128]. DLTs lack a clear boundary with surrounding tissue, show a formless morphology, localize between antigens, and activate an immune response. Lymphocytes in the LT migrate to regional lymph nodes and support proliferation and differentiation after contact with antigens, and their progenies migrate back to the lamina propria as effective B and T cells. Therefore, histoplanimetrical results would reflect the species-related differences in mucosal immunity, particularly their difference between organs and antigenic exposure status.

The mucosa of the vagina and vaginal vestibule is populated by several APC populations with distinct anti-inflammatory or immunological tolerance properties. Langerhans cells are a specialized DC population found in the epidermis of the skin and stratified squamous epithelium of the eye, vagina, cervix, and mouth

[49,84,109]. VEDCs are major APCs that are important in innate immune defense, as well as in the generation and regulation of the adaptive immune system against pathogens entering the female genital organ [20,52]. In this Chapter, the author showed M cell-like Langerin$^+$ DCs in the epithelium of the vaginal vestibule of both goats and pigs, which was consistent with previous studies on VEDCs in humans and several species of animals [20,49,52,70]. VEDCs can incorporate antigens from the lumen of the genital organ, move to the draining lymph nodes, present them to T cells, and initiate an immune reaction. This pathway of APC migration from the mucosa to the nearest lymph node may represent the inductive arm of the mucosal immune system in the lower portion of the female genital organ [37].

Humoral immune defense is mediated by antibodies produced by highly specialized cells that synthesize and secrete abundant quantities of proteins [30]. Antibody-secreting cells are generally divided into plasmablasts and plasma cells based on their proliferation capacity [81]. In this study, the author found IgA$^+$ cells in the lamina propria, epithelium, DLT, and surrounding LN. Interestingly, IgA$^+$ cells seem to move from the lamina propria to the lumen of the vaginal vestibule through the stratified squamous epithelium in the vaginal vestibule of goats and pigs. In the intestines, secretory IgA-producing cells are scattered in the intestinal lamina propria and aggregate around intestinal crypts [135]. Therefore, similar to alimentary tracts, the vaginal vestibule mucosa also contains IgA-producing cells to effectively defend the mucosal immune system. Additionally, this Chapter showed that the close-to-lumen characteristic is important for the ability of secretory IgA to form protective immunoglobulin barriers in the genital organ, which is important because when protective immunoglobulin barriers are destroyed, the genital organ is more vulnerable to pathogens.

Morphological differences in LTs between goats and pigs might be related to their estrus cycle variability or estrus stage at the time of euthanasia. However, the author could not determine age-related differences in the morphological changes of GOALT in goats. Goats are seasonally polyestrous, short-day breeders with several estrous cycles during the fall or winter, and pigs are polyestrous and can heat more than once throughout the year. Sex hormones precisely regulate most components of the innate and adaptive immune systems in the genital organ throughout the estrous cycle. Estradiol inhibits antigen presentation by vaginal cells and those vaginal cells, which in turn influences antigen presentation, as well as B and T cell proliferation [127]. Therefore, further studies using season-and estrus cycle-matched samples are needed, and female reproductive stage- and age-related changes of GOALT in each animal species would be important for the understanding of mucosal immunity of ductal genital organs.

Summary

In the Chapter 1, the author elucidated GOALT in the vaginal vestibule of adult, non-pregnant cows which constituted the genital lymphoid ring according to Waldeyer's ring. In this Chapter 2, the author investigated the gross anatomical and histological features of GOALTs in the vaginal vestibule of healthy, non-pregnant, adult goats and pigs. Their vaginal vestibules were composed of stratified squamous, non-keratinized epithelium, and various-sized dark-blue hematoxylin^{+} spots were observed in whole-mount specimens, which were diffusely distributed throughout the mucosal surfaces. These spots were histologically identified as LTs and consisted of LNs or DLTs. Both LNs and DLTs contained B cells, T cells, macrophages, DCs, plasma cells, and HEVs. Only the numbers of B cells were significantly higher in both the LNs and DLTs of pigs compared with goats. Furthermore, the surface of the vaginal vestibule epithelium covering the LTs was partially disrupted with a large intercellular space exposing abundant connective tissue fibers with numerous lymphocytes. Thus, the author clearly demonstrated GOALTs in the vaginal vestibule which would be common local immunological barriers in both examined animals.

Figures

Table 2-1. Antibodies

	Source	Detection (Application)	Dilution	Blocking	Antigen retrieval	Secondary antibody
Rabbit anti-IgA	Bethyl (Montgomery, Alabama, USA)	Plasma cell	1:100	10% NGS (SABPO(R) Kit, Nichirei)	20mM TB (pH 9.0) 115C	Goat anti-rabbit IgG antibody (SABPO(R) Kit, Nichirei)
Rabbit anti-IgG	Bethyl (Montgomery, Alabama, USA)	Plasma cell	1:100	10% NGS (SABPO(R) Kit, Nichirei)	10mM CB (pH 6.0) 115°C, 15 min	Goat anti-rabbit IgG antibody (SABPO kit, Nichirei)
Rabbit anti-langerin	Prointech (Rosemont, Illinois, USA)	Dendritic cell	1: 50	10% NGS (SABPO(R) Kit, Nichirei)	10mM CB (pH 6.0) 115°C, 15 min	Goat anti-rabbit IgG antibody (SABPO kit, Nichirei)

CB: citrate buffer. TB: tris buffer. NGS: normal goat serum

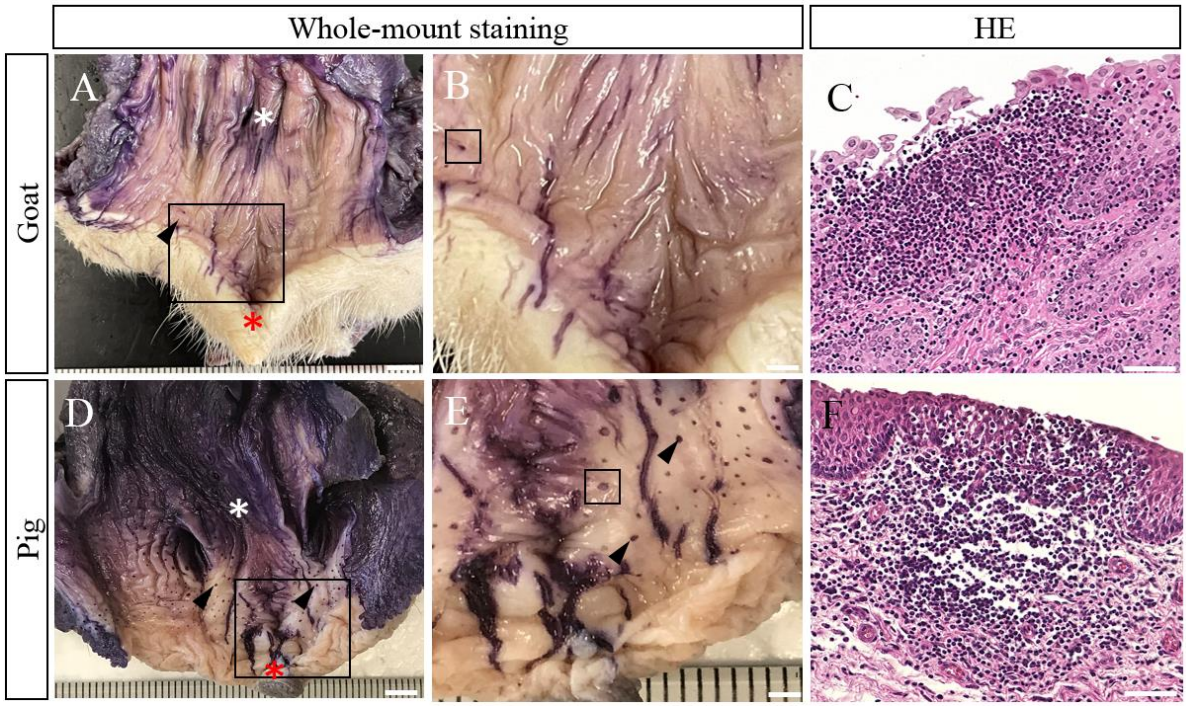

Figure 2-1. Scattered GOALTs distributed throughout the mucosa of the vaginal vestibule and EPGOs of goat and pig

(A, B) Goat (B) and pig (B) vaginal vestibule and EPGOs after the whole-mount staining with hematoxylin, showing navy-blue spots. White asterisks showed external urethral orifice. Red asterisks showed the clitorisBlack arrowheads indicated navy-blue spots. Scale bars = 5 mm. (C, D) Enlarged images of the vaginal vestibule mucosa squared areas in panels a, b. bars = 2 mm. (E, F) Histology of navy-blue spot squared areas in panel C, D. HE staining. Scale bar = 50 μm.

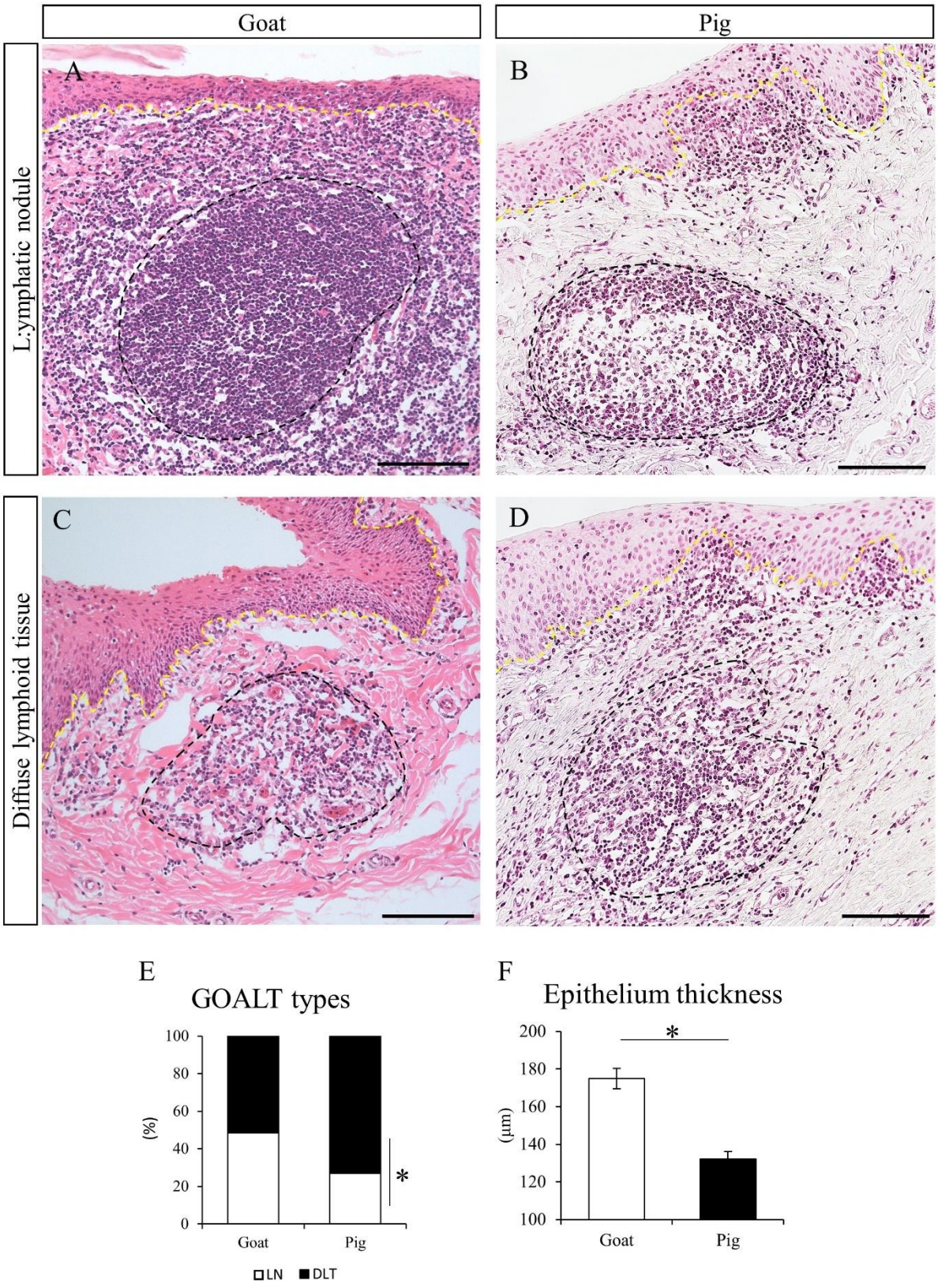

Figure 2-2. Histology of GOALTs found in the goat and pig vaginal vestibule

(A) Goat LN localizes in the LP while partially disrupting the structure of the epithelium of vaginal vestibule. (B) Pig LN localizes in the LP of vaginal vestibule, entirely neighbored with connective tissues. (C, D) Goat

and pig DLT localizes in LP of vaginal vestibule not disrupting epithelium. Diffusely distributed lymphocytes are shown between DLT and epithelium. Black dotted line shows the approximate boundary of GOALTs. Yellow dotted line indicates basement membrane. HE staining. Scale bars = 100 μm. (E) Appearance of the percentage of LNs and DLTs in the examined GOALTs of the vaginal vestibule. $n \geq 5$. (F) Epithelium thickness of vaginal vestibule. Values = mean ± SE. $n \geq 5$. Significant difference between the goat and pig was indicated by ∗, $P < 0.05$; Mann–Whitney *U* test.

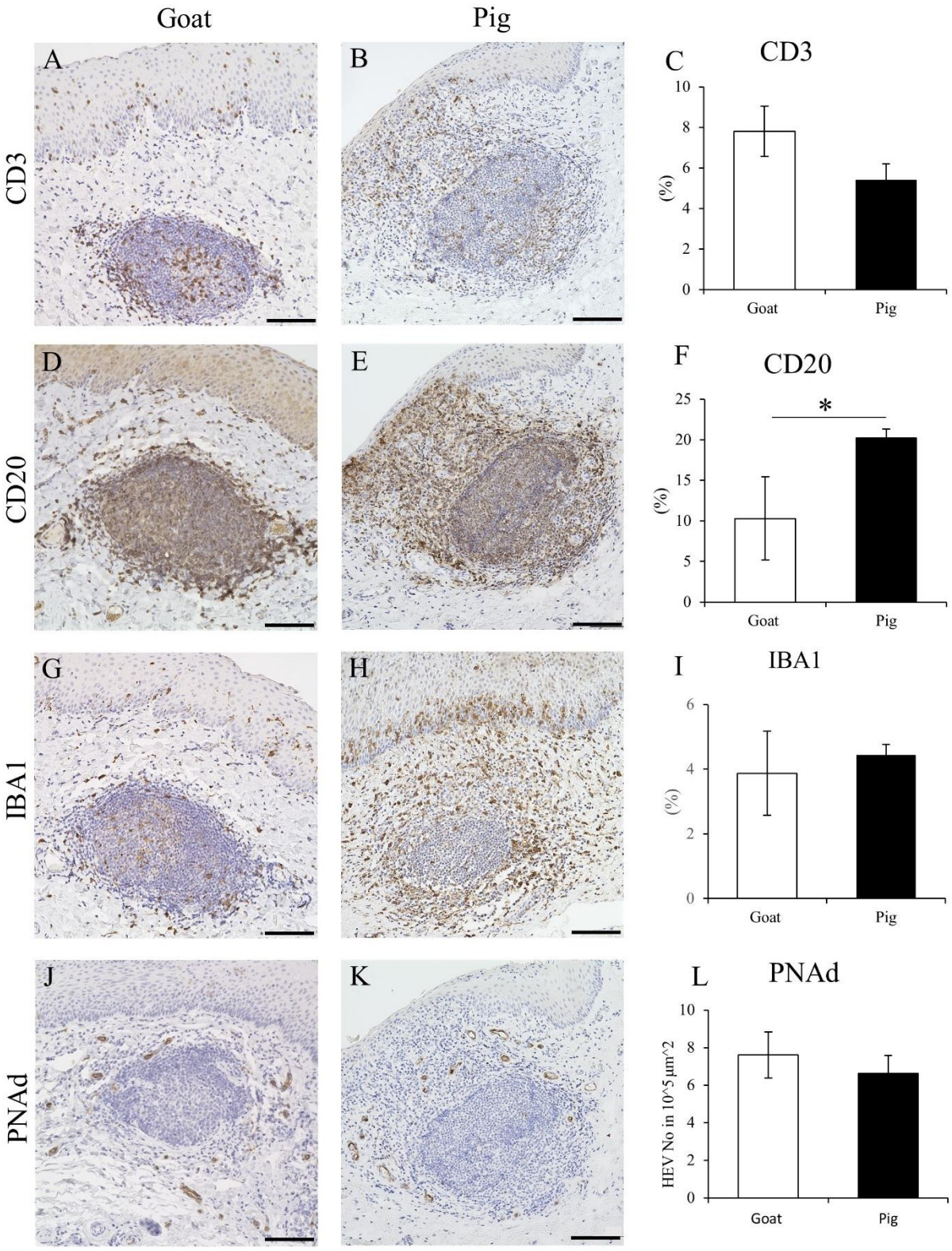

Figure 2-3. Immune cell characteristics composing LN in goat and pig vaginal vestibule

(A, B) CD3 for T cells of goat and pig. (C) Percentage of $CD3^+$ T cells localizing in the LN. Values = mean ± SE. n ≥ 4. (D, E) CD20 for B cells of goat and pig. (F) Percentage of $CD20^+$ B cells localizing in the LN.

Values = mean ± SE. n ≥ 4. Significant difference between the goats and pigs was indicated by ∗, $P < 0.05$; Mann–Whitney *U* test. (G, H) IBA1 for macrophages of goat and pig. (I) Percentage of $IBA1^+$ macrophages occupying the LN. Values = mean ± SE. n ≥ 4. (J, K) PNAd for HEVs of goat and pig. (L) Number of $PNAd^+$ HEVs in 10^5 μm^2 in LN. Values = mean ± SE. n ≥ 4. Scale bars = 100 μm.

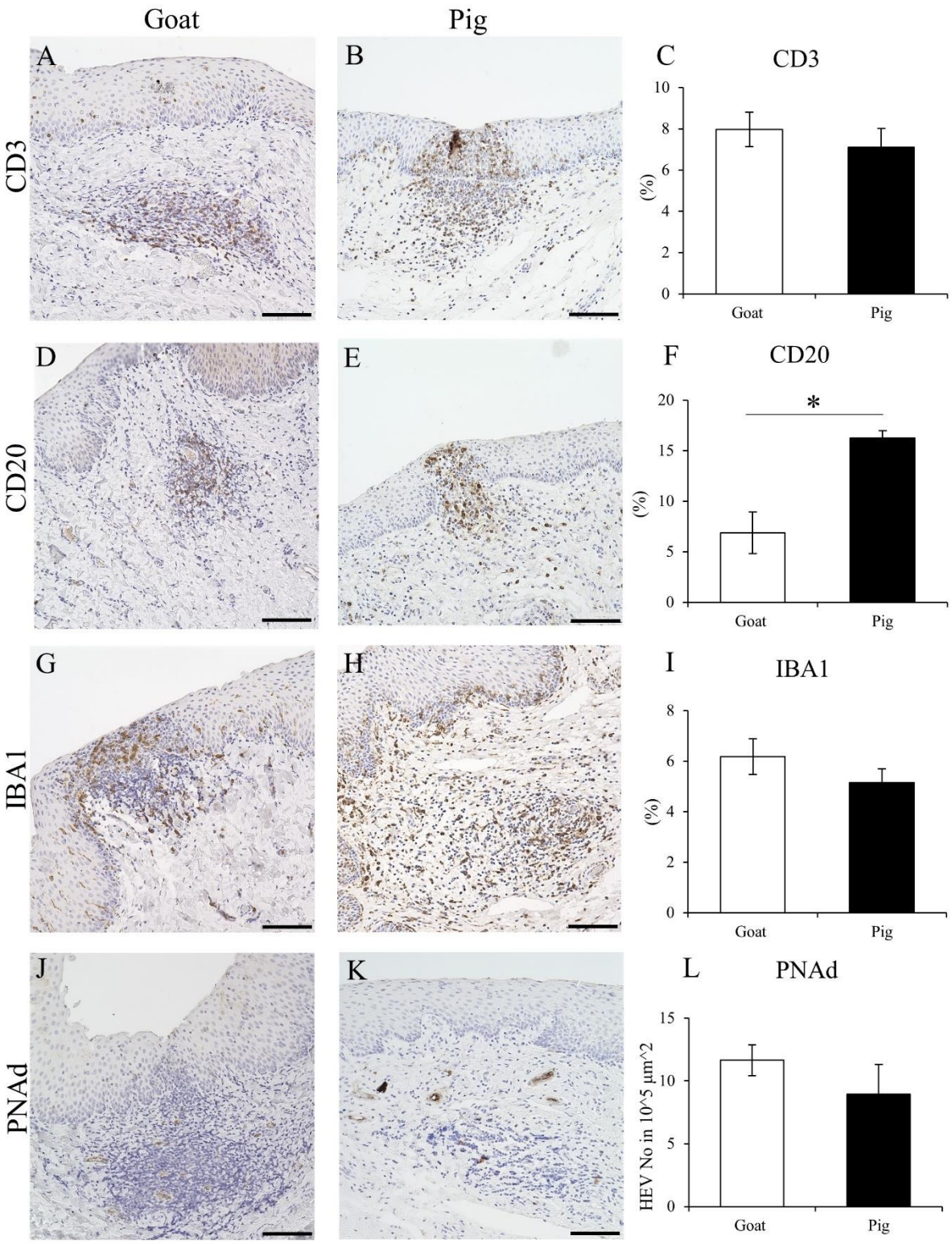

Figure 2-4. Immune cell characteristics composing LN in goat and pig vaginal vestibule

(A, B) CD3 for T cells of goat and pig. (C) Percentage of $CD3^+$ T cells localizing in the LN. Values = mean ± SE. n ≥ 4. (D, E) CD20 for B cells of goat and pig. (F) Percentage of $CD20^+$ B cells localizing in the LN. Values = mean ± SE. n ≥ 4. Significant difference between the goats and pigs was indicated by ∗, $P <$

0.05; Mann–Whitney *U* test. (G, H) IBA1 for macrophages of goat and pig. (I) Percentage of $IBA1^+$ macrophages occupying the LN. Values = mean ± SE. n ≥ 4. (J, K) PNAd for HEVs of goat and pig. (L) Number of $PNAd^+$ HEVs in 10^5 μm2 in LN. Values = mean ± SE. n ≥ 4. Scale bars = 100 μm.

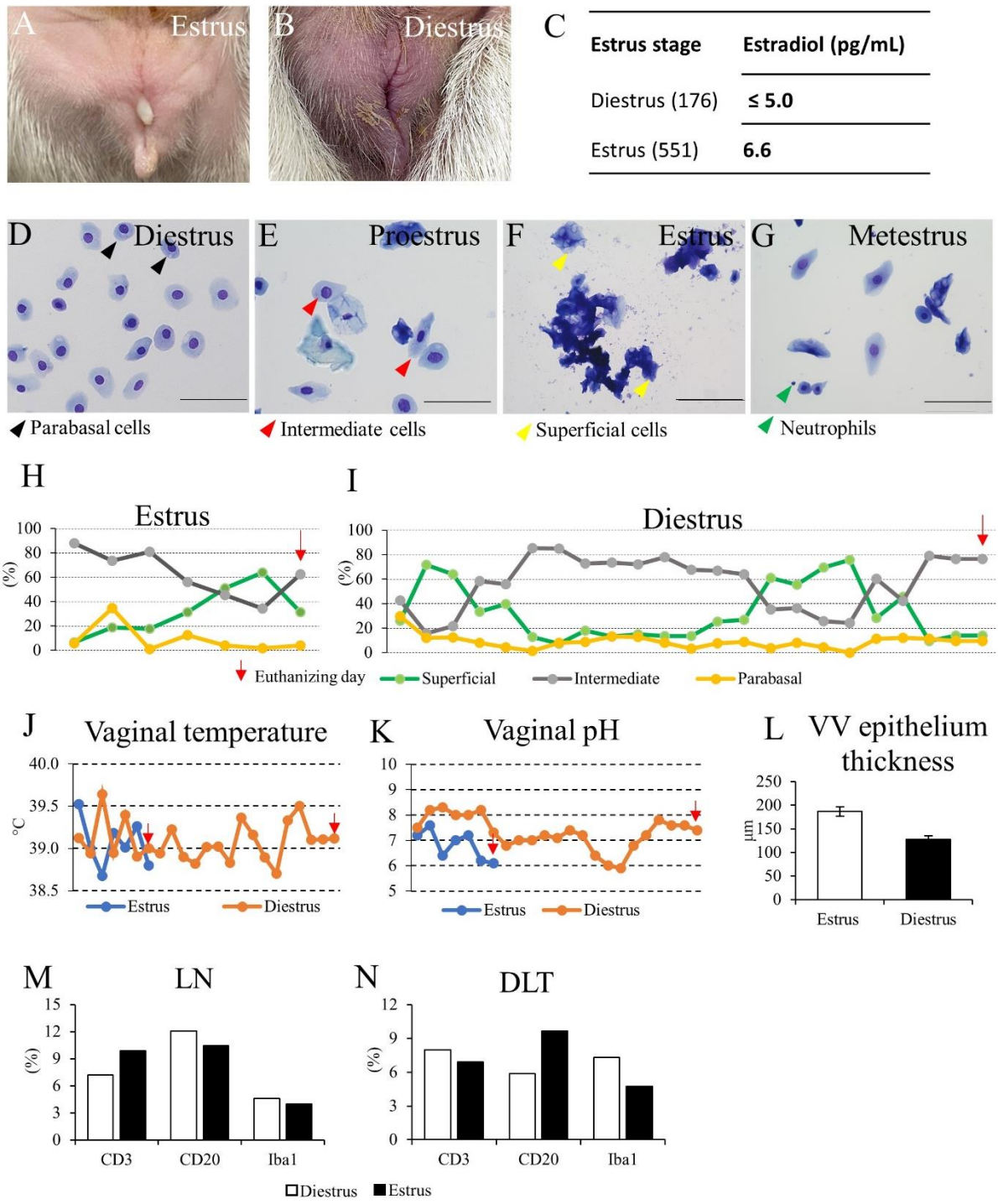

Figure 2-5. Immune cell composition in different stages of the estrus cycle

(A) Vulvar condition during the estrus stage, showing the discharge of sticky cloudy mucous, swelling, and redness. (B) Vulva condition during the diestrus stage. (C) Estradiol level in the blood serum of goats in different stages of the estrus cycle. (D, E, F, G) Vaginal cytology in diestrus, proestrus, estrus, and metestrus stages. Scale bars = 50 μm. (H, I) Daily percentage of exfoliative vaginal cells of goats expected as estrus (H) and diestrus (I) stages. (J) Daily vaginal temperature of goats. (K) Daily vaginal pH of goats. (L)

Epithelium thickness of vaginal vestibule in goats expected as estrus and diestrus stages. Values = mean ± SE. $n = 1$. (M) Percentage of immune cells occupying the LN during the estrus and diestrus stages. $n = 1$ in each stage. (N) Percentage of immune cells occupying the DLT during the estrus and diestrus stages. $n = 1$ in each stage.

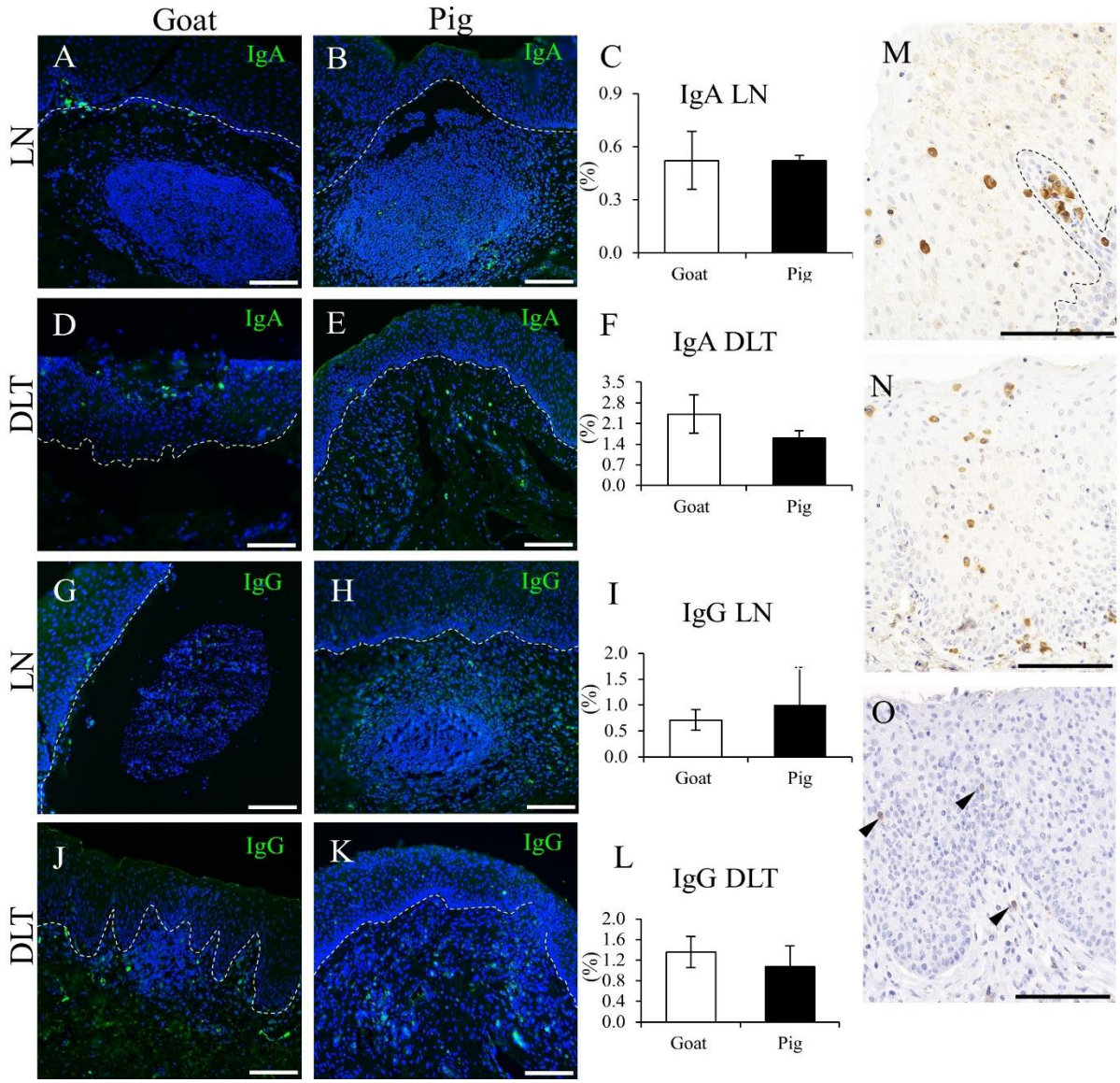

Figure 2-6. IgA$^+$, IgG$^+$ plasma cell characteristics in GOALT of goat and pig

(A, B) IgA$^+$ plasma cells in the LN of goat and pig. (C) Percentage of IgA$^+$ plasma cells localized the LN. Values = mean ± SE. n ≥ 4. (D, E) IgA$^+$ plasma cells in the DLT of goat and pig. (F) Percentage of IgA$^+$ plasma cells localized the DLT. Values = mean ± SE. n ≥ 4. (G, H) IgG$^+$ plasma cells in the LN of goat and pig. (I) Percentage of IgG$^+$ plasma cells localized the LN. Values = mean ± SE. n ≥ 4. (J, K) IgG$^+$ plasma cells in the DLT of goat and pig. (L) Percentage of IgG$^+$ plasma cells localized the DLT. (M, N) Goat IgA plasma cells in the epithelium of vaginal vestibule. (O) Pig IgA plasma cells in the epithelium of vaginal vestibule. Scale bars = 100 μm. Values = mean ± SE. n ≥ 4. Dotted lines indicated the approximate boundary between lamina propria and epithelium. Arrowheads showed IHC positive reaction. Scale bars = 100 μm.

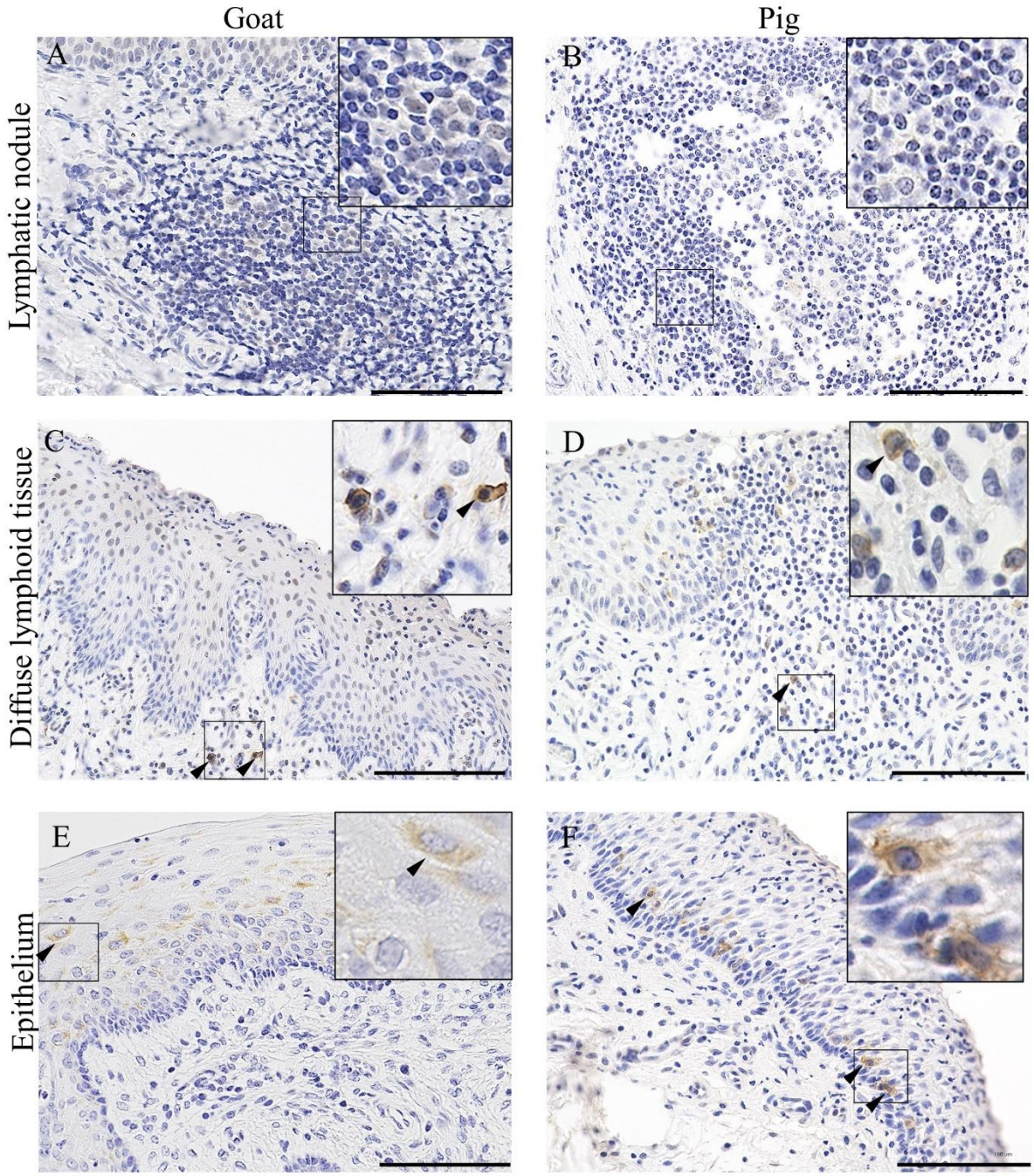

Figure 2-7. Dendritic cells characteristic in GOALT and epithelium of vaginal vestibule of goat and pig

(A, B) Langerin for DCs of LN of goat and pig. (C, D) Langerin for DCs of DLT of goat and pig. (E, F) Langerin for DCs of the epithelium of goat and pig. Black arrowheads show positive reaction for IHC. Scale bars = 100 μm.

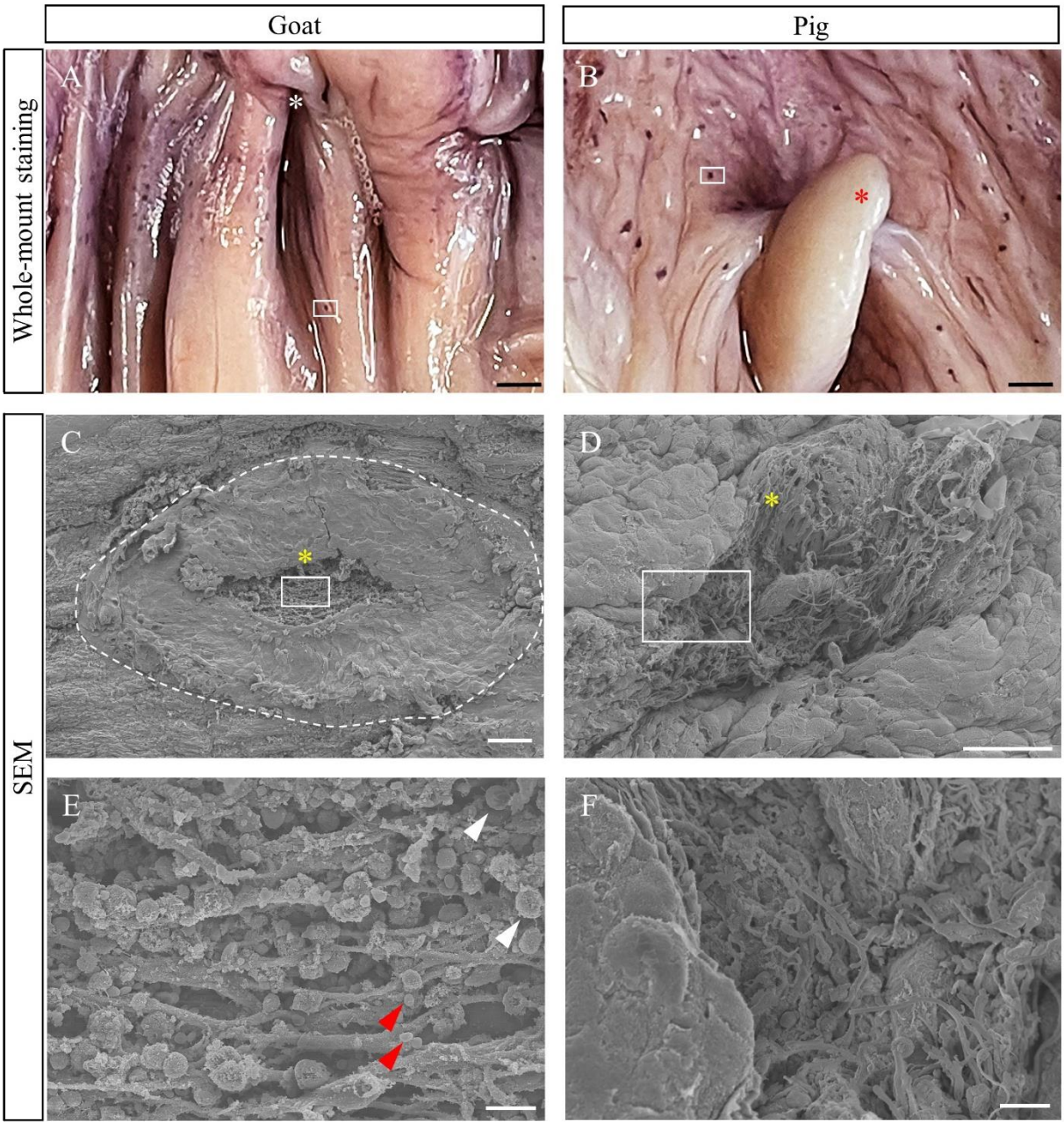

Figure 2-8. Ultrastructural characteristics of epithelium covering GOALT of the goat and pig

Goat (A) and pig (B) vaginal vestibule mucosa stained in whole-mount with hematoxylin. GOALTs were observed as hematoxylin-positive blue spots. White asterisk represents external urethral orifice. Red asterisk represents clitoris. Scale bars = 2 mm. Goat (C) and pig (D) vaginal vestibule mucosa were examined using SEM. The same areas as in panels A and B were examined. Dotted lines indicate GOALTs appeared on the surface of the epithelium. Yellow asterisks represent GOALTs opening into the vaginal vestibule lumen. Scale bars = 100, 50 μm. (E, F) Magnified areas squared in panels C and D. White arrowheads indicate infiltration of lymphocytes from the GOALT to the lumen of the vaginal vestibule. Red arrowheads indicate erythrocyte. Scale bars = 10 μm.

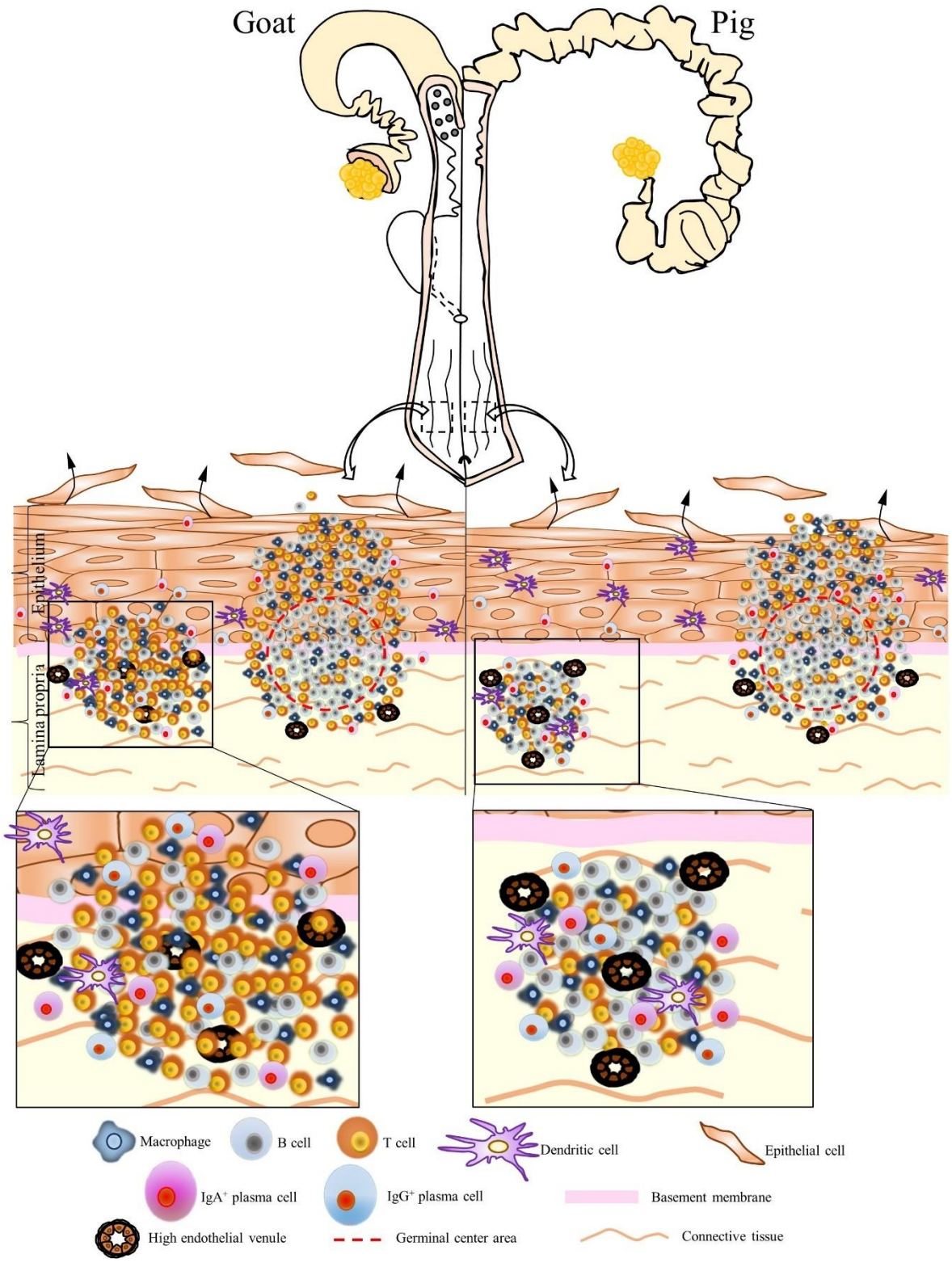

Figure 2-9. Graphical representation of GOALTs in the vaginal vestibule and reproductive organs of goat and pig

Vaginal vestibule is one of the compartments of the EPGO containing GOALTs. GOALTs consist of LNs and DLTs which localize in different parts of LP of the vaginal vestibule. LN and DLT comprised of B cells, T

cells, macrophages, and APCs. B cells are predominantly found in both LN and DLT of pigs. Germinal center mainly found in the center of the LN. HEVs observed among LT and neighboring connective tissues in the LP. Basically, the epithelium structure covered GOALTs is partly or thoroughly disrupted by the invasion of immune cells composing LNs and DLTs.

Chapter 3

Morphology and MALT structures in the large intestine of cotton rats

Introduction

In first two Chapters, the author showed morphology of GOALTs in the vaginal vestibule of ruminants (cow and goat) and non-ruminant animals (pig) and mucosal epithelium covering GOALTs. All examined animals showed two types of LTs; LN and DLT which consisted of B cells, T cells, macrophages, DCs, plasma cells, and HEVs. Furthermore, the epithelium structure covering GOALT differed from other parts in vaginal vestibule mucosa, and that was partially disrupted. Considerable differences were not observed in GOALT and epithelium morphology among examined species, suggesting GOALTs are normal common structures protecting the female lower ductal organs in cows, goats, and pigs immunologically. Therefore, this Chapter also focused focus on the MALTs in the lower ductal organs in other species, especially focusing on rodents which are globally used as experimental animals.

As previously described in Chapter 1 and 2, the vaginal vestibule is terminal part of the female genital organs, extends from the external urethral opening to the external vulva, combining urinary and reproductive tracts in cows, goats, and pigs. Vaginal vestibule lies mainly behind the ischial arch, slopes ventrally vulval opening [27,92]. In rodents, especially, in female mice, the external urethral orifice does not open into the vagina, meaning that vaginal vestibule would not be developed in these animals, because vaginal vestibule is defined as a part between the external urethral orifice and vulva. Therefore, the vagina of female mice ends in an area delimited by the labia of the vulva, which would be considered as a rudiment of the vaginal vestibule [111]. Thus, vaginal morphology of rodents was obviously different from cows, goats, and pigs, which studied in the previous Chapters.

Cotton rat is one of the valuable experimental rodent animals. Recent studies clarified several unique morphological phenotypes in cotton rats, such as the existence of pharyngeal pouch remnant, visceral fat tissue inflammation, abnormal adipose tissue accumulation in the pancreas without obesity, development of chronic kidney disease, and female genital organ-related disease such as a pyometra [50,51,89,90]. *Sigmodon hispidus* is most commonly used as an experimental animal among the seven species of cotton rats [31]. The first research of the use of cotton rats as laboratory animals began from 1939 when it was established that poliovirus induced paralysis in cotton rat [2]. It has since been shown that cotton rats can be infected with a variety of human viruses, bacteria, and parasitic pathogens: human immunodeficiency virus [113], herpes simplex virus type 1 [72], herpes simplex virus type 2 [133], adenovirus [102], measles virus[129], respiratory syncytial virus [86], human metapneumovirus [39,120,130], parainfluenza virus [87], influenza A virus [99], *Helicobacter pylori* [78], *Staphylococcus aureus* [125], *Mycobacterium tuberculosis* [29], *Borrelia burgdorferi* [98], *Francisella tularensis* [77], and *Leishmania donovani* [4]. The excessive susceptibility to efficient infection is probably related to similarities among cotton rats and humans of their antipathogen response, which completely differs from mice [83]. The secondary advantage of the cotton rat is its properly described genetics

and growing pool of reagents, for that reason offering a laboratory animal model for measles virus research [94], however; their characteristics of immune system, including MALT structure in lower ductal organs, have not been clarified yet.

Therefore, this Chapter aimed to identify morphology of MALT located in the lower ductal organs of cotton rat and to discuss its physiological function and pathogenesis. As a result, cotton rats did not possess vaginal vestibule same to the other rodents, and vaginal structure differed from examined farm animals. No LT was found in the vagina of cotton rat, but the author alternatively found and elucidated three different types of MALTs in the large intestine as well as sex-related differences in the ascending colon morphology in cotton rats.

Materials and methods

Animal and sample preparation

Animal experiments were performed according to the guidelines of the Hokkaido Institute of Public Health (Sapporo, Japan; Approval No.: K27-03). Male and female cotton rats (1–12 months old; HIS/Hiph strain) were maintained under conventional conditions at the Hokkaido Institute of Public Health and continuously inbred. A previous study showed four distinct life stages in cotton rats: 1–75 days; juveniles, 76–200 days; young adults, 201–300 days; adults, and 300 days onward; old adults [31,58]. In this Chapter, for large intestinal study, cotton rats (n = 65) were divided into six groups based on age and sex: young (1–3 months old) males (n = 21) and females (n = 12), adult (4–6 months old) males (n = 11) and females (n = 8), and old (10–12 months old) males (n = 6) and females (n = 7).

The author compared a part of the large intestine morphology among cotton rats, mice (male, C57BL/6N, 2 months old, n = 4), and hamsters (male, SLC: Syrian, 6 months old, n = 4). The mice and hamsters were purchased from Japan SLC (Hamamatsu, Japan). These animal experiments were approved by the Institutional Animal Care and Use Committee of the Graduate School of Veterinary Medicine, Hokkaido University (approval numbers 18-0052 and 20-0012). Investigators adhered to the Guide for the Care and Use of Laboratory Animals of Hokkaido University, Faculty of Veterinary Medicine.

Cotton rats were placed under deep anesthesia using isoflurane and euthanized by cutting the abdominal aorta. Other animals were euthanized using CO_2 inhalation. The whole organs of cotton rats, mice (large intestine and female reproductive organ) and hamsters (large intestine) were fixed using 10% NBF or Bouin's solution, and then the gastrointestinal tract (GIT) and genital organs were collected. Body weight was measured. The position of the internal organs in these specimens were photographed and recorded before removing the GITs.

Next, after fixation, cotton rats (6 months, n = 4) and mice (2 months, n = 4) EPGO; clitoris and vagina were separated from the obtained genital organs.

Morphological analyses

The lengths of the cecum and ascending colon (spiral loop like flexure, SLLF; horseshoe-like flexure, HSLF) of the large intestine were measured on the antimesenteric border using a pliable, non-stretchable cord. The intestinal walls were cut open longitudinally along opposite sides of the mesenteric border and gently rinsed out. The length of the single longitudinal mucosal fold (SLMF) found in the large intestine was measured using a pliable, non-stretchable cord. The diameter of the LN and height of the SLMF were measured by using an liquid crystal displayed digital caliper having an accuracy of 0.001 mm, (AD-5763-150; A&D Company, Tokyo, Japan) then LN area was calculated. The number of LNs found in the cecum

and ascending colon were identified based on their gross anatomy. Photographs were taken as previously described in Chapter 1.

Histological analysis

To evaluate the histology of the large intestine and EPGO each part of the large intestine was dehydrated and embedded in paraffin. Then, 3-μm paraffin sections were prepared and stained with HE. Histological digital images were captured as previously described in Chapter 1.

Statistical analyses

Results are expressed as mean ± SE. The Mann-Whitney *U* test was used to compare the data between male and female cotton rats ($P < 0.05$). The Kruskal-Wallis test was used to compare data between the age groups, and multiple comparisons were performed using Scheffé's method when a significant difference was noted ($P < 0.05$).

Result

Gross anatomical structure of the EPGO of rodents

The author evaluated EPGO of cotton rat and mouse to confirm existence of GOALT. As mentioned in previous Chapters, vaginal vestibule localizes within the canal of genital organ, elongated from the external urethral opening until the ventral commissure of the labia; however vaginal vestibule was absent in mice and cotton rats. Three openings were found on the exterior, caudal part of the body of examined rodents; anus, vaginal opening, and external urethral orifice (Fig. 3-1A-D). Mouse and cotton rat vagina was ventrally flattened, and its mucosa lined with cornified stratified squamous epithelium (Fig. 3-1B, D). Diffusely distributed immune cells were found in under the epithelium; however, LT or immune cells aggregation was not found. Principally, vaginal morphology of cotton rats was obviously different from cow, goat, and pig which studied in previous Chapters. For that reason, the author studied MALTs in large intestine because large intestine and vaginal vestibule are both related to the lower ductal organs.

Gross anatomical features of the large intestine in cotton rats

Firstly, the author characterized the morphology of large intestine in cotton rats and compared them between male and female. Figure 3-2A shows the running pattern of the large intestine of adult male cotton rats (six months old) from the ventral view. The ileum was connected to the large intestine via the ileal orifice, and the left and right sides of the large intestine from the ileal opening were the cecum and ascending colon, respectively (Fig. 3-2A). The cecal base was mostly located in the middle of the central part of the abdomen toward the left half, and its flexure patterns differed among individual animals. Generally, the well-developed, sacculated, long cecum began by twisting counterclockwise and showed various pattern shapes such as semilunar, sigmoidal, curved, comma, or round. It then became localized to the caudal part of the abdominal cavity and finished with a spacious apex. A vermiform appendix was not observed at the end of the cecum and its wall was thinner (data not shown) compared to other parts of the large intestine.

Opposite the ileal opening, the beginning of the ascending colon showed a large diameter, similar to the cecum, and ran to the right half of the abdomen. It then suddenly decreased in diameter just before running to the cranial side (Fig. 3-2A). The subsequent ascending colon showed unique and complex flexures. Briefly, on the right half of the abdomen, several spiral loops were observed, which were tightly connected to each other by connective tissue and mesentery (Fig. 3-2A). These SLLFs began on the right caudoventral side of the abdomen (just after the ascending colon decreased in diameter) and ran to the caudo-dorsal side, making double or triple loops. Then, the ascending colon ran slightly to the caudal ventral side, and diagonally in the cranial direction. Subsequently, the ascending colon continued in to a dorsal-lying HSLF toward the right half of the abdomen by running in the cranial, caudal, and again cranial directions. At the right dorsal cranial

side of the abdomen, the HSLF was connected to the right colic flexure. A relatively short transverse colon then crossed cranial dorsal to the root of the mesentery, connected to the left colic flexure, and continued caudally to the descending colon, which has a higher fat content than the jejunum. By entering the pelvis, the descending colon became the rectum (Fig. 3-2A). The running pattern of the large intestine found in male cotton rats is summarized in Figure 3-2B.

The morphology of the large intestine in female cotton rats was similar to that in males (Fig. 3-2C); however, the number of SLLFs was significantly higher in females than in males. The large intestine of male cotton rats mostly contained two loops; however, in female rats, there were three. The running pattern of the large intestine in female cotton rats is summarized in Figure 3-2D.

For the large intestine of the other rodents, the SLLF was identified in hamsters and found to be similar to that in cotton rats, but not in mice. The HSLF was identified in both mice and hamsters; however, their lengths were significantly shorter and longer, respectively, than those of the cotton rats, and the latter showed a quadruple pattern in the HSLF (Fig. 3-3A–D). Hamsters and mice did not show sex differences in large intestine morphology (data not shown).

Morphometry of the cecum and ascending colon in cotton rats

The author compared the body weight and cecum, SLLF, and HSLF lengths between sexes and among the young (1–3 months old), adult (4–6 months old), and old (10–12 months old) groups (Fig. 3-4). Body weight was significantly increased from the adult period onward in both sexes, and the body weight of males was significantly higher than that of females in the adult and old groups (Fig. 3-4A). The length of the measured large intestine was not related to body weight. For the cecum lengths, there were no significant differences among the groups for both sexes; however, the female ceca were longer than those of the males, and a significant sex-related difference was observed in the adult groups (Fig. 3-4B). In contrast, the SLLF length differed between the sexes and groups (Fig. 3-4C). The SLLF was longer in the young group than in the other groups, and significant differences were observed between the young and adult male groups. The lengths of the SLLF were significantly longer in female rats than in male rats in the adult and old groups without any age-related significant differences. The HSLF length was the highest in the old group for both sexes, and males showed significant differences between the old group and other groups in HSLF length. The adult group had significantly longer HSLFs in females than in males (Fig. 3-4D). Figure 3-4E shows the total ascending colon length. There were no age-related ascending colon differences in males; however, females had significantly longer ascending colon lengths in the adult and old groups compared to those in the young group. Additionally, the adult group had a significantly longer ascending colon length in females than in males.

The author calculated the length of the small intestine and the large intestine ratio in mice, cotton rats, and hamsters (Fig. 3-5A–D). The small intestine and large intestine ratio of the cotton rats were significantly higher than those of hamsters, and significantly lower than those of mice (Fig. 3-5D).

Detailed morphology of the SLLF in cotton rats

Next, the author focused on the morphology of the SLLF, which had a curved, loop-like structure. Figure 3-6 show the representative adult (six months old) SLLF of both sexes from the ventral and dorsal aspects. The males and females usually had two and three flexures, respectively, and the SLLF of the females was longer and more complicated than that of males (Fig. 3-6A-H). Figure 3-6I summarizes the number of flexures in the SLLF of both sexes. Almost all males had two flexures (76%–83%), whereas the adult and old female groups had three flexures (88% and 100%, respectively), with only some of the young female group having two flexures (33%). From the comparison of the average number of flexures in the SLLF, females showed significantly higher values than males in all examined groups (Fig. 3-6J).

Inner features of the ascending colon in cotton rats

Figure 3-7A shows the inner features from the cecum to the ascending colon in adult males (four months old). The SLMF originated from the ileal papilla to the beginning of the SLLF and was located along the mesenteric border (Fig. 3-7A and B). The length of the SLMF is shown in Figure 3-7C: it significantly increased with age in both sexes, with females having a significantly longer SLMF than males in the adult group. The author examined the histology of the ascending colon with SLMF by dividing it into three parts (Fig. 3-7D–F). The SLMF was lined with the large intestine epithelium and the number of goblet cells increased from the beginning of the SLMF to the SLLF. Some areas of the SLMF possessed several LNs in their lamina propria (Fig. 3-7D and F). Subsequently, the SLMF height was measured in three different parts of the ascending colon; its height gradually diminished toward the distal part of the ascending colon (Figure 3-7D–F) in both sexes, and all groups had a decreased luminal diameter of ascending colon. However, there were no sex- or age-related differences.

Additionally, the author confirmed the absence of the SLMF in hamsters (cotton rats and hamsters belong to the same family: *Cricetidae)* and mice (Fig. 3-8). Hamsters and mice had a transverse mucosal fold (semilunar shaped) that began near the cecal side of the ileal opening and continued up to the beginning of the ascending colon, which partly separated the cecum and ascending colon while cotton rats having longitudinal fold (Fig. 3-8A–F). Lastly, the author established the appearance of the SLMF in neonatal (0 days old), 4-day, and two months-old cotton rats respectively (Fig. 3-8G–I).

LTs localized in the large intestine of cotton rats

Finally, the author characterized the LTs of the large intestine (Fig. 3-9) and found three types of LTs classified by their size and shape (Fig. 3-9A). First, a large protuberant LT was located near the apex of the cecum (Fig. 3-9A and B; large-type). Second, small protuberant LTs were found from the cecum to the beginning of the HSLF (Fig. 3-9A and B; small-type). Third, thin, flat LTs were observed in the HSLF and transverse colon (Fig. 3-9A and C; flat-type).

Histologically, large-type LTs showed aggregation with germinal centers in the lamina propria to the submucosa at the apex of the cecum (Fig. 3-9D). Small-type LTs were found in the lamina propria from the cecum to the beginning of the HSLF with a germinal center, mainly at the top of the beginning and base of the end part of the longitudinal fold (Fig. 3-9E–G). Flat-type LTs were observed in the lamina propria of the HSLF and transverse colon without a germinal center (Fig. 3-9H and I). Thus, all types of LTs seemed to be classified as LNs according to the presence of germinal center and immune cell localizations which are not diffusely distributed.

Figure 3-9J–M shows the results of the morphometric analysis of the number and size of LNs in the large intestine, including the cecum, SLLF, and HSLF, and their total data. For the LN number, female rats showed a significantly higher number in adults than in old groups in the cecum, and the total number was significantly higher in females than in male adult rats (Fig. 3-9J-M). Regarding the ratio of LN number to large intestine unit length, female rats had significantly higher values in the old group than in the adult group in the cecum, indicating a higher density of cecum LNs (Fig. 3-9N-Q). For this parameter, there were no significant sex- or age-related differences. For the LN area or the ratio of LN area to large intestine unit length, there were no significant age-related differences in each part (Fig. 3-9R-U); however, females had significantly lower values than males in the total values of the ratio of LN area to large intestine unit length (Fig. 3-9R-U).

Discussion

Cow, goat, pig GOALTs in the vaginal vestibules were morphologically evaluated in Chapter 1 and 2. The author also tried to elucidate GOALTs in EPGO of experimental rodents; however vaginal vestibule area was not developed in examined rodents. Principal experimental rodents such as rats [42], mice [111] , and hamsters [105] do not possess vaginal vestibule, and their external urethral orifice directly opens to the outside locating ventrally to the anal and vaginal openings. Additionally, any LTs were not developed in the vagina of examined cotton rats and mice. Therefore, MALT in the large intestine, localization beside the genital organs, was evaluated for the reason, large intestine and vaginal vestibule are both related to the lower ductal organs.

Firstly, the author clarified the morphological features of the large intestine in cotton rats. Sex differences were found in the ascending colon, and the presence of the SLLF and HSLF was unique to cotton rats compared to other mammals and contributed to increasing the total length of the large intestine. Similar SLLF and HSLF structures were observed in hamsters but not in mice (Fig. 3-3). Similar to other mammals, rodent feeding behavior, digestive tract morphology, and body weight are closely associated [91]. Laboratory mice originate from the wild *Mus musculus* and are usually omnivorous animals. Syrian hamsters, *Mesocricetus auratus*, are also omnivorous rodents, originating from northwest Syria, especially from dry and stony areas. Their natural diet mainly includes grains, and occasionally insects, fruit, and green plants [82]. The cotton rat is a member of the Cricetidae family, which includes hamsters. These animals are mainly distributed in the southern United States, Mexico, Central America, Columbia, and Venezuela, in areas that are commonly surrounded by grassy, dense forests, and marshland areas. Cotton rats are omnivorous and their diet principally consists of plants and seeds, and they only occasionally eat invertebrates, eggs, and small birds [26]. The food habits of the animals, including laboratory rodents, would be reflected in their large intestine morphology, especially in the ascending colon, because herbivores large intestine develop to digest grass (high-fiber food). The ratio of the large intestine to the small intestine was larger in the hamster, cotton rats, and mice, in that order (Fig. 3-4). These data might therefore reflect omnivory in mice, omnivory with a tendency toward herbivory in hamsters, and intermediate diet type in cotton rats.

At the beginning of the ascending colon, the author found an SLMF possessing several protuberant or small-sized LNs; the SLMF grew in length but not in height with the age of the animals. The presence of the SLMF in neonatal cotton rats suggests that the mucosal fold is an innate structure and is not dependent on feeding behavior for its development in this species. In mammals, the colon is part of the large intestine, which contains the largest population of microorganisms in the GIT, and plays a major role in the absorption of liquid and minerals [121]. Kararli [56] found that colon anatomy significantly differed among species. Furthermore, numerous rodents were found to have various shaped mucosal folds in the ascending colon that

enable the formation of wrinkles, which maintain their nutrient supply system. In general, in comparison to large animals, small herbivorous animals require a special digestive strategy in the large intestine to utilize plant nitrogen in a short time, owing to their higher metabolic rate, restriction of passage speed, and short digestive transit time [114]. As studied by Sperber [10] and Sakaguchi [114], this digestive strategy comprises a colonic separation mechanism that separates colonic contents by digestion rate. This allows coarse particles to be distinguished and eliminated in a short time through the digestive tract, while maintaining the accumulation of microorganisms in the cecum. This mechanism has been established in different species of mammals and birds [11], including rabbits [10], marsupials [11], Scandinavian lemmings, rats [10], guinea pigs, and chinchillas [45]. These findings show that the morphological and histological structures of the colonic mucosal fold in several rodent (mouse, cotton rat, hamster) species are similar to those reported in other rodent species, and this is consistent with what is expected in omnivores.

Adult female cotton rats showed a significantly longer ascending colon with a higher number of SLLFs compared to males. SLMF length was also longer in adult females. However, sex-related differences were not found in mice and hamsters. The author assume that sex differences were only identified in cotton rats due to the genetic background, feeding behavior, and geography of the original wild individuals. These results are a critical and valuable finding of the existence of sex-related differences in the large intestine lining. Sex-related hormones are strongly correlated with gut biology. Androgen and estrogen receptors are expressed in GIT cells, including the interstitial cells of the lamina propria and submucosa and epithelial cells in the gastric glands, small intestines, and large intestine [126]. Estrogen receptor β (ERβ) is the dominant estrogen receptor and is expressed in the colonic mucosal tissues of humans, especially in vascular smooth muscle and endothelial cells [65]. In humans, ERβ receptors are known to regulate intestinal barrier function [74] and could play an important role in diseases showing sex differences, such as colorectal cancer (where ERβ is more highly expressed in females than in males [95]) and inflammatory bowel disease [60]. In addition, the total excretion of bile acid in humans is lower, the digestive transition time is slower, the ability to digest neutral detergent fiber is higher, and stool consistency is harder in females than in males [68]. Here, for the first time, the author found sex-related differences in the large intestine length and its lining in cotton rats. Data is limited for comparing this study to; however, this species could play a crucial role in elucidating the mechanisms behind large intestine diseases that show sex differences.

Importantly, the author found various types of LN in the cecum and ascending colon of cotton rats, including protuberant and flat nodules. The LT, including the patch type or solitary intestinal LT (SILT), has been well studied in the small intestine [18]. For the murine large intestine, colonic patches that are developed during the embryonic stage are positioned in the submucosa between the muscular layers and muscular mucosa. SILT, which originates during the postpartum period, is located in the lamina propria, making direct

contact with the intestinal epithelium, toward the intraluminal area [6]. Therefore, flat LNs in the HSLF and transverse colon and protuberant LNs in the cecum and SLLF might be types of colonic patch and SILT, respectively. These localization patterns indicate the developmental differences of LNs in the large intestine. The shape of the LNs might also be related to the hardness of feces in the large intestine. The water content of feces gradually decreases from the beginning of the colon to the rectum; therefore, the physical pressure of feces on the intestinal wall differs among the large intestine regions. LNs were localized to the SLMF and an appendix was not observed; however, the author found large LNs near the apex of the cecum, surrounded by several small LNs. Thus, these data emphasized the crucial role of the cecum and ascending colon in mucosa-associated LT, potentially serving as a "safe house" [14] or reservoir for commensal bacteria in case of normal microbiome and immunological barrier function loss (the appendix in primates and rabbits).

In conclusion, cotton rats, one of the most valuable experimental rodents, did not develop the vaginal vestibule. On the other hand, the author found that their large intestines showed a unique morphological structure and pattern and SLMF, and various types of LNs and sex-related differences. Thus, this rodent may serve as a principal model for elucidating species-specific digestive tract function, gastrointestinal disorders, and their sex-related characteristics. Further studies are required to investigate the mechanisms of sex differences in their lower ductal organs, especially focusing on mucosal immunity.

Summary

The previous Chapters elucidated the GOALT morphology as an immune system protecting the female lower ductal organs in cows, goats, and pigs. This Chapter also try to examine them in rodents; especially the author examined the cotton rats which have been used for testing various diseases and mucosal vaccination studies. Firstly, the author elucidated that cotton rats did not develop the vaginal vestibule and GOALT; therefore, the GALT and structure of cecum and ascending colon of young (1–3-month old), adult (4–6-month old), and old (10–12-month old) cotton rats were examined as an alternative lower ductal organs of body. The large intestine in cotton rats is composed of the cecum, ascending colon, transverse and descending colons, and rectum, and is similar to that of other mammals. The ascending colon begins with a double or triple spiral SLLF and ends with a coupled HSLF. A SLMF was found at the beginning of the ascending colon along the mesentery line and developed with age. Furthermore, the SLMF contained several lymphatic nodules (LNs), indicating their role in digestive and immunological functions. Small and large protuberant LNs were found in the cecum and SLLF, respectively, whereas thin and flat LNs were observed in the HSLF and transverse colon, respectively. Regarding sex-related differences, adult females had a significantly longer ascending colon with a higher number of SLLFs compared to males. The SLMF length and LN number were also longer and higher, respectively, in adult females compared to adult males. Thus, this Chapter clarified the different types of GALTs with the unique morphology of the large intestine in cotton rats, and these data would crucial to consider the immune system of lower ductal organ and its species- and sex-related differences in animals.

Figures

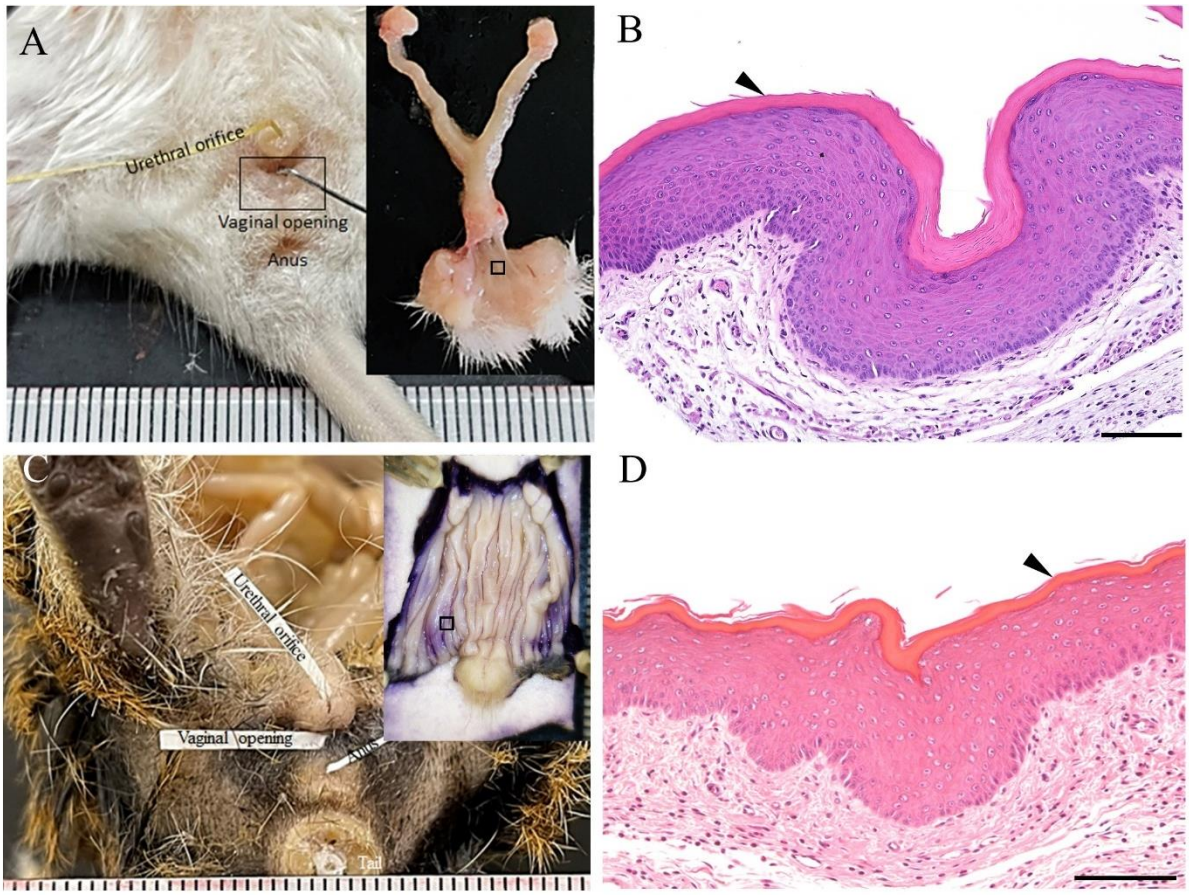

Fig. 3-1. External part of reproductive organ structure in mouse and cotton rats.

(A) External genitalia of female adult mouse contained three separate openings at the caudal part of the body. Dorsally, anal opening, ventrally urethral orifice, and between them located vaginal opening. Right upper photo showed gross anatomy of reproductive organ of female adult mice. One scale of the ruler is 1 mm. (B) Histology of mouse vagina. Arrowhead indicated cornified epithelium. HE staining. Bar = 100 μm. (C) External genitalia of female adult cotton rats. Right upper photo showed vagina after whole-mount staining with hematoxylin. Anus, vaginal opening, urethral orifice were located caudal part of the body. One scale of the ruler is 1 mm. (D) Histology of cotton rat vagina. Arrowhead indicated cornified epithelium. HE staining. Bar = 100 μm.

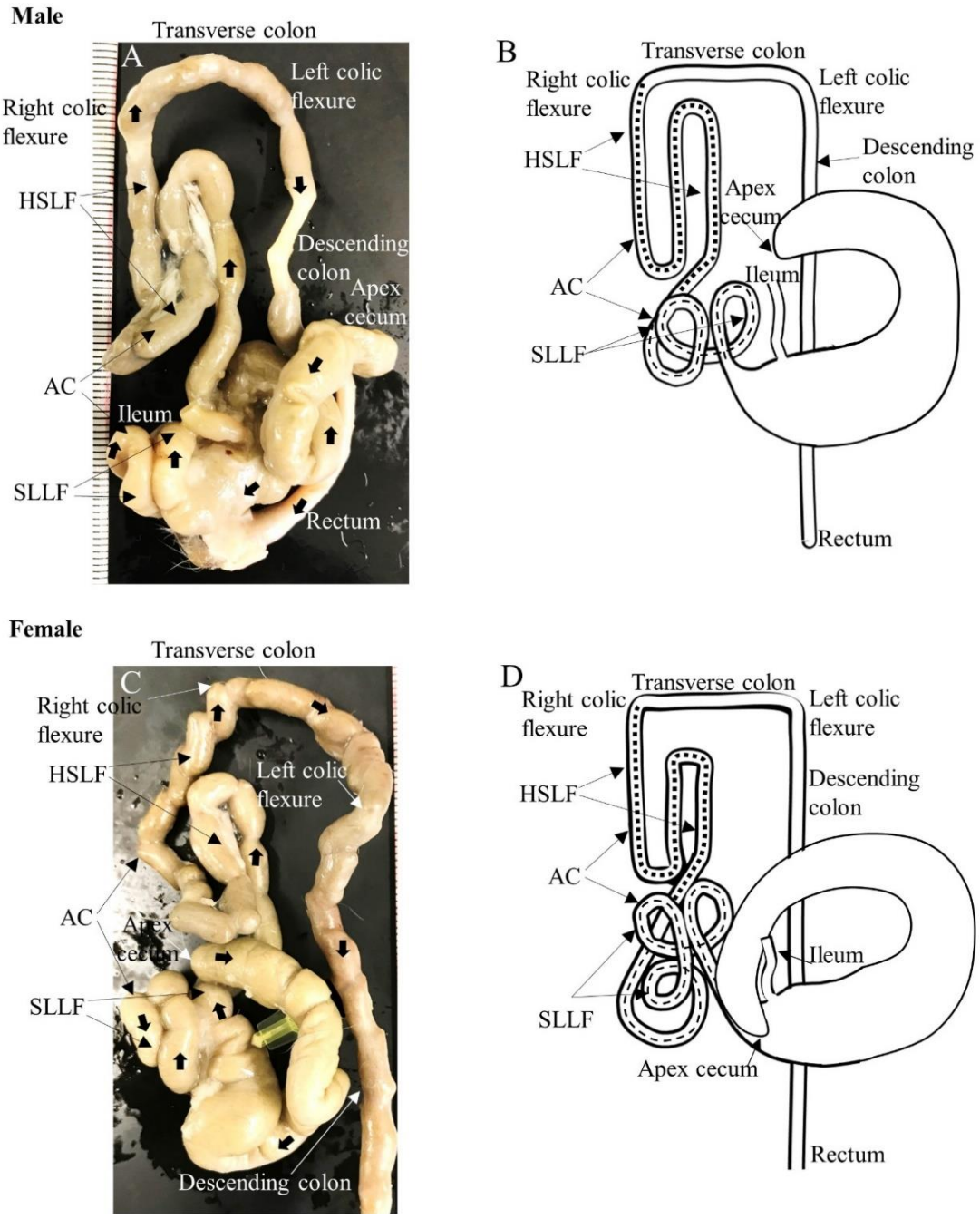

Figure 3-2. Gross anatomical features of the large intestine in cotton rats

(A and B) Male. Panel A shows a picture from the ventral view at 6 months old. Panel B summarizes the morphology and running pattern of the large intestine from the ventral view. (C and D) Female. Panel C shows a picture from the ventral view at 6 months old. Panel D summarizes the morphology and running pattern of the large intestine from the ventral view. Thick arrows represent the direction of intestines toward the rectum (A and C). Flat dashed lines and square dashed lines represent a spiral loop-like flexure (SLLF) and horseshoe-like flexure (HSLF), respectively. LI: large intestine, AC: ascending colon. Ruler = 1 mm.

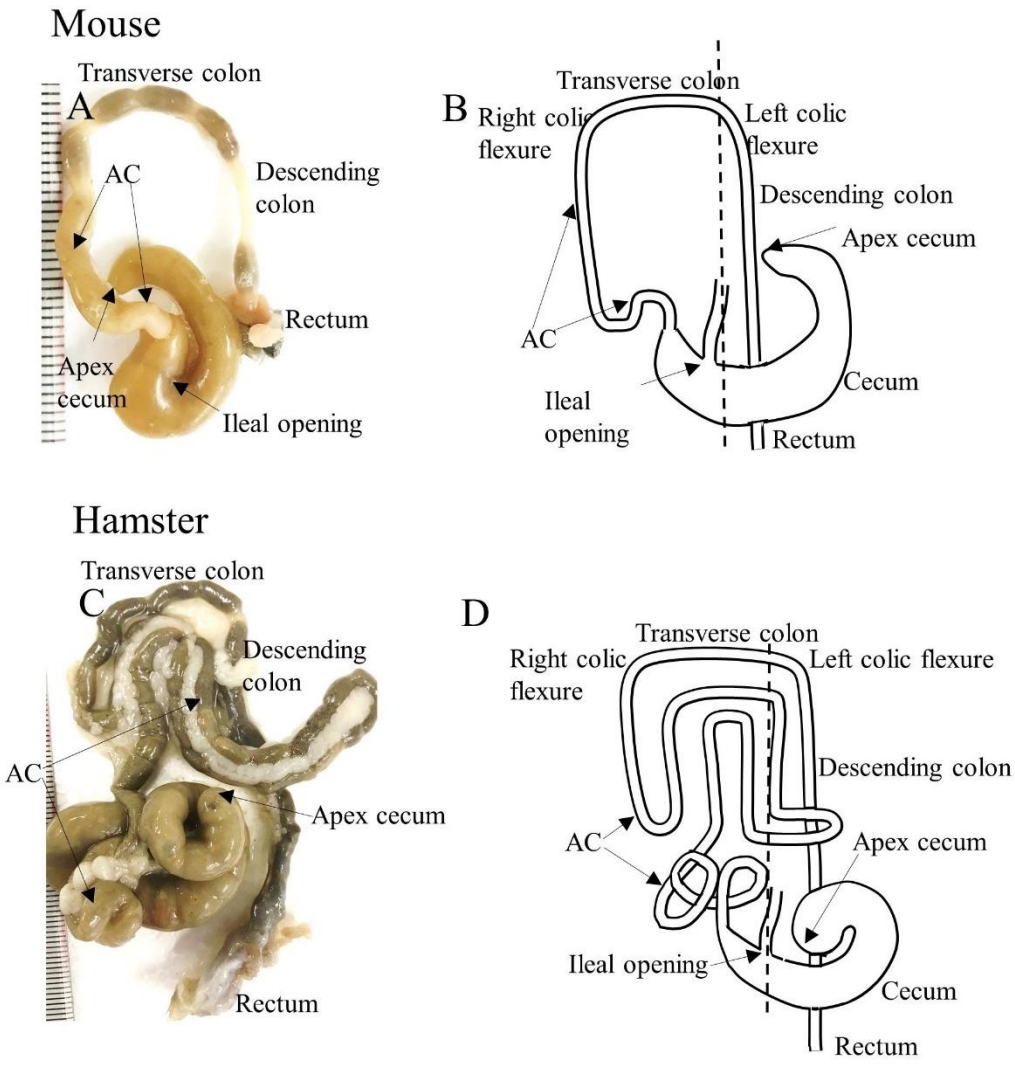

Figure 3-3. Morphology of large intestines in different rodents

A and B Male mouse at 2 months. Panel (A) shows a picture from the ventral view. Panel (B) summarizes the morphology and running pattern of the large intestine from the ventral view. (C and D) Male cotton rat at 6 months. Panel (C) shows a picture from the ventral view. Panel (D) summarizes the morphology and running pattern of the large intestine from the ventral view. (E and F) Male hamster at 6 months. Panel (E) shows a picture from the ventral view. Panel (F) summarizes the morphology and running pattern of the large intestine from the ventral view. Ruler = 1 mm.

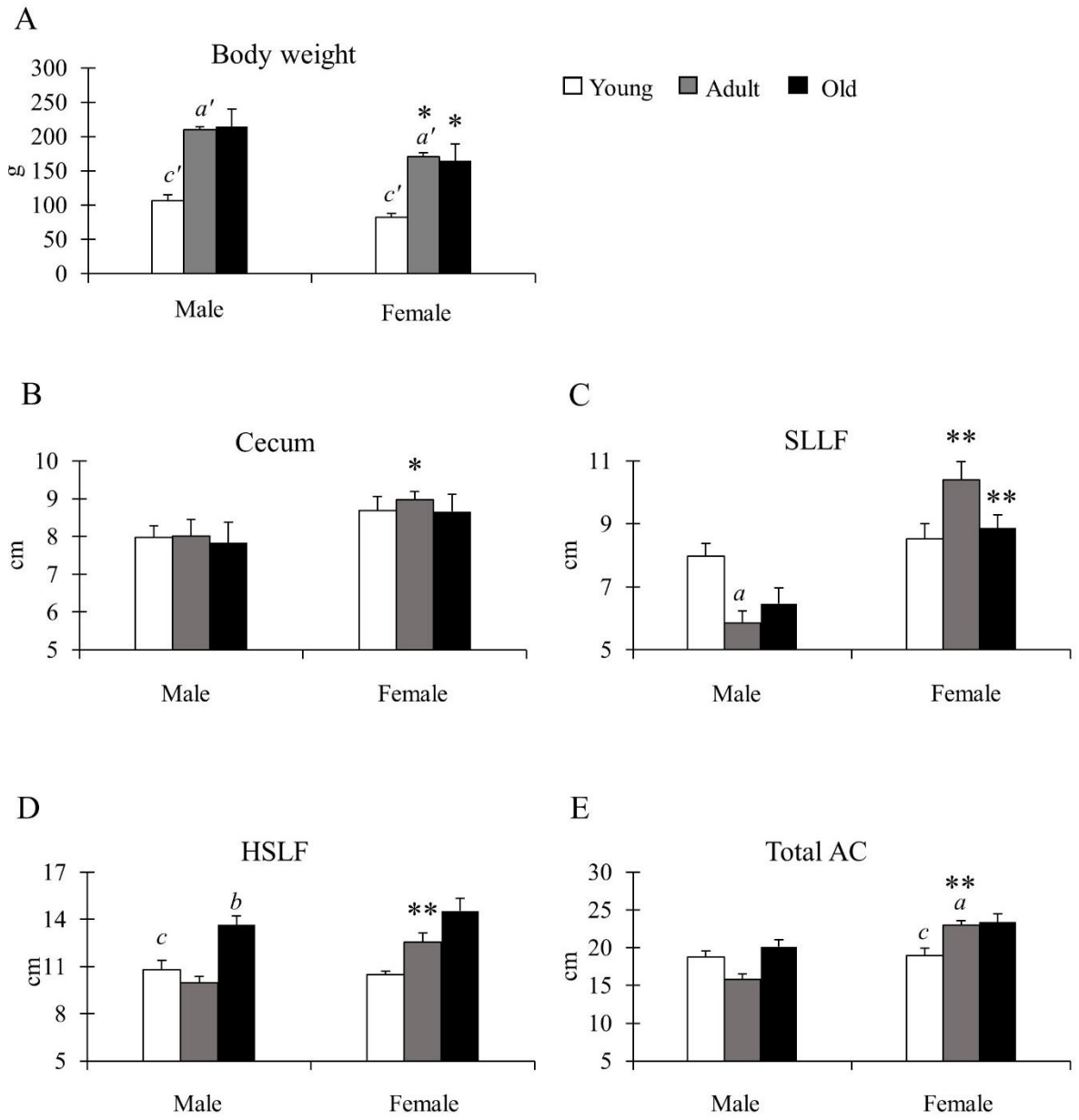

Figure 3-4. Body weight, and cecum and ascending colon lengths in cotton rats

(A) Body weight. Significant differences between the young and adult groups are indicated by *a′*. Significant differences between the young and old groups are indicated by *c′*. (*a′, c′ P* < 0.01; Kruskal-Wallis test followed by Scheffé's method). (B–E) Lengths of cecum (B), spiral loop-like flexure (SLLF; C), horseshoe-like flexure (HSLF; D), and total ascending colon (E). Values = mean ± standard error. *n* = 21 (male, young age group), *n* = 12 (female, young age group), *n* = 11 (male, adult age group), *n* = 8 (female, adult age group), *n* = 6 (male, old age group), and *n* = 7 (female, old age group). Significant sex-related differences in the same age group are indicated by * (*P* < 0.05) or ** (*P* < 0.01; Mann-Whitney *U* test). Significant differences between the young and adult groups are indicated by *a*. Significant differences between the adult and old groups are indicated by *b.* Significant differences between the old and young groups are indicated by *c* (*a*, *b,* *c P* < 0.05; Kruskal-Wallis test followed by Scheffé's method).

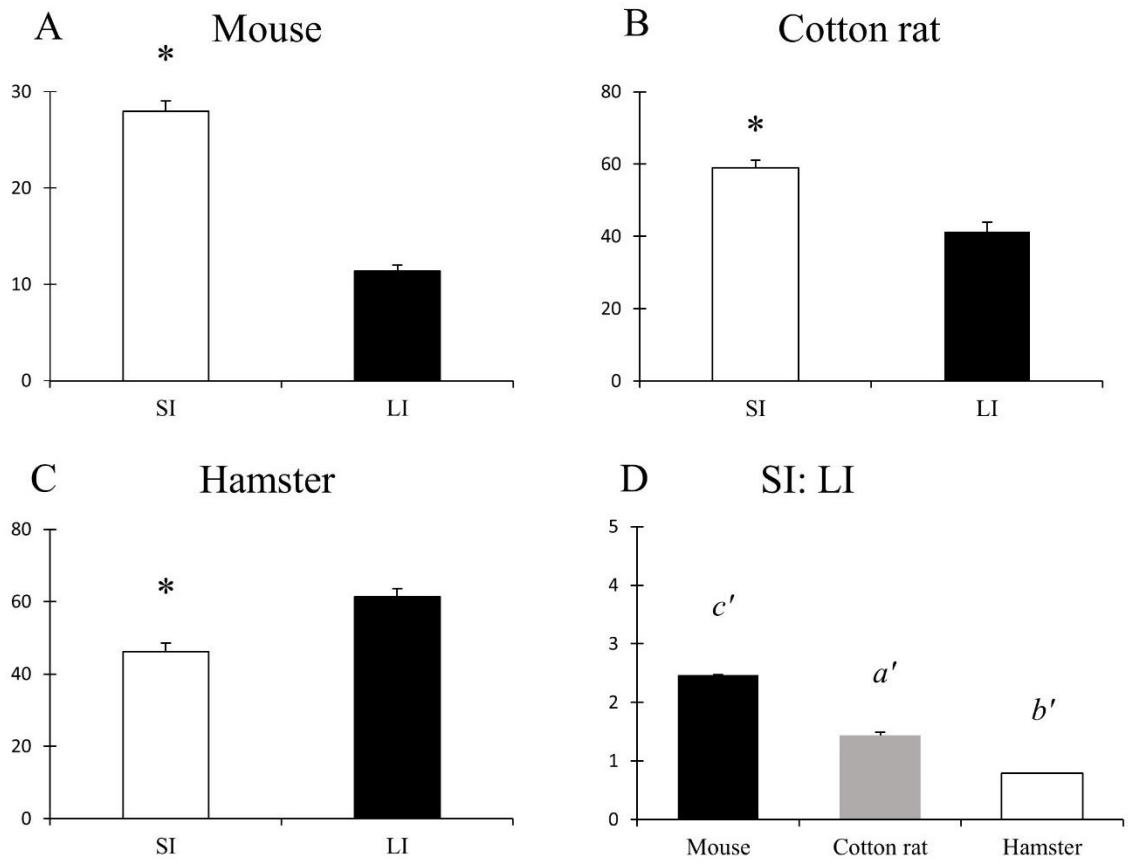

Figure 3-5. Body weight, and cecum and ascending colon lengths in cotton rats

(A) Mouse at 2 months. (B) Cotton rat at 6 months. (C) Hamster at 6 months. (D) Ratio of small intestine to large intestine length. Values are presented as mean ± standard error. $n = 4$ (each group). Significant differences between the small intestine and large intestine are indicated by *($P < 0.05$) (Mann-Whitney *U* test). Significant differences between the young and adult groups are indicated by *a*. Significant differences between the adult and old groups are indicated by *b*. Significant differences between the old and young groups are indicated by *c*. ($P < 0.05$) (Kruskal-Wallis test followed by the Scheffé's method).

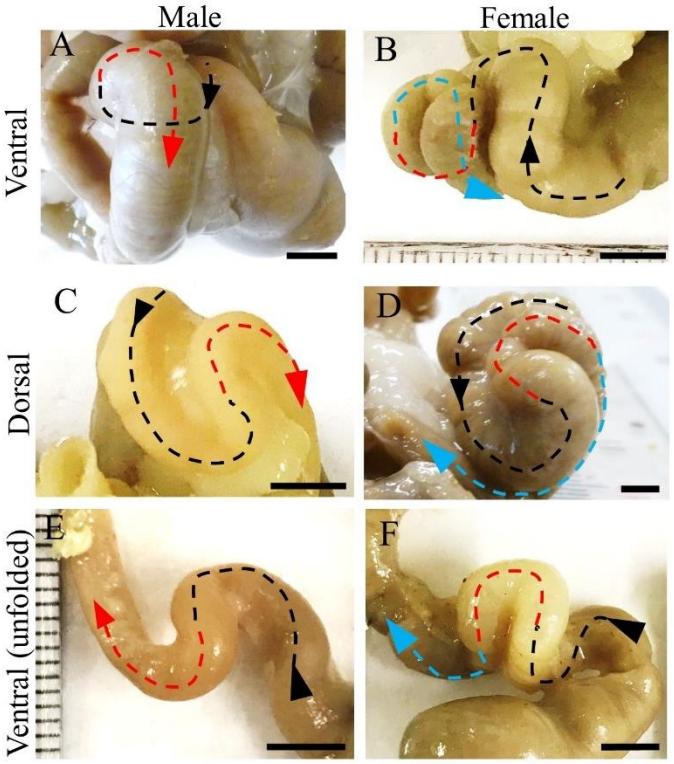

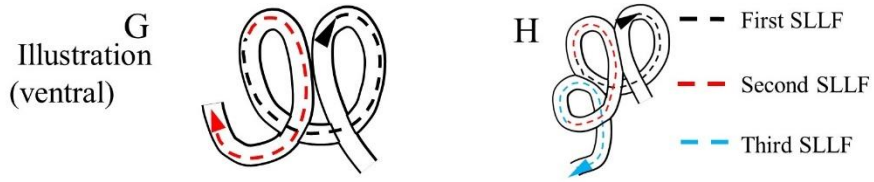

I

SLLF No	Male			Female		
	Young	Adult	Old	Young	Adult	Old
II	76% (16)	82% (9)	83% (5)	33% (4)	12% (1)	0%(0)
III	24% (5)	18% (2)	17% (1)	67% (8)	88% (7)	100%(7)
Total No	21	11	6	12	8	7

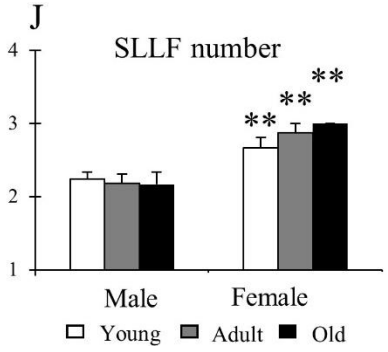

Figure 3-6. Morphological features of the SLLF in the ascending colon of cotton rats

(A-H) Sex-related differences of the SLLF from the ventral and dorsal views. Black, red, and blue arrows indicate the first and second and their flexures of SLLF with direction toward the rectum. Number of SLLFs

regarding appearance (I) and mean values (J). Values = percentage (I) or mean ± standard error (J). n = 21 (male, young age group), n = 12 (female, young age group), n = 11 (male, adult age group), n = 8 (female, adult age group), n = 6 (male, old age group), and n = 7 (female, old age group). Significant sex-related differences in the same age group are indicated by ** ($P < 0.01$; Mann-Whitney U test).

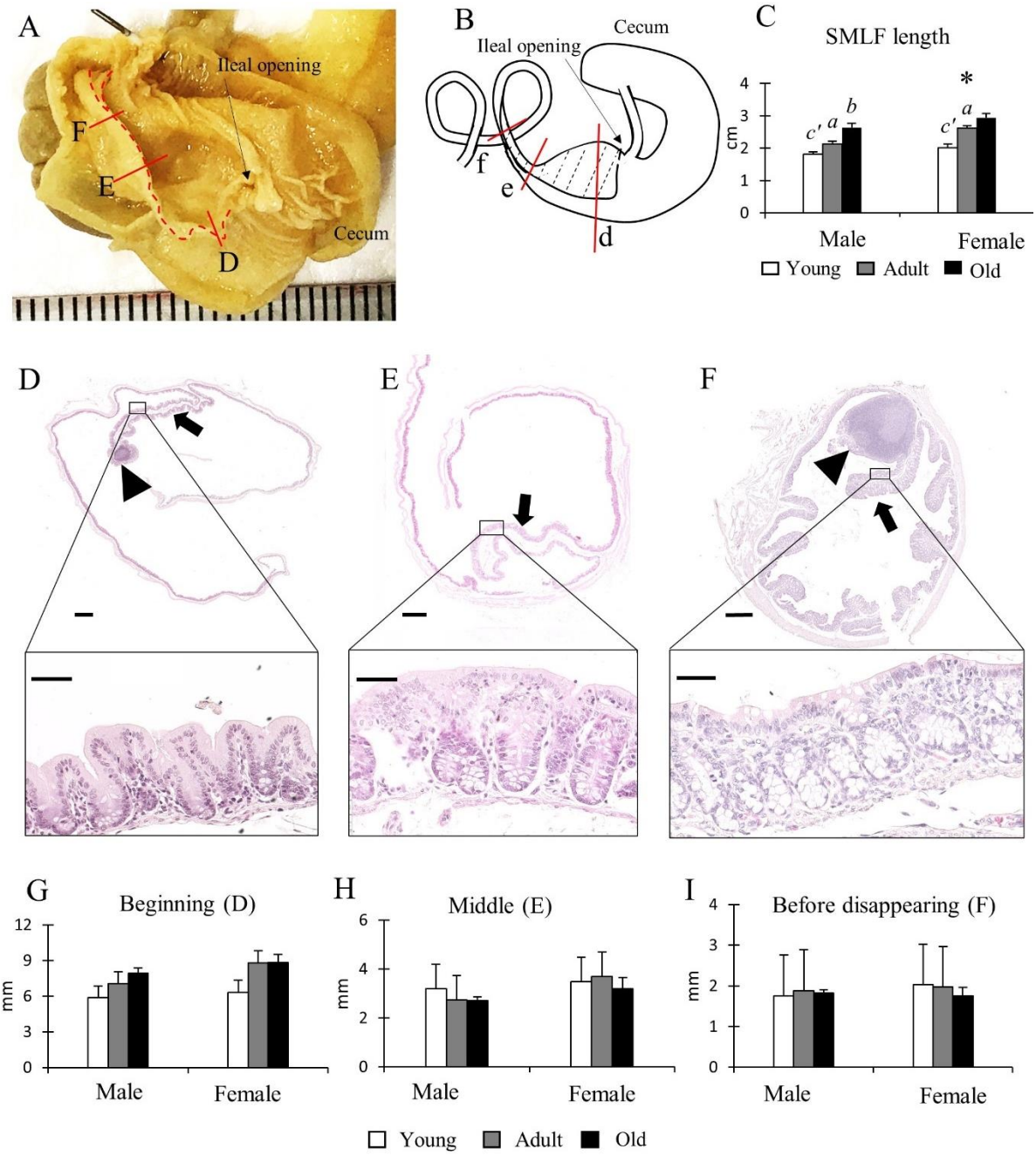

Figure 3-7. Morphological and histological features of the single SLMF in the ascending colon of cotton rats

Morphological and histological features of the single SLMF in the ascending colon of cotton rats. (A) Inner features of the cecum to the beginning of the SLLF. The SLMF is indicated by a dotted line. (B) Localization of the SLMF. The SLMF is indicated by a dotted-line area. (C) SLMF length. Values are presented as the mean ± standard error. n = 21 (male, young age group), n = 12 (female, young age group), n = 11 (male, adult age group), n = 8 (female, adult age group), n = 6 (male, old age group), and n = 7 (female, old age group). Significant sex-related differences in the same age group are indicated by ∗ ($P < 0.05$; Mann-Whitney U test).

Significant differences between the young and adult groups are indicated by a or a'. Significant differences between the adult and old groups are indicated by b or b' (a, b $P < 0.05$; a', b' $P < 0.01$; Kruskal-Wallis test followed by Scheffé's method). (D–F) Histological features of SLMFs. Panels (D–F) correspond to the areas shown with red lines indicated in panels (A, B). Beginning of the SLMF just after ileal opening (D), middle position of the SLMF where the colon begins to decrease its diameter (E), 3 mm before disappearing SLMF (F). Arrows and arrowheads indicate the SLMF and lymphatic nodule (LN), respectively. The lower panels indicate the high-magnification area of the square area in the upper panels. Hematoxylin and eosin staining. (G) SLMF height. Values are presented as the mean ± standard error. n = 4 (male, young age group), n = 5 (female, young age group), n = 4 (male, adult age group), n = 5 (female, adult age group), n = 4 (male, old age group), and n = 5 (female, old age group).

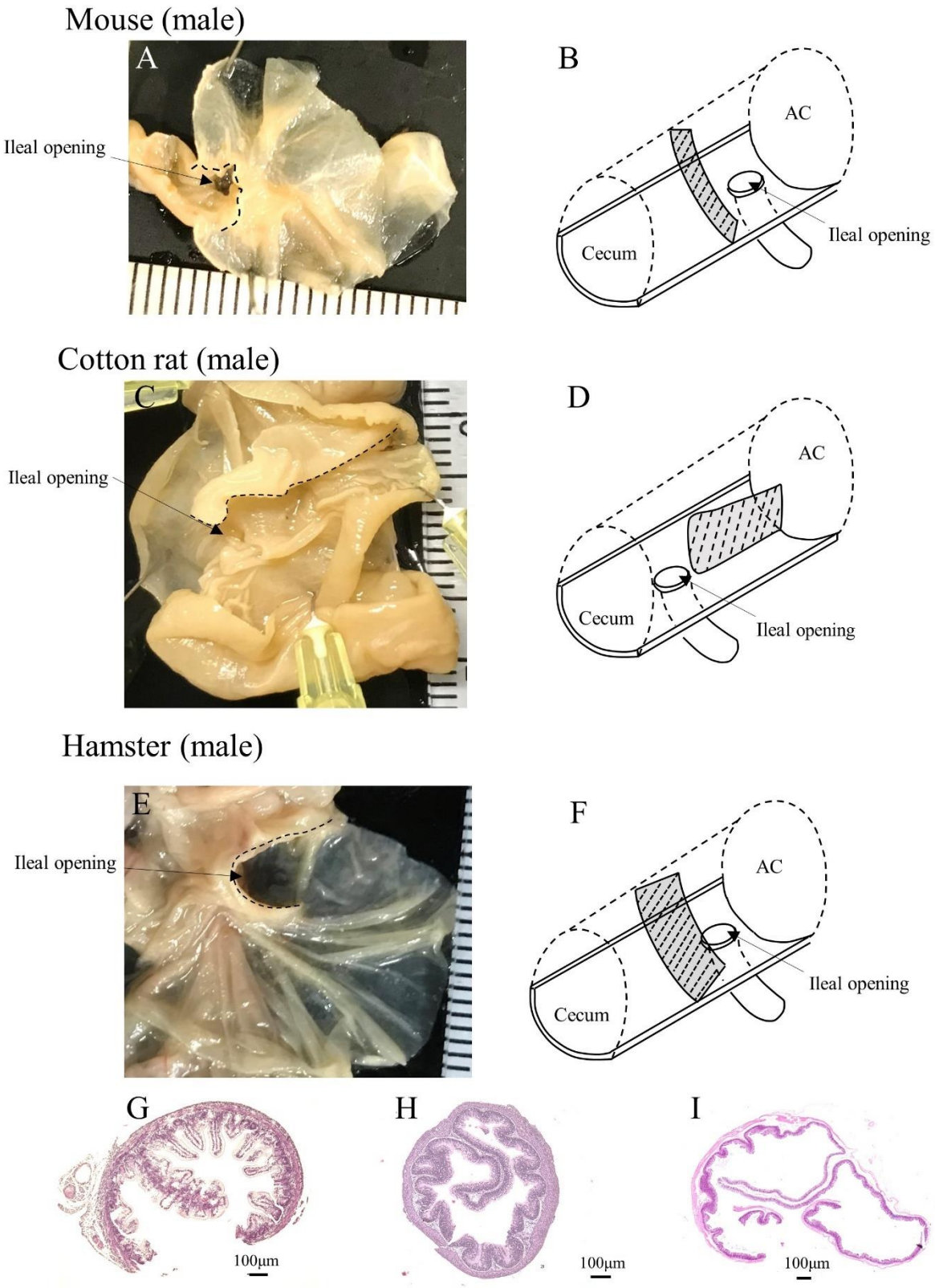

Figure 3-8. Morphological comparison of mucosal fold in the ascending colon of several rodents and SLMF appearance at different aged cotton rats.

(A and B) Male mouse at 2 months. Panel (A) shows a picture of the inner features at the border between the

cecum and colon. Panel (B) summarizes the morphology at the border between the cecum and colon. The gray dotted line area indicates the simple mucosal fold. (C and D) Male cotton rat at 6 months. Panel (C) shows a picture of the inner feature at the border between the cecum and colon. Panel (D) summarizes the morphology at the border between the cecum and colon. The gray dotted line area indicates the simple mucosal fold. (E and F) Male hamster at 6 months. Panel (E) shows an image of the inner feature at the border between the cecum and colon. Panel (F) summarizes the morphology at the border between the cecum and colon. The gray dotted line area indicates the simple mucosal fold. (G–I) Single mucosal longitudinal fold of cotton rats at 0 day (G), 4 days (H), and 4 months (I). Hematoxylin and eosin staining.

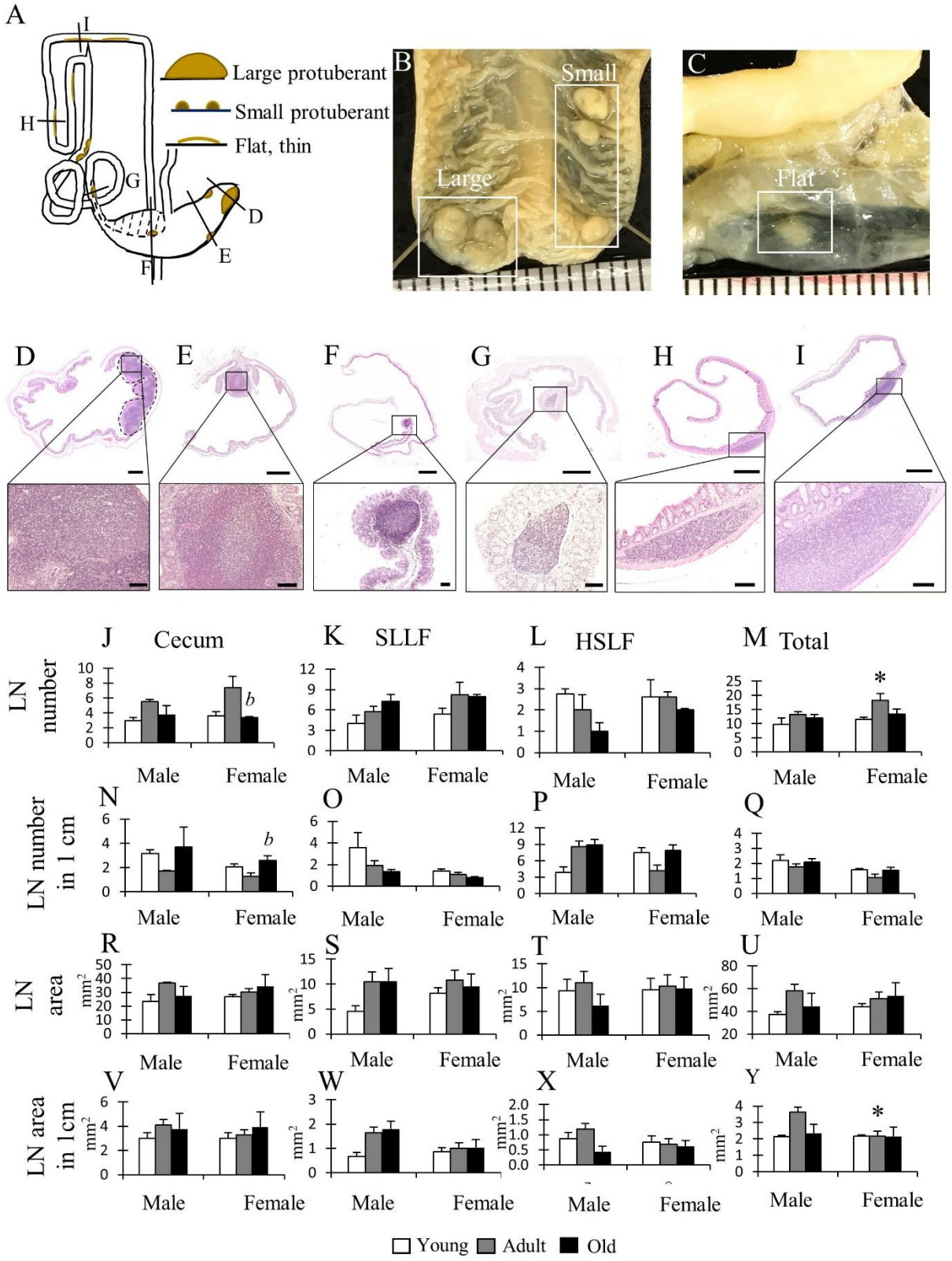

Figure 3-9. Morphological and histological features of LTs in the cecum and colon of cotton rats.

(A) Summarized localization and shapes of LNs found in the cecum and colon. Dotted line area indicates the localization of the single longitudinal mucosal fold (SLMF). Ventral view. (B, C) Gross anatomical features of LNs found in the cecum (B) or colon (C). Ruler = 1 mm. (D–I) Histological features of the LN. Panels D–

I correspond to the areas indicated with black lines in panel A. Near the apex of cecum (D), middle position of cecum (E), after ileal opening (F), before end of spiral loop-like flexure (SLLF) (G), horseshoe-like flexure (HSLF) (H), and transverse colon (I). The lower panels indicate magnified images of the square areas in the upper panels. Hematoxylin and eosin staining (J–Y) LN number (J-M), LN number in unit length (N-Q), LN area (R-U), and LN area in unit length (V-Y). Values are presented as the mean ± standard error. n = 4 (each group). Significant sex-related differences in the same age group are indicated by $*P < 0.05$; Mann-Whitney U test. Significant differences between the adult and old groups are indicated by b (Kruskal-Wallis test followed by Scheffé's method).

Conclusion

Mucosal immunology is an attractive field of science due to a great potential for the development of mucosal vaccination and immunotherapy among human and veterinary medicine because almost all infections and environmental allergies utilize mucosa as an entry portal. Importantly, genital organs of female mammals closely contact with the outer environment and maintains innate and adaptive immune systems by constructing the physical epithelial barrier, the production of antimicrobial agents and inflammatory mediators, and the various immune cells. Therefore, this thesis focused on the MALTs formed in the lower ductal organs of female mammals and analyzed them to understand the morphological characteristics crucial for the correct diagnosis and effective therapy in their pathological conditions.

In Chapter1 and 2, the author characterized LTs in the mucosa clitoris, vulva, and vaginal vestibule of healthy, non-pregnant, adult cow, goat, and pig. The gross anatomical and histological features of LTs in the mucosa of EPGOs were examined using whole-mount staining with hematoxylin, HE, IHC, IF, and SEM. Whole-mount specimens revealed that several hematoxylin^{+} spots were arranged in a ring in the mucosa. Histologically, these spots contained aggregated immune cells, and the author defined them as GOALTs. GOALTs were composed of LNs or DLTs at different depths of lamina propria. All examined LTs were comprised of B cells, T cells, macrophages, DCs, plasma cells, and HEVs. B cells were dominant both in LNs and DLTs of all examined species. Abundant collagenous fibers were stretched across the lamina propria of vaginal vestibule, whereas reticular fibers were primarily observed in the DLTs rather than LNs. Furthermore, the vaginal vestibule epithelium covering LTs was disrupted by a large intercellular space, and immune cells directly contacted the intraluminal space through this area lacking epithelium. The author did not find obvious differences in the morphology of GOALTs and immune cell components among examined animal species. These data strongly suggested that GOALT is a conserved local immunological barrier and "genital lymphoid ring" in cow, goat, and pig, which would functions as immunological gate systems as Waldeyer's pharyngeal ring in the head.

In addition to the above farm animals, the Chapter 3 focused on the major laboratory animal rodents including cotton rats, mice, rats, and hamsters, but these rodents did not anatomically develop a vaginal vestibule, and no clear GOALT was found. Therefore, the author focused on GALTs in the large intestine as a structure which maintains the immune function of the lower ductal organs. This Chapter analyzed the GALT in the large intestines of the cotton rat, which is useful as an experimental animal but lacks anatomical knowledge, with their intestinal running patterns and morphological characteristics. In particular, the running pattern of large intestines and the morphology of mucosal fold in the caecum differed between cotton rats and other rodents. Briefly, the proximal and distal parts of ascending colon formed the SLLF and HSLF respectively, and they were unique morphologies in the large intestines of cotton rats compared to other

rodents in both sexes. The author also clarified morphologically different types of LTs on the mucosal surface of the cecum and ascending colon in both sexes of cotton rats, including protuberant and flat LNs. Furthermore, adult female cotton rats showed a significantly longer ascending colon with a higher number of SLLFs compared to males. At the beginning of the ascending colon, author found an SLMF possessing several protuberant or small-sized LTs; the SLMF grew in length but not in height with the age of the animals. In summary, this Chapter has clarified the morphological characteristics of the lower ductal organs of rodents, especially cotton rats.

The present study revealed GOALTs forming the genital lymphoid ring in the vaginal vestibule of cow, goat, and pigs, in their adulthood. These GOALTs would be immunological barriers in the lower ductal organs of farm animals and would have a critical role in the pathogenesis relating to female reproductive organs in farm animals. On the other hand, in the present study, examined rodents do not develop the GOALTs due to the absence of obvious vaginal vestibules, but the author considered that their terminal part of GITs might maintain the immunological environment in the lower ductal organs of females, including reproductive and digestive organs. These novel fundamental knowledge on GOALTs and GALTs would be crucial to understand the pathology of mammalian reproductive organ- and GIT-related disorders, which contribute the development of diagnosis and therapeutic strategies utilizing the mucosal immunity in animal and human medicines from the viewpoint of one health concept and zoobiquity.

Conclusion in Japanese

管状臓器の粘膜は外来抗原やアレルゲンの侵入門戸となるため、動物とヒトの医学双方において、それらの粘膜免疫を利用したワクチン法や治療法の開発が進んでいる。特に、雌性生殖器は外界と密接に関連するため、その粘膜は物理的な上皮バリアや種々の免疫細胞を配備し、抗菌物質や炎症関連物質の産生を介して粘膜免疫を担う。本論文では、雌性動物の下部管状臓器に形成される粘膜関連リンパ組織（MALT）に着目し、適正な病態診断や効果的治療の実施に重要となる形態学的特徴の理解を目的とし、解析を進めた。

第一章と二章では、非妊娠時のウシ、ヤギ、ブタの腟前庭と外部生殖器（陰核、外陰部）の粘膜におけるリンパ組織（LT）を検索した。LT の形態学的特徴を各臓器のホールマウント標本や走査型電子顕微鏡標本の観察、組織切片のヘマトキシリン・エオジン染色や免疫染色による解析で評価した。腟前庭のホールマウント標本において、ヘマトキシリンに濃染する複数の小円領域が全動物の粘膜に観察され、それらはリング状に配置された。組織学的解析から、当該小円領域には免疫細胞が集簇しており、著者はこれらを“生殖器関連リンパ組織（GOALT）”と定義した。GOLAT はリンパ小節（LN）もしくは散在性リンパ組織（DLT）の形態様式を示し、これらは粘膜固有層や粘膜下組織に局在し、B 細胞、T 細胞、マクロファージ、樹状細胞、形質細胞や毛細血管後細静脈を包含した。また、腟前庭の GOALT では、豊富な膠原線維が立体的に構築され、細網線維構築は LN よりも DLT で発達する傾向にあった。さらに、GOALT 直上の腟前庭粘膜上皮は部分的に脱落・欠如し、免疫細胞が直接管腔に面していた。これら GOALT の形態やその構成細胞に顕著な動物種差はなかった。以上より、GOALT は雌のウシ、ヤギ、ブタの下部管状臓器、特に腟前庭で発達する免疫学的障壁であり、頭部におけるワルダイエルの咽頭輪のように、“陰部リンパ輪”として下部管状臓器の局所免疫を担うと考えた。

上記の産業動物に加え、第三章では主要な実験動物齧歯目であるコットンラット、マウス、ラット、ハムスターに焦点を当てたが、これら齧歯目では解剖学的に腟前庭が発達せず、明瞭な GOALT を見出せなかった。そこで、大腸の腸管関連リンパ組織（GALT）を下部管状臓器の粘膜免疫を担う構造として着目した。本章では実験動物として有用だが、その解剖学的知見が不足しているコットンラットの大腸 GALT を腸の走行や形態学的特徴と共に解析した。特に、コットンラットの結腸の走向や盲腸粘膜ヒダの形態が他の齧歯目とは異なった。雌雄コットンラットの上行結腸前半部はラセン状屈曲を、その後半部は馬蹄状屈曲を形成し、これらは他の齧歯目に比べて特徴的な形態だった。雌雄コットンラットの盲腸と上行結腸の粘膜には隆起型あるいは平坦型のリンパ小節がみられた。さらに上行結腸の形態は雌雄で大きく異なり、特に雌の上行結腸は雄に比べて長く、上行結腸の前半部分に形成されるラセン状屈曲の数が雄よりも雌で多かった。また、上行結腸起始部には隆起型もしくは小型のリンパ濾胞を複数有する粘膜の縦ヒダ構造がみられ、その丈は解析週齢間で同等だった一方、加齢と共に腸管走向方向への長さを増した。以上、

本章では齧歯目、特にコットンラットの下部管状臓器の形態学的特徴を明らかにした。

本論文では、成体のウシ、ヤギ、ブタの腟前庭を解析し、リンパ陰部輪を形成する GOALT の形態を明らかにした。GOALT はこれら主要な産業動物の下部管状臓器における免疫学的障壁となり、雌性生殖器関連疾患において重要な役割を果たすと考えられた。一方、本解析に供した齧歯目は明瞭な腟前庭を欠き、GOALT を発達させなかったが、これらの種の消化管後半部分は生殖器や消化器を含む雌の下部管状臓器の免疫学的環境の維持に貢献する可能性を考えた。これらの GOALT や GALT の新たな基礎的知見は、生殖器ならびに消化器の病態発生機序を理解する上で重要であり、動物やヒトにおける粘膜免疫を利用した診断法ならびに治療法の開発に貢献する。

Acknowledgement

I would like to express my sincere gratitude to my supervisor Professor Yasuhiro Kon for giving me the opportunity to fulfill my graduate studies, providing valuable guidance and feedback, and challenging me to grow as a scientist. I am deeply grateful to Associate professor Osamu Ichii for his invaluable supervision, support, and tutelage. His astonishing editing and teaching skills always inspired from a teacher's and researcher's viewpoint. I would like to extend my sincere thanks to Professor Mitsuyoshi Takiguchi and Professor Takashi Kimura for their critical comments and suggestions for this thesis. I would also like to thank all members of the Laboratory of Anatomy, especially my friend Takashi Namba for his kind support for this research and my PhD student life. I would like to express my gratitude to my parents, husband, and my children for all of their unconditional support in these very intense academic years. Finally, I sincerely express my deepest sorrow and gratitude to all animals supporting this research.

References

1) Anderson ML, Moore PF, Hyde DM, Dungworth DL. Bronchus associated lymphoid tissue in the lungs of cattle: relationship to age. Res Vet Sci 41, 211-220, 1986.
2) Armstrong C. The Experimental transmission of poliomyelitis to the eastern cotton rat, sigmodon hispidus hispidus. Public Heal Reports 54, 1719-1721, 1939.
3) Astley RA, Kennedy RC, Chodosh J. Structural and cellular architecture of conjunctival lymphoid follicles in the baboon (Papio anubis). Exp Eye Res 76, 685-694, 2003.
4) Azazy AA, Devaney E, Chance ML. A peg-elisa for the detection of Leishmania donovani antigen in circulating immune complexes. Trans R Soc Trop Med Hyg 88, 62-66, 1994.
5) Azzali G. Structure, lymphatic vascularization and lymphocyte migration in mucosa-associated lymphoid tissue. Immunol Rev 195, 178-189, 2003.
6) Baptista AP, Olivier BJ, Goverse G, Greuter M, Knippenberg M, Kusser K, Domingues RG, Veiga-Fernandes H, Luster AD, Lugering A, Randall TD, Cupedo T, Mebius RE. Colonic patch and colonic SILT development are independent and differentially regulated events. Mucosal Immunol 6, 511-521, 2013.
7) Barone R. *Anatomia Comparata Dei Mammiferi Domestici*. 1st ed. Edagricole New Business Media; 1993.
8) Bennett JE, Dolin R, Blaser MJ. *Principles and Practice of Infectious Diseases*. 9th ed. Elsevier; 2019.
9) Bienenstock J, McDermott MR. Bronchus- and nasal-associated lymphoid tissues. Immunol Rev 206, 22-31, 2005.
10) Bjornhag G, Sperber I, Holtenius K. A Separation mechanism in the large intestine of equines. Can J Anim Sci 64, 89-90, 1984.
11) Björnhag G. Transport of water and food particles through the avian ceca and colon. J Exp Zool 252, 32-37, 1989.
12) Blazquez NB, Batten EH, Long SE, Perry GC. Amount and distribution of vestibular-associated lymphoid tissue in calves and adult cows. Res Vet Sci 43, 239-242, 1987.
13) Blazquez NB, Batten EH, Long SE, Perry GC. Histology and histochemistry of the bovine reproductive tract caudal to the cervix part I. The vestibule and associated glands. Br Vet J 143, 328-337, 1987.
14) Bollinger RR, Barbas AS, Bush EL, Lin SS, Parker W. Biofilms in the normal human large bowel: Fact rather than fiction. Gut 56, 1481-1482, 2007.

15) Brandtzaeg P, Kiyono H, Pabst R, Russell MW. Terminology: Nomenclature of mucosa-associated lymphoid tissue. Mucosal Immunol 1, 31-37, 2008.

16) Brandtzaeg P, Pabst R. Let's go mucosal: communication on slippery ground. Trends Immunol 25, 570-577, 2004.

17) Budras KD, E.Habel R. *Bovine Anatomy*. 1st ed. Schlutersche; 2003.

18) Buettner M, Lochner M. Development and function of secondary and tertiary lymphoid organs in the small intestine and the colon. Front Immunol 7, 2016.

19) Bulmer JN, Earl U. The expression of class II MHC gene products by fallopian tube epithelium in pregnancy and throughout the menstrual cycle. Immunology 61, 207-213, 1987.

20) Caucheteux S, Piguet V. Vaginal epidermal dendritic cells: Defense against HIV-1 or a safe haven? J Clin Invest 128, 3228-3230, 2018.

21) Cesta MF. Normal structure, function, and histology of mucosa-associated lymphoid tissue. Toxicol Pathol 34, 599-608, 2006.

22) Chodosh J, Nordquist RE, Kennedy RC. Comparative anatomy of mammalian conjunctival lymphoid tissue: A putative mucosal immune site. Dev Comp Immunol 22, 621-630, 1998.

23) Cole HH. A study of the mucosa of the genital tract of the cow, with special reference to the cyclic changes. Am J Anat 46, 261-301, 1930.

24) Crespo-Moral M, García-Posadas L, López-García A, Diebold Y. Histological and immunohistochemical characterization of the porcine ocular surface. PLoS One 15, e0227732, 2020.

25) Croitoru K, Bienenstock J. *Handbook of Mucosal Immunology*. 1st ed. Elsevier; 1994.

26) Curlee JF, Cooper DM. *The Laboratory Rabbit, Guinea Pig, Hamster, and Other Rodents*. 1st ed. Elsevier Inc.; 2012.

27) Dadarwal D, Palmer C, Griebel P. Mucosal immunity of the postpartum bovine genital tract. Theriogenology 104, 62-71, 2017.

28) Dyce KM, Sack WO, Wensing CJG. *Textbook of Veterinary Anatomy*. 1st ed. Saunders; 1987.

29) Elwood R, Wilson S, Blanco J, Yim K, Tuberculosis LP-, 2007 U. The American cotton rat: a novel model for pulmonary tuberculosis. Tuberculosis 87, 145-154, 2007.

30) Fagraeus A. Plasma cellular reaction and its relation to the formation of antibodies in vitro. Nature 159, 499-499, 1947.

31) Faith RE, Montgomery CA, Durfee WJ, Aguilar-Cordova E, Wyde PR. The cotton rat in biomedical research. Lab Anim Sci 47, 337-345, 1997.

32) Forchielli ML, Walker WA. The role of gut-associated lymphoid tissues and mucosal defence.

Br J Nutr 93, 41-48, 2005.

33) Gahlot PK, Kumar P. Gross localization and distribution of gut associated lymphoid tissue in goat (Capra Hircus). Haryana Vet 57, 159-160, 2018.

34) Giuliano EA, Moore CP, Phillips TE. Morphological evidence of M cells in healthy canine conjunctiva-associated lymphoid tissue. Graefes Arch Clin Exp Ophthalmol 240, 220-226, 2002.

35) Green WB, Eaton K, Krakowka S. Porcine gastric mucosa associated lymphoid tissue (MALT): stimulation by colonization with the gastric bacterial pathogen, Helicobacter pylori. Vet Immunol Immunopathol 56, 119-131, 1997.

36) Grishina I, Fenton A, Sankaran-Walters S. Gender differences, aging and hormonal status in mucosal injury and repair. Aging Dis 5, 160-169, 2014.

37) Hagiwara H, Ohwada N, Aoki T, Fujimoto T. Langerhans cells in the human oviduct mucosa. Ital J Anat Embryol 103, 253-258, 1998.

38) Hamada H, Hiroi T, Nishiyama Y, Takahashi H, Masunaga Y, Hachimura S, Kaminogawa S, Takahashi-Iwanaga H, Iwanaga T, Kiyono H, Yamamoto H, Ishikawa H. Identification of multiple isolated lymphoid follicles on the antimesenteric wall of the mouse small intestine. J Immunol 168, 57-64, 2002.

39) Hamelin M-È, Yim K, Kuhn KH, Cragin RP, Boukhvalova M, Blanco JCG, Prince GA, Boivin G. Pathogenesis of human Metapneumovirus lung Infection in BALB/c mice and cotton rats. J Virol 79, 8894-8903, 2005.

40) Hammond J. The physiology of reproduction in the cow. Nature 120, 37-39, 1927.

41) Häussler M, Liebler E., Daugschies A, Pohlenz J. Changes in the number of lymphocyte subsets, macrophages, mast cells and eosinophils in the large intestine of pigs during infection with Oesophagostomum dentatum. Eur J Vet Pathol 2, 20-21, 1996.

42) Hayakawa T, Iwaki T. *A Color Atlas of Sectional Anatomy of the Rat*. 1st ed. Adthree; 2008.

43) Hellings P, Jorissen M, Ceuppens J. The Waldeyer's ring. Acta Otorhinolaryngol Belg 54, 237-241, 2000.

44) Hickey DK, Patel M V., Fahey J V., Wira CR. Innate and adaptive immunity at mucosal surfaces of the female reproductive tract: Stratification and integration of immune protection against the transmission of sexually transmitted infections. J Reprod Immunol 88, 185-194, 2011.

45) Holtenius K, Björnhag G. The colonic separation mechanism in the guinea-pig (Cavia porcellus) and the chinchilla (Chinchilla laniger). Comp Biochem Physiol A Comp Physiol 82, 537-542, 1985.

46) Huang YT, Chu RM, Liu RS, Weng CN. Morphologic studies of intrapulmonary airway mucosa-

associated lymphoid tissues in swine. Vet Immunol Immunopathol 25, 13-22, 1990.

47) Hume ID, Morgan KR, Kenagy GJ. Digesta retention and digestive performance in Sciurid and Microtine rodents: Effects of hindgut morphology and body size. Physiol Zool 66, 396-411, 1993.

48) Hunt JS. Immunologically relevant cells in the uterus. Biol Reprod 50, 461-466, 1994.

49) Hussain LA, Lehner T. Comparative investigation of Langerhans' cells and potential receptors for HIV in oral, genitourinary and rectal epithelia. Immunology 85, 475-484, 1995.

50) Ichii O, Nakamura T, Irie T, Kouguchi H, Nakamura D, Nakamura S, Sato S, Yokoyama K, Horino T, Sunden Y, Elewa YHA, Kon Y. Female cotton rats (Sigmodon hispidus) develop chronic anemia with renal inflammation and cystic changes. Histochem Cell Biol 146, 351-362, 2016.

51) Ichii O, Nakamura T, Irie T, Otani Y, Hosotani M, Masum MA, Islam RM, Horino T, Sunden Y, Elewa YHA, Kon Y. Age-related glomerular lesions with albuminuria in male cotton rats. Histochem Cell Biol 153, 27-36, 2020.

52) Iijima N, Linehan MM, Saeland S, Iwasaki A. Vaginal epithelial dendritic cells renew from bone marrow precursors. Proc Natl Acad Sci U S A 104, 19061-19066, 2007.

53) J.Haley P. The lymphoid system: A review of species differences. J Toxicol Pathol 30, 111-123, 2017.

54) Jericho KWF, Derbyshire JB, Jones JET. Intrapulmonary lymphoid tissue of pigs exposed to aerosols of haemolytic streptococcus group L and porcine adenovirus. J Comp Pathol 81, 1-11, 1971.

55) Jørgensen PB, Eriksen LL, Fenton TM, Bailey M, Agace WW, Mörbe UM. The porcine large intestine contains developmentally distinct submucosal lymphoid clusters and mucosal isolated lymphoid follicles. Dev Comp Immunol 131, e collection, 2022.

56) Kararli TT. Comparison of the gastrointestinal anatomy, physiology, and biochemistry of humans and commonly used laboratory animals. Biopharm Drug Dispos 16, 351-380, 1995.

57) Kathrine E, Steen J. A review of the human vs. porcine female genital tract and associated immune system in the perspective of using minipigs as a model of human genital Chlamydia infection. Vet Res 46, 1-13, 2011.

58) Kawase S, Ishikura H. Female-predominant occurrence of spontaneous gastric adenocarcinoma in cotton rats. Lab Anim Sci 45, 244-248, 1995.

59) Kenneth Murphy CW. *Janeway's Immunobiology*. 9th ed. Garland Science, Taylor & Francis Group; 2017.

60) Kim YS, Kim N. Sex-gender differences in irritable bowel syndrome. J Neurogastroenterol Motil

24, 544-558, 2018.

61) Kiyono H, Fukuyama S. NALT- versus Peyer's-patch-mediated mucosal immunity. Nat Rev Immunol 4, 699-710, 2004.

62) Knop E, Knop N. The eye-associated lymphoid tissue (EALT) - A basis of the anatomy and immunology at the ocular surface. Acta Ophthalmol 89, 2431 e pub, 2011.

63) Komban RJ, Strömberg A, Biram A, Cervin J, Lebrero-Fernández C, Mabbott N, Yrlid U, Shulman Z, Bemark M, Lycke N. Activated Peyer′s patch B cells sample antigen directly from M cells in the subepithelial dome. Nat Commun 10, 1-15, 2019.

64) Konig H, Liebich H. *Veterinary Anatomy of Domestic Mammals: Textbook and Colour Atlas*. 3rd ed. Schattauer; 2007.

65) Konstantinopoulos PA, Kominea A, Vandoros G, Sykiotis GP, Andricopoulos P, Varakis I, Sotiropoulou-Bonikou G, Papavassiliou AG. Oestrogen receptor beta (ERβ) is abundantly expressed in normal colonic mucosa, but declines in colon adenocarcinoma paralleling the tumour's dedifferentiation. Eur J Cancer 39, 1251-1258, 2003.

66) Kracke A, Hiller AS, Tschernig H, Kasper M, Kleemann WJ, Troger HD, Pabst R. Larynx-associated lymphoid tissue (LALT) in young children. Anat Rec 248, 413-420, 1997.

67) Kuper CF, Koornstra PJ, Hameleers DMH, Biewenga J, Spit BJ, Duijvestijn AM, Vriesman VB, Peter CJ, Sminia T. The role of nasopharyngeal lymphoid tissue. Immunol Today 12, 219-224, 1992.

68) Lampe JW, Fredstrom SB, Slavin JL, Potter JD, Paul S. Sex differences in colonic function: a randomised trial. Gut 34, 531-536, 1993.

69) Lanzkowsky P, Lipton JM, Fish JD. *Lanzkowsky's Manual of Pediatric Hematology and Oncology*. Academic Press; 2016.

70) Lee SK, Kim CJ, Kim D-J, Kang J. Immune cells in the female reproductive tract. Immune Netw 15, 16-26, 2015.

71) Lehner T, Panagiotidi C, Bergmeier LA, Tao L, Brookes R, Gearing A, Adams S. Genital-associated lymphoid tissue in female non-human primates. Adv Exp Med Biol 371, 357-365, 1995.

72) Lewandowski G, Zimmerman MN, Denk LL, Porter DD, Prince GA. Herpes simplex type 1 infects and establishes latency in the brain and trigeminal ganglia during primary infection of the lip in cotton rats and mice. Arch Virol 147, 167-179, 2002.

73) Liebler-Tenorio E, Pabst R, Liebler E, Liebler-tenorio EM. MALT structure and function in farm animals. Vet Res 37, 257-280, 2006.

74) Looijer-van Langen M, Hotte N, Dieleman, A L, Albert E, Mulder C, Madsen KL. Estrogen receptor-β signaling modulates epithelial barrier function. Am J Physiol Liver Physiol 300, 621-626, 2011.

75) Lorenzen E, Agerholm JS, Grossi AB, Bojesen AM, Skytte C, Erneholm K, Follmann F, Jungersen G. Characterization of cytological changes, IgA, IgG and IL-8 levels and pH value in the vagina of prepubertal and sexually mature Ellegaard Göttingen minipigs during an estrous cycle. Dev Comp Immunol 59, 57-62, 2016.

76) Lorenzen E, Follmann F, Jungersen G, Agerholm JS. A review of the human vs. porcine female genital tract and associated immune system in the perspective of using minipigs as a model of human genital Chlamydia infection. Vet Res 46, 1-13, 2015.

77) Lowery G. *Mammals of Louisiana and Its Adjacent Waters*. 1st ed. Louisiana State University; 1974.

78) Mähler M, Heidtmann W, Niewiesk S, Gruber A, Fossmark R, Beil W, Hedrich H, Wagner S. Experimental Helicobacter pylori infection induces antral-predominant, chronic active gastritis in Hispid cotton rats (Sigmodon hispidus). Helicobacter 10, 332-344, 2005.

79) Mair KH, Sedlak C, Käser T, Pasternak A, Levast B, Gerner W, Saalmüller A, Summerfield A, Gerdts V, Wilson HL, Meurens F. The porcine innate immune system: An update. Dev Comp Immunol 45, 321-343, 2014.

80) Manesse M, Delverdier M, Abella-Bourges N, Sautet J, Cabanié P, Schelcher F. An immunohistochemical study of bovine palatine and pharyngeal tonsils at 21, 60 and 300 days of age. Anat Histol Embryol 27, 179-185, 1998.

81) Manz RA, Thiel A, Radbruch A. Lifetime of plasma cells in the bone marrow. Nature 388, 133-134, 1997.

82) Mark, A S; Karla, A S; Ronald PW. Hamster. In: *The Laboratory Rabbit, Guinea Pig, Hamster, and Other Rodents*. Academic Press; 2012.

83) Mestas J, Hughes CCW. Of mice and not men: differences between mouse and human immunology. J Immunol 172, 2731-2738, 2004.

84) Miller CJ, McChesney M, Moore PF. Langerhans cells, macrophages and lymphocyte subsets in the cervix and vagina of rhesus macaques. Lab Investig 67, 628-634, 1992.

85) Moyron-Quiroz JE, Rangel-Moreno J, Kusser K, Hartson L, Sprague F, Goodrich S, Woodland DL, Lund FE, Randall TD. Role of inducible bronchus associated lymphoid tissue (iBALT) in respiratory immunity. Nat Med 10, 927-934, 2004.

86) Murphy BR, Sotnikov A V., Lawrence LA, Banks SM, Prince GA. Enhanced pulmonary

histopathology is observed in cotton rats immunized with formalin-inactivated respiratory syncytial virus (RSV) or purified F glycoprotein and challenged with RSV 3-6 months after immunization. Vaccine 8, 497-502, 1990.

87) Murphy TF, Dubovi EJ, Clyde WA. The cotton rat as an experimental model of human parainfluenza virus type 3 disease. Exp Lung Res 2, 97-109, 1981.

88) Nair PNR, Schroeder HE. Duct-associated lymphoid tissue (DALT) of minor salivary glands and mucosal immunity. Immunology 57, 171-180, 1986.

89) Nakamura T, Ichii O, Irie T, Mizoguchi T, Shinohara A, Kouguchi H, Sunden Y, Otsuka-Kanazawa S, Elewa YHA, Koshimoto C, Nagasaki KI, Kon Y. Cotton rats (Sigmodon hispidus) possess pharyngeal pouch remnants originating from different primordia. Histol Histopathol 33, 555-565, 2018.

90) Nakamura T, Ichii O, Irie T, Kouguchi H, Sotozaki K, Chihara M, Sunden Y, Nagasaki K ichi, Tatsumi O, Elewa YHA, Kon Y. Cotton rat (Sigmodon hispidus) develops metabolic disorders associated with visceral adipose inflammation and fatty pancreas without obesity. Cell Tissue Res 375, 483-492, 2019.

91) Naya DE, Feijoo M, Lessa EP, Pardi˜nas UFJ, Pardi˜nas P, Teta P, Tomasco IH, Valdez L, D'el´ia G, El´ia E. Digestive morphology of two species of Abrothrix (Rodentia, Cricetidae): comparison of populations from contrasting environments. J Mammal 95, 1222-1229, 2014.

92) Nguyen JD, Duong H. *Anatomy, Abdomen and Pelvis, Female External Genitalia*. StatPearls Publishing; 2022.

93) Nie X, Xie R, Tuo B. Effects of estrogen on the gastrointestinal tract. Dig Dis Sci 63, 583-596, 2018.

94) Niewiesk S, Prince G. Diversifying animal models: the use of hispid cotton rats (Sigmodon hispidus) in infectious diseases. Lab Anim 36, 357-372, 2002.

95) Nüssler NC, Reinbacher K, Shanny N, Schirmeier A, Glanemann M, Neuhaus P, Nussler AK, Kirschner M. Sex-specific differences in the expression levels of estrogen receptor subtypes in colorectal cancer. Gend Med 5, 209-217, 2008.

96) Ochiel DO, Fahey J V., Ghosh M, Haddad SN, Wira CR. Innate immunity in the female reproductive tract: role of sex hormones in regulating uterine epithelial cell protection against pathogens. Curr Womens Health Rev 4, 102-117, 2008.

97) Oláh I, Takács L, Törö I. Formation of lymphoepithelial tissue in the sheep's palatine tonsil. Acta Otolaryngol Suppl 454, 7-17, 1988.

98) Oliver JH, Chandler FW, James AM, Sanders FH, Hutcheson HJ, Huey LO, McGuire BS, Lane

RS. Natural occurrence and characterization of the Lyme disease spirochete, Borrelia burgdorferi, in cotton rats (Sigmodon hispidus) from Georgia and Florida. J Parasitol 81, 30-36, 1995.

99) Ottolini MG, Blanco JCG, Eichelberger MC, Porter DD, Pletneva L, Richardson JY, Prince GA. The cotton rat provides a useful small-animal model for the study of influenza virus pathogenesis. J Gen Virol 86, 2823-2830, 2005.

100) Owen R, Jones A. Epithelial cell specialization within human Peyer's patches: an ultrastructural study of intestinal lymphoid follicles. Gastroenterology 66, 189-203, 1974.

101) Pabst R. The anatomical basis for the immune function of the gut. Anat Embryol (Berl) 176, 135-144, 1987.

102) Pacini DL, Dubovi EJ, Clyde WA. A new animal model for human respiratory tract disease due to adenovirus. J Infect Dis 150, 92-97, 1984.

103) Parham P, Janeway C. *The Immune System*. 3rd ed. Garland Science; 2009.

104) Parsons KR, Howard CJ, Jones B V, Sopp P. Investigation of bovine gut associated lymphoid tissue (GALT) using monoclonal antibodies against bovine lymphocytes. Vet Pathol 26, 396-408, 1989.

105) Popesko P, Viera; R, Jindrich H. *Colour Atlas of Anatomy of Small Laboratory Animals*. 2nd ed. Saunders; 2003.

106) Randall TD. Bronchus-associated lymphoid tissue (BALT). Structure and function. Adv Immunol 107, 187-241, 2010.

107) Rehman A, Ahmad E, Arshad U, Riaz A, Akhtar MS, Ahmad T, Khan JA, Mohsin I, Shi Z, Sattar A. Effects of immunization against inhibin α-subunit on ovarian structures, pregnancy rate, embryonic and fetal losses, and prolificacy rate in goats where estrus was induced during the non-breeding season. Anim Reprod Sci 224, 106654. Epub, 2021.

108) Reynolds JD, Pabst R. The emigration of lymphocytes from Peyer's patches in sheep. Eur J Immunol 14, 7-13, 1984.

109) Romani N, Clausen BE, Stoitzner P. Langerhans cells and more: Langerin-expressing dendritic cell subsets in the skin. Immunol Rev 234, 120-141, 2010.

110) Rothkotter HJ. Lymphocyte subsets in jejunal and ileal Peyer's patches of normal and gnotobiotic minipigs. Immunology 67, 103-108, 1989.

111) Ruberte J, Carretero A, Navarro M. Female genital organs. In: *Morphological Mouse Phenotyping : Anatomy, Histology and Imaging*. 1st ed. Academic Press; 2017:227-251.

112) Russell MW, Mestecky J. Humoral immune responses to microbial infections in the genital tract. Microbes Infect 4, 667-677, 2002.

113) Rytik P, Müller KW. The use of the polymerase chain reaction in modelling HIV infection in animals. Zh Mikrobiol Epidemiol Immunobiol 8, 86-89, 1995.

114) Sakaguchi E. Digestive strategies of small hindgut fermenters. Anim Sci J 74, 327-337, 2003.

115) Sakimoto T, Shoji J, Inada N, Saito K, Iwasaki Y, Sawa M. Histological study of conjunctiva-associated lymphoid tissue in mouse. Jpn J Ophthalmol 46, 364-369, 2002.

116) Samuelson DA. *Textbook of Veterinary Histology*. 1st ed. Saunders Elsevier; 2006.

117) Schneider P, Takatsuka H, Wilson A, Mackay F, Tardivel A, Lens S, Cachero TG, Finke D, Beermann F, Tschopp J. Maturation of marginal zone and follicular B cells requires B cell activating factor of the tumor necrosis factor family and is independent of B cell maturation antigen. J Exp Med 194, 1691-1697, 2001.

118) Silva FMO, Guimarães JP, Vergara-Parente JE, Carvalho VL, Carolina A, Meirelles O, Marmontel M, Oliveira BSSP, Santos SM, Becegato EZ, Evangelista JSAM, Miglino MA. Morphology of mucosa-associated lymphoid tissue in odontocetes. Microsc Res Tech 79, 845-855, 2016.

119) Sisson S, Grossman JD, Getty R. *Sisson and Grossman's The Anatomy of the Domestic Animals*. 5th ed. Saunders; 1975.

120) Steinbach MM, Duca CJ. Experimental Tuberculosis in the Cotton Rat (Sigmodon hispidus littoralis). Proc Soc Exp Biol Med 44, 288-290, 1940.

121) Stevens CE. Physiological implications of microbial digestion in the large intestine of mammals: relation to dietary factors. Am J Clin Nutr 31, 161-168, 1978.

122) Tommola P, Bützow R, Unkila-Kallio L, Paavonen J, Meri S. Activation of vestibule-associated lymphoid tissue in localized provoked vulvodynia. Am J Obstet Gynecol 212, 476.e1-e8, 2015.

123) Wang J, Gusti V, Saraswati A, Lo DD. Convergent and divergent development among M cell lineages in mouse mucosal epithelium. J Immunol 187, 5277-5285, 2011.

124) Wang Y, Sui Y, Kato S, Hogg AE, Steel JC, Morris JC, Berzofsky JA. Vaginal type-II mucosa is an inductive site for primary CD8+ T-cell mucosal immunity. Nat Commun 6, 1-13, 2015.

125) Weidenmaier C, Kokai Kun J. Role of teichoic acids in Staphylococcus aureus nasal colonization, a major risk factor in nosocomial infections. Nat Med 10, 243-245, 2004.

126) Winborn WB, Sheridan PJ, McGill HC. Sex steroid receptors in the stomach, liver, pancreas, and gastrointestinal tract of the baboon. Gastroenterology 92, 23-32, 1987.

127) Wira CR, Rossoll RM, Kaushic C. Antigen-presenting cells in the female reproductive tract: influence of estradiol on antigen presentation by vaginal cells. Endocrinology 141, 2877-2885, 2000.

128) Wojciech P, Ross MH. *Histology: A Text and Atlas: With Correlated Cell and Molecular Biology*. 8th ed. Wolters Kluwer; 2020.

129) Wyde PR, Moore-Poveda DK, Daley NJ, Oshitani H. Replication of clinical measles virus strains in hispid cotton rats. Proc Soc Exp Biol Med 221, 53-62, 1999.

130) Wyde P, Chetty S, Jewell A. Development of a cotton rat–human metapneumovirus (hMPV) model for identifying and evaluating potential hMPV antivirals and vaccines. Antiviral Res 66, 57-66, 2005.

131) Yan Z, Wang JB, Gong SS, Huang X. Cell proliferation in the endolymphatic sac in situ after the rat waldeyer ring equivalent immunostimulation. Laryngoscope 113, 1609-1614, 2003.

132) Yang H, Parkhouse RME. Phenotypic classification of porcine lymphocyte subpopulations in blood and lymphoid tissues. Immunology 89, 76-83, 1996.

133) Yim KC, Carroll CJ, Tuyama A, Cheshenko N, Carlucci MJ, Porter DD, Prince GA, Herold BC. The cotton rat provides a novel model to study genital herpes infection and to evaluate preventive strategies. J Virol 79, 14632-14639, 2005.

134) Zhang J, Kuolee R, Patel G, Chen W. Intestinal M cells: the fallible sentinels? World J Gastroenterol 13, 1477-1486, 2007.

135) Zhang WD, Wang WH, Jia S. The distribution of siga and igg antibody-secreting cells in the small intestine of bactrian camels (camelus bactrianus) of different ages. PLoS One 11, e0156635, 2016.

136) Zhou JZ, Way SS, Chen K. Immunology of the uterine and vaginal mucosae. Trends Immunol 39, 302-314, 2018.